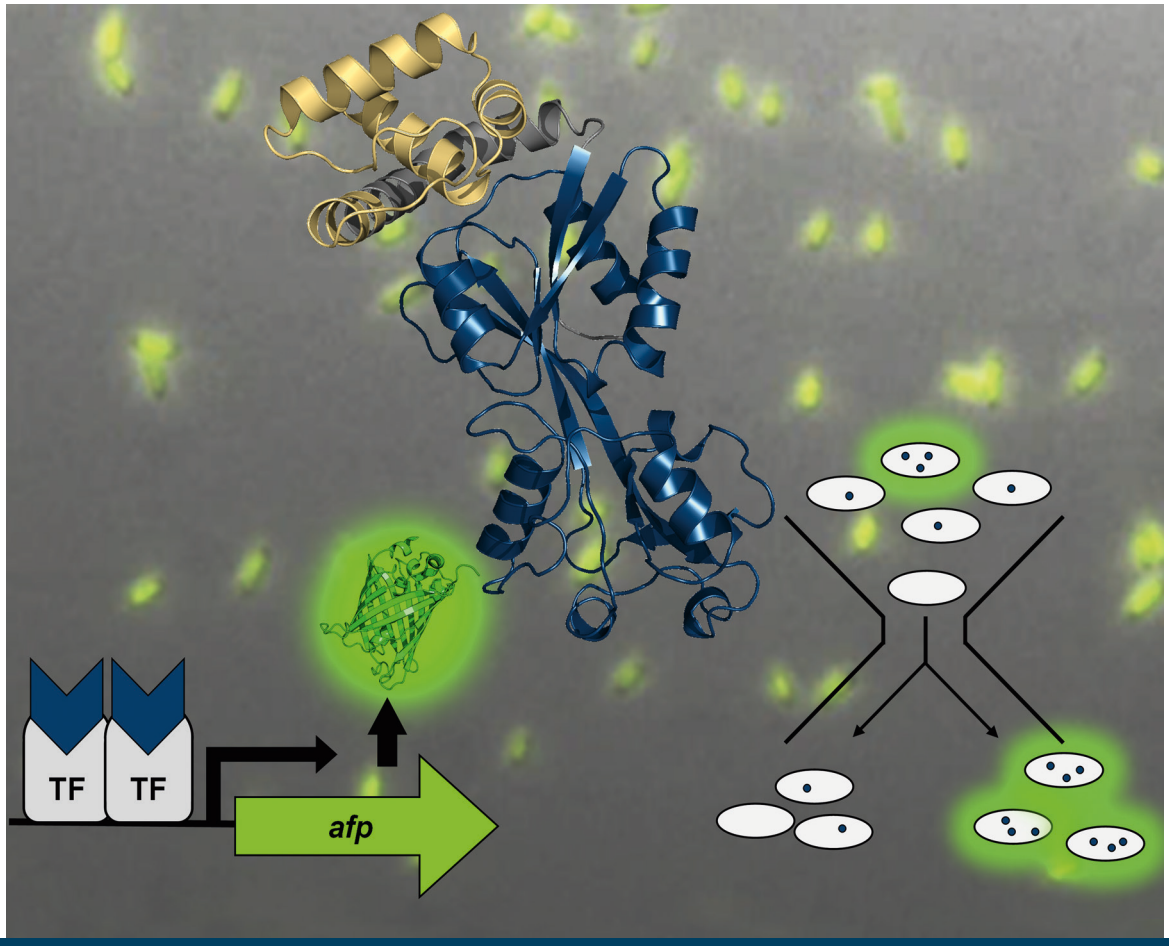

Development of a transcriptional biosensor and reengineering of its ligand specificity using fluorescence-activated cell sorting

Lion Konstantin Flachbart

Schlüsseltechnologien / Key Technologies
Band / Volume 226
ISBN 978-3-95806-515-4

Mitglied der Helmholtz-Gemeinschaft

JÜLICH
Forschungszentrum

Schriften des Forschungszentrums Jülich
Reihe Schlüsseltechnologien / Key Technologies Band / Volume 226

Forschungszentrum Jülich GmbH
Institut für Bio-und Geowissenschaften
Biotechnologie (IBG-1)

Development of a transcriptional biosensor and reengineering of its ligand specificity using fluorescence-activated cell sorting

Lion Konstantin Flachbart

Schriften des Forschungszentrums Jülich
Reihe Schlüsseltechnologien / Key Technologies Band / Volume 226

ISSN 1866-1807 ISBN 978-3-95806-515-4

Bibliografische Information der Deutschen Nationalbibliothek.
Die Deutsche Nationalbibliothek verzeichnet diese Publikation in der
Deutschen Nationalbibliografie; detaillierte Bibliografische Daten
sind im Internet über http://dnb.d-nb.de abrufbar.

Herausgeber und Vertrieb:	Forschungszentrum Jülich GmbH Zentralbibliothek, Verlag 52425 Jülich Tel.: +49 2461 61-5368 Fax: +49 2461 61-6103 zb-publikation@fz-juelich.de www.fz-juelich.de/zb
Umschlaggestaltung:	Grafische Medien, Forschungszentrum Jülich GmbH
Druck:	Grafische Medien, Forschungszentrum Jülich GmbH
Copyright:	Forschungszentrum Jülich 2020

Schriften des Forschungszentrums Jülich
Reihe Schlüsseltechnologien / Key Technologies, Band / Volume 226

D 61 (Diss. Düsseldorf, Univ., 2019)

ISSN 1866-1807
ISBN 978-3-95806-515-4

Vollständig frei verfügbar über das Publikationsportal des Forschungszentrums Jülich (JuSER)
unter www.fz-juelich.de/zb/openaccess.

This thesis in hand has been performed at the Institute of Bio- and Geosciences, IBG-1: Biotechnology, Forschungszentrum Jülich GmbH, from May 2015 until June 2019 under the supervision of Prof. Dr. Michael Bott and Prof. Dr. Jan Marienhagen.

Printed with the permission of
the Faculty of Mathematics and Natural Sciences
of the Heinrich Heine University Düsseldorf

Examiner: Prof. Dr. Michael Bott
Institute of Bio- and Geosciences, IBG-1: Biotechnology
Forschungszentrum Jülich GmbH

Co-examiner: Prof. Dr. Holger Gohlke
Institute for Pharmaceutical and Medicinal Chemistry
Heinrich Heine University Düsseldorf

Date of oral examination:

14.10.2019

Results presented in this thesis will be published in two original articles. At the time of printing this thesis, one original article was published. The second original article was close to submission.

Flachbart, L. K., Sokolowsky, S. & Marienhagen, J. (2019). Displaced by deceivers - Prevention of biosensor cross-talk is pivotal for successful biosensor-based high-throughput screening campaigns. ACS Synth. Biol. 8, acssynbio.9b00149. https://doi.org/10.1021/acssynbio.9b00149

Flachbart, L. K., Gertzen, C., Gohlke, H. & Marienhagen, J. (2020). Development of a biosensor platform for various phenolic compounds using a transition ligand strategy. *To be submitted.*

Table of contents

Table of contents III

Abstract V

Zusammenfassung VI

Abbreviations VII

1. Scientific context and key results of the thesis 1

1.1. Industrial Biotechnology - key to a future bio-based economy 1

1.2. Engineering of enzymes and microorganisms 2

1.3. Recombinant DNA technologies 4

1.4. Genetically encoded biosensors 6

1.4.1. RNA-aptamer-based biosensors 7

1.4.2. Biosensors employing Förster resonance energy transfer 7

1.4.3. Transcription factor-based biosensors 8

1.4.4. Fluorescence activated cell sorting 9

1.5. Microbial production of plant polyphenols 13

1.6. Aims of this thesis 16

1.6.1. Application of transcription factor-based biosensors for directed enzyme evolution 16

1.6.2. Development of transcription-factor-based biosensors 17

1.7. Key results 18

1.7.1. A *trans*-cinnamic acid biosensor 18

1.7.2. Optimization of heterologous gene expression enables CA production and biosensor-mediated product detection in *E. coli* 18

1.7.3. Prevention of biosensor cross-talk is a prerequisite for any FACS applications using pSenCA 20

1.7.4. Directed evolution of an ammonia lyase by multistep FACS screening 22

1.7.5. Identifying a promiscuity hotspot in the transcriptional regulator HcaR 24

1.7.6. Multistep FACS-campaign enables the isolation of biosensors with novel specificities 27

1.8. Conclusions and Outlook 30

2. Publications 32

2.1. Displaced by deceivers - Prevention of biosensor cross-talk is pivotal for successful biosensor-based high-throughput screening campaigns 32

2.1.1. Displaced by deceivers - Manuscript 32

2.1.2. Displaced by deceivers - Supporting information 45

2.2. Development of a biosensor platform for phenolic compounds using a transition ligand strategy 52

2.2.1. Biosensor platform development - Manuscript 52

2.2.2. Biosensor platform development - Supporting information 78

3. Bibliography 84

4. Appendix 100

4.1. Author contributions 100

Danksagung 101

Erklärung 102

Abstract

Important chemical compounds of our daily life such as amino acids, antibiotics or vitamins are produced by microorganisms at large-scale. Also, there is growing interest in the microbial synthesis of many other compounds including pharmaceutically interesting secondary metabolites from plants. However, development and improvement of the microbial producer strains is time-consuming and cost-intensive. In this context, biosensor-based fluorescence-active cell sorting (FACS) to identify suitable production strain variants represents a promising approach to tackle these challenges.

In this dissertation, the application of transcription factor-based biosensors in combination with FACS for high-throughput screening of enzyme libraries was investigated in *Escherichia coli*. Furthermore, the construction of biosensors with modified ligand spectrum from an existing biosensor was pursued to expand the repertoire of biosensor-detectable substances.

Initially, the transcription factor-based biosensor pSenCA which can be used to convert cytosolic concentrations of the phenylpropanoid *trans*-cinnamic acid (CA) to a fluorescence output signal, was constructed and characterized. The biosensor is composed of the transcriptional regulator HcaR from *Escherichia coli* and its target promoter P_{hcaE}, transcriptionally fused with the *eyfp* gene encoding an autofluorescent protein.

This biosensor was subsequently used to optimize an L-phenylalanine/L-tyrosine ammonia lyase from *Trichosporon cutaneum* (Xal_{Tc}), by a directed evolution approach. Aromatic amino acid ammonia lyases represent the key enzyme in many plant polyphenol biosynthetic pathways. The use of an expression system with titratable expression strength of the ammonia lyase gene as well as a significant reduction of the initial cell density prior to screening were prerequisites for an effective isolation of CA producers from mixed cultures with non-producers. The established screening method was subsequently used to screen a randomly mutagenized ammonia lyase library of 2.4×10^6 variants for improved fluorescence. All 182 clones isolated by FACS were CA producers, 138 produced at least 10 % more CA compared to the parent strain. The best strain showed a 60 % increase in CA production. Seven Xal_{Tc} variants investigated *in vitro* exhibited up to 12 % increased specific activity and up to 20 % increased substrate affinity.

In the second project, 15 amino acids in the ligand binding site of the regulator protein HcaR, which were identified by *in silico* structure analysis, were randomized by site saturation mutagenesis. The resulting HcaR biosensor libraries were screened for variants with increased specificity for 3,5-dihydroxyphenylpropionate using FACS. These experiments resulted in the isolation of pSenGeneral, a sensor variant with a significantly broadened ligand spectrum. In a second round of biosensor evolution, additional libraries based on pSenGeneral were constructed and screened for variants with specificity for various compounds of biotechnological interest. As a result, biosensor variants for the detection of 4-hydroxybenzoic acid, 6-methylsalicylate, *p*-coumaric acid, or 5-bromoferulic acid could be isolated. In the future, these newly designed biosensors for small aromatic compounds could find an application during microbial strain development and might represent a good starting point for the development of additional biosensors for other aromatic molecules of biotechnological interest.

Zusammenfassung

Wichtige chemische Verbindungen unseres täglichen Lebens wie Aminosäuren, Antibiotika oder Vitamine werden von Mikroorganismen im großen Maßstab produziert. Darüber hinaus wächst das Interesse an der mikrobiellen Synthese zahlreicher weiterer Substanzen, einschließlich pharmazeutisch interessanter sekundärer Metaboliten aus Pflanzen. Die Entwicklung und Verbesserung der mikrobiellen Produzentenstämme ist jedoch zeitaufwendig und kostenintensiv. In diesem Zusammenhang stellt die biosensorbasierte, Fluoreszenz-aktivierte Zellsortierung (FACS) einen vielversprechenden Ansatz zur Bewältigung dieser Herausforderungen dar.

In dieser Arbeit wurde die Anwendung von Transkriptionsfaktor-basierten Biosensoren in Kombination mit FACS für das Hochdurchsatzscreening von Enzymbibliotheken in *Escherichia coli* untersucht. Darüber hinaus wurde die Konstruktion von Biosensoren mit modifiziertem Ligandenspektrum, ausgehend von einem bestehenden Biosensor, verfolgt, um das Repertoire an Substanzen zu erweitern, die duch Biosensoren detektierbar sind

Zunächst wurde der transkriptionelle Biosensor pSenCA, der zytosolische Konzentrationen des Phenylpropanoids *trans*-zimtsäure (CA) in ein Fluoreszenzsignal umwandelt, konstruiert und charakterisiert. Der Biosensor besteht aus dem Transkriptionsregulator HcaR aus *Escherichia coli* und dessen Zielpromotor P_{hcaE}, transkriptionell fusioniert mit dem *eyfp*-Gen, das ein fluoreszierendes Reporterprotein kodiert.

Im Anschluss wurde pSenCA genutzt, um eine L-Phenylalanin/L-Tyrosin-Ammoniak-Lyase aus *Trichosporon cutaneum* (Xal_{Tc}), durch einen gerichteten Evolutionsansatz zu optimieren. L-Phenylalanin/L-Tyrosin-Ammoniak-Lyasen katalysieren einen Schlüsselschritt in der Biosynthese vieler pflanzlicher Polyphenole. Die Verwendung eines Expressionssystems mit titrierbarer Expressionsstärke des Ammoniak-Lyase-Gens sowie eine signifikante Reduktion der anfänglichen Zelldichte vor dem Screening waren Voraussetzung für eine effektive Isolierung von CA-Produzenten aus Mischkulturen mit Nicht-Produzenten. Die etablierte Screeningmethode wurde anschließend verwendet, um eine ungerichtet mutagenisierte Ammoniak-Lyase-Bibliothek mit $2{,}4\times10^6$ Varianten auf erhöhte Fluoreszenz zu überprüfen. Alle 182 Klone, die mittels FACS isoliert wurden, waren CA-Produzenten, 138 produzierten signifikant (> 10 %) mehr CA als der Ausgangsstamm. Der beste Stamm zeigte einen Anstieg der CA-Produktion um 60 %. Sieben *in vitro* untersuchte Xal_{Tc}-Mutanten zeigten eine bis zu 12 % erhöhte Aktivität und eine bis zu 20 % erhöhte Substrataffinität.

Im zweiten Projekt wurden 15 Aminosäuren in der Ligandenbindestelle des Regulatorproteins HcaR, die mittels *in silico*-Strukturanalyse identifiziert wurden, durch eine Sättigungsmutagenese zielgerichtet mutagenisiert. Die resultierenden HcaR-Biosensorbibliotheken wurden mittels FACS auf Varianten mit erhöhter Spezifität für 3,5-Dihydroxyphenylpropionat durchmustert. Diese Experimente führten zur Isolation von pSenGeneral, einer Sensorvariante mit einem deutlich vergrößerten Spektrum detektierbarer Liganden. In einer zweiten Runde der Biosensorevolution wurden zusätzliche Bibliotheken auf Basis von pSenGeneral erstellt und nach Sensoren mit Spezifität für verschiedene Verbindungen von biotechnologischem Interesse durchsucht. So konnten Biosensorvarianten für den Nachweis von 4-Hydroxybenzoesäure, 6-Methylsalicylat, *p*-Cumarsäure oder 5-Bromoferulasäure isoliert werden. Diese neu entwickelten Biosensoren für kleine Aromaten könnten in Zukunft eine Anwendung bei der mikrobiellen Stammentwicklung finden und auch einen guten Ausgangspunkt für die Entwicklung weiterer Biosensoren für andere aromatische Moleküle von biotechnologischem Interesse darstellen.

Abbreviations

3,4DHBA	3,4 dihydroxybenzoic acid
3,5DHPP	3,5-dihydroxyphenylpropionic acid
3HCA	3-hydroxycinnamic acid
3HPP	3-hydroxy phenylpropionic acid
4CL	4-coumaryl-CoA ligase
4HBA	4-hydroxybenzoic acid
5BFA	5-bromoferulic acid
5BFA	5-bromoferulic acid
6MSA	6-methylsalicylic acid
AFP	autofluorescent protein
AL	aromatic amino acid ammonia lyase
BA	benzoic acid
BP	band-pass filter
CA	*trans*-cinnamic acid
CA^-	*Escherichia coli coli* DH10B Δ*hcaREFCBD* pSenCA pBAD
CA^+	*Escherichia coli coli* DH10B Δ*hcaREFCBD* pSenCA pBAD-xal_{Tc}
CAD	cinnamyl alcohol dehydrogenase
CAF	caffeic acid
CCR	cinnamoyl-CoA reductase
cells/s	cells per second
CHI	chalcone isomerase
CHS	chalcone synthase
CRISPR/Cas	clustered regularly interspaced short palindromic repeats-associated proteins
DIR	Dirigent proteins
E. coli	*Escherichia coli*
e.g.	(lat.) exempli gratia
et al.	(lat.) et alii
FA	ferulic acid
FACS	fluorescence-activated cell sorting
FES	fluorescence-activated cell sorting-enrichment step(s)
FRET	förster resonance energy transfer
FSC	Forward scatter characteristics
GOI	gene of interest

HT	high throughput
iOD_{600}	optical density of inoculum at 600 nm
LAC	laccase
L-Ara	L-arabinose
LBD	ligand binding domain
LP	long-pass dichroic mirror
L-Phe	L-phenylalanine
L-Tyr	L-tyrosine
MOI	molecule of interest
MON	P 450 monooxygenase
OMT	*O*-methyltransferase
PAL	L-phenylalanine ammonia lyase
*p*HCA/4HCA	*p*-coumaric acid
PMT	Photomultiplier Tube
PP	phenylpropionic acid
SA	salicylic acid
SDM	site-directed mutagenesis
SNP	single nucleotide polymorphism
SSC	Side scatter characteristics
SSM	site saturation mutagenesis
STS	stilbene synthase
TAL	L-tyrosine ammonia lyase
TF	transcription factor
WT	wild type
Xal_{Tc}	aromatic amino acid ammonia lyase from *Trichosporon cutaneum*
xal_{Tc}	synthetic construct encoding Xal_{Tc}, codon optimized for *E. coli*

1. Scientific context and key results of the thesis

1.1. Industrial Biotechnology - key to a future bio-based economy

In defiance of all technological progress, the energetic consumption (transportation, heating) or material use of fossil fuels is ever increasing. Mainly refined from fossil resources, simple chemical units are the building blocks for the synthesis of multitudinous substances used as solvents, fuels, polymers, textiles, nutrient, flavours and pharmaceuticals (Harmsen et al., 2014; Wieschalka et al., 2013). In addition, the consumption of fossil fuels for transportation and industrial processes releases CO_2, which accelerates global warming and thus contributes to the climate change (Kucherov et al., 2018; Watts et al., 2015).

In this context, industrial biotechnology can help to reduce the dependence on fossil fuels by applying microorganisms or isolated enzymes for the production of base chemicals, building blocks for polymer production and specialty chemicals from renewable feedstocks (Scarlat et al., 2015) (Figure 1). The replacement of fossil raw material-dependent production processes by more sustainable processes based on renewable biological resources for the production value-added products such as food, feed, bio-based products, and bioenergy is of central importance in the European commission's vision for a bio-based economy (bioeconomy) in Europe. Therefore, biotechnology is seen as one of the key technologies on the way towards a sustainable bioeconomy (Scarlat et al., 2015).

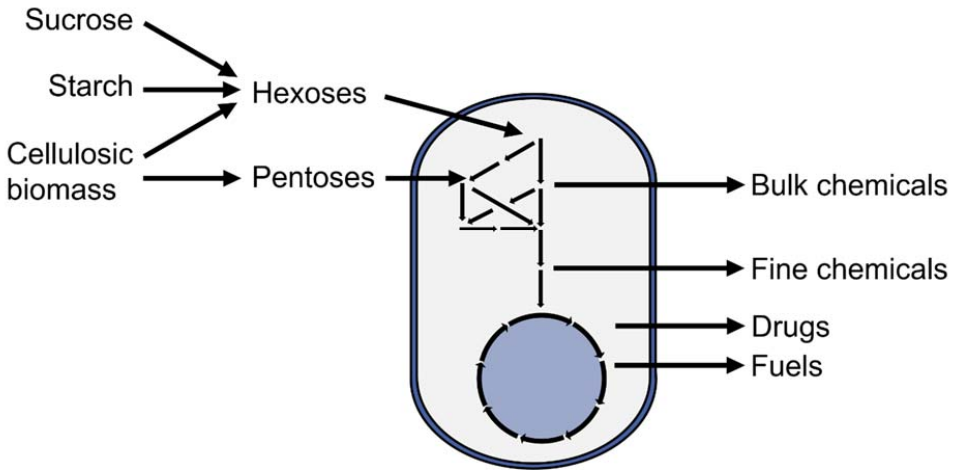

Fig. 1: Conversion of sugars derived from sucrose, starch or cellulosic biomass to value added products by the means of a microbial production strain.

1.2. Engineering of enzymes and microorganisms

Microorganisms harbour diverse metabolic pathways, which enable the conversion of basic carbon sources into complex, value-added compounds. Optimized by evolution towards resource efficiency, however, pathway activities are stringently controlled and metabolites are only produced in quantities necessary to enable proliferation and survival of the respective organism (Nielsen, 2001). Triggered by certain growth conditions, excess metabolite formation may nevertheless occur. Examples for this are the production of ethanol by *Saccharomyces cerevisiae* under anaerobic and microaerobic conditions and the overproduction of L-glutamate in *Corynebacterium glutamicum* under biotin limitation (Gutmann et al., 1992; Hoppe and Hansford, 1984).

Despite mankind using microbial fermentation to produce food and beverages for thousands of years without knowledge about the underlying mechanisms, it was not until 1857 that Louis Pasteur concluded the presence of "lactic yeast" is responsible for the production of lactic acid, thereby laying the foundation for targeted application and engineering of microbial organisms (Pasteur, 1857; Schürrle, 2018; Sibbesson, 2019).

Even without in-depth knowledge of microbial metabolism, production capabilities of the organisms in question can be altered by undirected mutagenesis and screening for a production phenotype. Thus, a classic strain engineering technique is the introduction of random mutations followed by isolation of metabolite-producing mutants. Iterative exposure to chemical mutagens or ultraviolet/nuclear radiation induces random genetic mutations throughout the entire genome of the organism in question (Ghribi et al., 2004; Hughes et al., 2012). Strains with the desired production phenotype are subsequently identified by time- and cost-intensive screening, which means cultivation and analysis of individual strain variants (Figure 2) (Sauer, 2001; Schallmey et al., 2014). Besides beneficial mutations, resulting in overproduction of the molecule of interest (MOI), silent mutations and mutations with adverse effects on growth speed and stress tolerance occur (Kaplan et al., 1989). An advantageous option for identifying improved producers is selection. For this, the production strain is modified to be auxotrophic for the MOI, whereby only mutants that produce the MOI survive. However, this technique is mostly restricted to intermediates or products of the microbial metabolism. Furthermore, once the MOI production is high enough to support cellular growth, more potent strain variants are difficult to distinguish from their respective parent strains (Dietrich et al., 2010).

A principle similar to mutagenesis and screening of microorganisms, referred to as directed evolution, is used for the optimization of enzymes regarding their overall activity, pH resistance, thermal resilience, solvent tolerance, substrate specificity or their substrate spectrum (Bornscheuer et al., 2019). Here, mutagenesis is mostly performed *in vitro* employing PCR-based methods such as error-prone polymerase chain reaction (epPCR) (Cirino et al., 2003). Subsequently, the generated gene

libraries are expressed to produce the corresponding protein variants and single variants are individually characterized (Lutz and Iamurri, 2018). This characterization of is often performed *in vitro* as this enables an easier control of the reaction conditions (Arnold and Georgiou, 2003). Subsequently, the isolated variants can be used as starting points for further rounds of mutagenesis and screening (Figure 2). A disadvantage of directed protein evolution *in vitro* is an often limited applicability of the improved enzyme variants *in vivo* where parameters important for the overall enzyme performance, such as pH, substrate concentration or cofactor availability, are different (Bulter et al., 2003; Fasan et al., 2007). Ideally, a mutein is screened in exactly the same environment and with exactly the same substrates that will be used in the desired application.

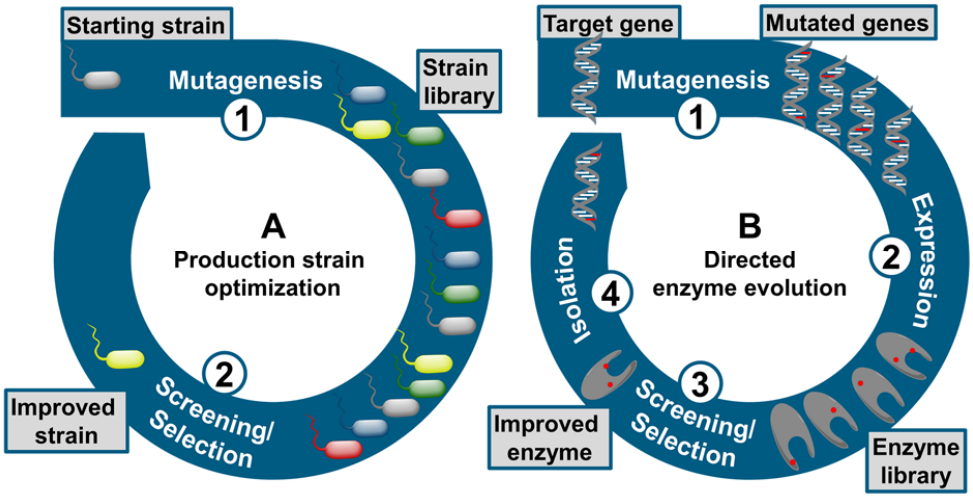

Fig. 2: Optimization of microbial production strains and directed evolution of enzymes (A) ① Introduction of random mutations, *e.g.* by chemical mutagens or radiation, resulting in a strain library. ② Identification of improved producer strain either by screening or by selection for the desired phenotype. Isolated strains can be used for subsequent cycles. **(B)** ① Introduction of random mutations into the target gene, *e.g.* by error-prone PCR. ② Transformation of a suitable host with the library and expression of mutated genes results in an enzyme library. ③ Identification of improved enzyme variant either by screening or by selection for the desired property. ④ Isolation of the gene encoding such an improved enzyme variant can be used for subsequent cycles of site-directed evolution.

In the last decades, the understanding of structure-function relationships in many enzymes or proteins greatly improved. As a result, localizable protein traits such as enantioselectivity can be improved by rational redesign and subsequent screening of rather small enzymes libraries, which significantly reduces the screening effort for identifying improved enzyme variants (Lutz and Iamurri, 2018).

1.3. Recombinant DNA technologies

In strain development, recombinant DNA technologies such as the overexpression or deletion of endogenous genes and the overexpression of heterologous genes enabled a more targeted approach (Lee et al., 2009). The generation of data sets necessary for a systemic overview became possible with the development of the "omics" methods, enabling the analysis of the entire genetic information (genomics) of an organism, its transcripts (transcriptomics), proteins (proteomics), metabolites (metabolomics), and pathway fluxes (fluxomics) (Furusawa et al., 2013; Niedenführ et al., 2015; Petzold et al., 2015; Woolston et al., 2013). The rational strain design enables the overproduction of cellular metabolites like alcohols, acids, or vitamins. By combination of knowledge gained in previous mutagenesis and screening approaches and stoichiometric deliberations, competitive producer strains can be constructed (Bott, 2015).

The development of an artificial toggle switch enabling bistable gene expression/repression without continuous inductor supply to drive expression and an oscillator circuit that periodically induces gene expression marked the beginning of synthetic biology (Elowitz and Leibler, 2000; Gardner et al., 2000). Synthetic biology uses various biological methods and concepts from engineering sciences to create artificial biological systems and develop foundational technologies that make the design and construction of engineered biological systems easier (Church et al., 2014; Endy, 2005). Well-known examples are the complete chemical synthesis, assembly, and cloning of a *Mycoplasma genitalium* genome and the standardization of genes and genetic regulatory elements by means of the BioBrick standard (Gibson et al., 2008; Knight, 2003).

Several tools have been established that significantly increase the accuracy and/or speed of classical engineering methods or offer unprecedented manipulation possibilities. While transcription activator-like effector nucleases (TALEN) and zinc-finger nucleases (ZFN) can be tailored to induce DNA double strand breaks at defined positions, the target sequence of clustered regularly interspaced short palindromic repeats-associated proteins (CRISPR/Cas) can be quickly altered by modification of the CRISPR RNA, given a protospacer adjacent motif is present (Carroll, 2011; Gaj et al., 2013; Jinek et al., 2012; Miller et al., 2011). DNA deletions or, if a suitable DNA fragment is provided, DNA insertions can thus be achieved with high efficiency. Whilst the incorporation of heterologous DNA into eukaryotic cells is performed by endogenous homology-directed repair, a recombinase gene has to be

co-expressed in prokaryotic cells to facilitate DNA insertions (Jakočiūnas et al., 2018; McVey and Lee, 2008; Reisch and Prather, 2015). Further examples for innovative technologies are multiplexed-automated genome engineering (MAGE, or in combination with CRISPR/Cas CRMAGE), optogenetic tools for the construction of artificial networks and for biocontainment and genomically recoded organisms (Chan et al., 2016; Elowitz and Leibler, 2000; Fredens et al., 2019; Möglich and Hegemann, 2013; Ronda et al., 2016; Rovner et al., 2015; Sowa et al., 2015; Wang et al., 2009).

Despite all technological progress, most of today's industrial production strains still stem from undirected mutagenesis and screening campaigns, or are a result of combining rational strain engineering and random mutagenesis/screening strategies (Bott, 2015). A reason for this is that even extensively studied model organisms, such as *E. coli* or *S. cerevisiae*, contain hundreds of genes whose function is not, or not fully, understood. These genes represent potential targets for strain engineering during the development of microbial production strains (Binder et al., 2012; Bott, 2015). A similar situation applies to enzyme engineering approaches, where mutations that cannot be inferred in advance, can result in dramatically improved properties. Therefore, the combination of random mutagenesis and screening still represents a powerful and often used strategy in strain and enzyme engineering campaigns. For the screening of strain as well as enzyme libraries, the characteristics of the MOI and the available resources in the laboratory dictate the available screening options. In most screening procedures, the production of the MOI in single candidate strains must be assessed using *e.g.* chromatographic methods that can only be scaled to allow for a screening throughput of 10^2 - 10^3 variants. Seldom, the MOI is chromogenic or fluorogenic, which allows for the development of microtiter plate-based screenings with higher throughput (10^4 – 10^5 variants) (Lin et al., 2017). A significantly higher throughput is possible with auxotrophy screenings that couple the target enzyme activity to the growth of the host strain (Dietrich et al., 2010). As opposed to the successful use of auxotrophic screenings for the engineering of novel catabolic activities, the coupling of growth to anabolic metabolism is much more demanding (Dietrich et al., 2010; Hall, 1981). Recurrently, the overproduction phenotype proved deleterious for the host strains fitness (Martin et al., 2003; Pitera et al., 2007). A generalized approach that decouples the screened producer cells from the growth restraint is the use of an auxotrophic whole cell biosensor. For example, a library of mevalonate-producing *E. coli* cells was screened for enhanced production (Pfleger et al., 2007). After parallel cultivation of the library variants, cell-free supernatant was transferred into cultures inoculated with mevalonate-auxotrophic *E. coli* cells constitutively expressing an autofluorescent reporter gene. Growth of the auxotrophic strain resulted in increasing fluorescence, generating a mevalonate-responsive whole cell biosensor.

1.4. Genetically encoded biosensors

A significantly higher screening throughput compared to auxotrophic whole cell biosensors is possible if the production strain itself harbours a genetically encoded biosensor. The different types of genetically coded biosensors all contain a transduction element that modulates gene expression or signal intensity upon ligand binding. Regulatory mechanisms to alter gene expression, based on RNA aptamer structures in riboswitches, transcriptional regulators, and enzymes offer a repertoire of tools to construct biosensors for intracellular metabolite detection (Mahr and Frunzke, 2015).

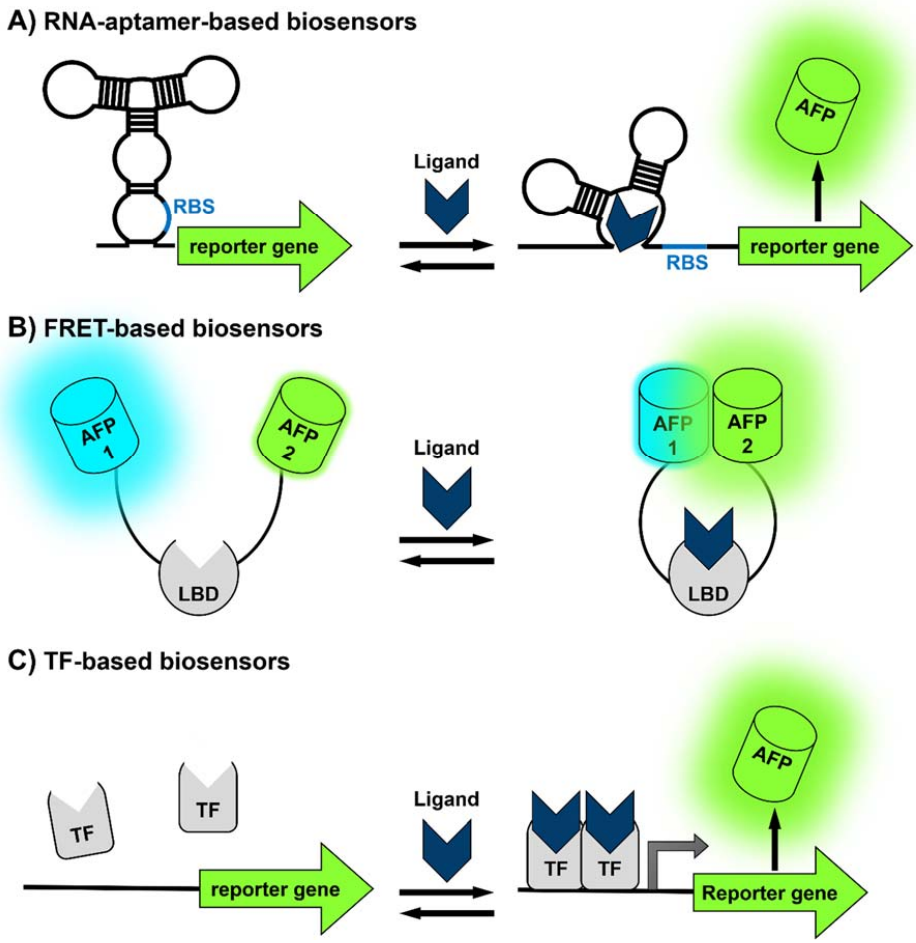

Fig. 3: Different biosensor types in OFF state (left, ligand absent) and ON-state (right, ligand present). (A) RNA-aptamer-based biosensors**. (B)** FRET-based biosensors. **(C)** TF-based biosensors. **Abbreviations:** FRET, Förster resonance energy transfer; AFP, autofluorescent protein; AFP1, donor autofluorescent protein; AFP2, acceptor autofluorescent protein; RBS, ribosome binding site; TF, transcription factor.

1.4.1. RNA-aptamer-based biosensors

RNA aptamer-based biosensors are riboswitches that change their structure upon binding of a ligand molecule, resulting in the alteration of gene expression, RNA stability or the enzymatic activity of ribozymes (Aboul-ela et al., 2015; Kang et al., 2014; Serganov and Nudler, 2013) (Figure 3 A). The effect of riboswitches on gene regulation was initially described for the response to thiamine pyrophosphate, flavin mononucleotide, and coenzyme B12 (Nahvi et al., 2002; Winkler et al., 2002a, 2002b). Natural metabolite-binding RNAs can be identified using algorithms such as Riboswitch Explorer (http://132.248.32.45:8080/cgi-bin/ribex.cgi) or Riboswitch Finder (http://riboswitch.bioapps.biozentrum.uni-wuerzburg.de/server.html) (Abreu-Goodger and Merino, 2005; Bengert and Dandekar, 2004). An *in vitro* method termed SELEX (systematic evolution of ligands by exponential enrichment) enables the selection of RNA aptamers with high affinity for diverse MOI (Ellington and Szostak, 1990). However, synthetic and *in vitro* selected RNA aptamers are often unsuitable for *in vivo* applications due to poor intracellular folding capacities (Kopniczky et al., 2015; Liang et al., 2011; Lin et al., 2017)

More recently, by fusing RNA aptamers to a selectable marker, riboselectors for the screening of L-lysine and L-tryptophan production in *E. coli* were constructed and the production of L-lysine in *C. glutamicum* was controlled using both an L-lysine-ON and an L-lysine-OFF riboswitch (Jang et al., 2015; Yang et al., 2013; Zhou and Zeng, 2015). The advantage of the immediate response to changes in the effector concentration contrasts with the effortful construction of *in vivo* functional aptamers with novel specificities.

1.4.2. Biosensors employing Förster resonance energy transfer

An alternative sensor type that enables the transduction of intracellular MOI formation into a measureable output makes use of Förster resonance energy transfer (FRET) (Figure 3 B). FRET sensors employ two autofluorescent proteins (AFPs) with overlapping emission spectrum of the FRET donor and excitation spectrum of the FRET acceptor. The FRET donor AFP transfers its excitation energy to the FRET acceptor AFP if both are in close proximity (<10 nm). Both AFPs are connected through a linker that contains a ligand binding domain (LBD) for the MOI. Upon MOI binding, the LBD undergoes a conformational change, that alters the intramolecular distance of both AFPs, either increasing or reducing FRET, resulting in altered fluorescence ratio of both AFPs (Lin et al., 2017). FRET biosensors for a wide range of applications have been reported, including sensors for acids, sugars, amino acids, ions, redox states, hydrogen peroxide, oxygen, and hormones (Ameen et al., 2016; Bilan et al., 2013; Feng et al., 2015; Hessels and Merkx, 2015; Mohsin et al., 2013; Nadler et al., 2016; Potzkei et al., 2012; San Martín et al., 2013; Yano et al., 2010). FRET sensors are able to monitor increases and decreases in ligand concentration in a high temporal resolution and were used to investigate fundamental questions regarding intracellular metabolite concentrations in plant and mammalian tissues, as well as

in microbial cells (Hamers et al., 2014; Kaschubowski et al., 2020; Mohsin and Ahmad, 2014; Zhu et al., 2017). To date, however, no biotechnological screening application involving FRET-based sensors has been described.

1.4.3. Transcription factor-based biosensors

Transcription factors (TF) have been widely used for the construction of genetically encoded biosensors (Lin et al., 2017). In biosensors that utilize a transcriptional activator, upon binding of an effector molecule, the TF undergoes conformational changes that enable the recruitment of the RNA polymerase to a target promoter of the TF, initiating transcription (Figure 3 C). Many TFs bind small molecule effectors, but gene expression control in response to inorganic ions, temperature or pH shifts, protein-protein interactions or protein modification has also been reported (Mahr and Frunzke, 2015). To construct a TF-based biosensor, a target promoter including the DNA-binding site of the TF is combined with a reporter gene, encoding *e.g.* an AFP, thereby facilitating the transduction of effector molecule accumulation into a fluorescent output. Online databases enable extensive data mining for the construction of new biosensors. Example database exclusively for the model organism *E. coli* are EcoCyc and RegulonDB (http://EcoCyc.org and http://regulondb.ccg.unam.mx/), corynebacterial and mycobacterial TF and gene regulatory networks are listed at CMRgNet (http://www.lgcm.icb.ufmg.br/cmregnet/home/index.php), while the prokaryotic database of gene regulation (PRODORIC, http://prodoric.tu-bs.de/), the transcriptional regulon database RegPrecise (http://regprecise.lbl.gov/RegPrecise/), and the DNA-binding domain database (DBD, http://www.transcriptionfactor.org) enable a broader research (Abreu et al., 2015; Keseler et al., 2013; Munch et al., 2003; Novichkov et al., 2013; Salgado et al., 2006; Wilson et al., 2008). For many years, whole cell biosensors were applied as detection systems for heavy metals and environmental toxins (Billinton et al., 1998; De Lorenzo et al., 1993; Ikariyama et al., 1997; Sticher et al., 1997). Nowadays, TF-based biosensors are applied as sensor reporter systems to identify improved producers in strain libraries and for the identification of suitable synthetic pathways or cultivation conditions (Dietrich et al., 2013; Rogers and Church, 2016; Snoek et al., 2018). Another recent application is the dynamic feedback regulation of heterologous pathways in response to the intracellular concentration of pathway intermediates (Chou and Keasling, 2013; Xu et al., 2014; Zhang et al., 2016). Furthermore, TF-based biosensors were used to examine the heterogeneity of bacterial cultures at the single cell level and for the isolation of desired characteristics from metagenome libraries (Kiviet et al., 2014; Mustafi et al., 2014; Uchiyama and Miyazaki, 2010; Williamson et al., 2005; Yeom et al., 2018).

1.4.4. Fluorescence activated cell sorting

Fluorescence activated cell sorting (FACS) is a technology that dates back to the 1960s, when the first cytometers were constructed to detect cellular DNA by using intercalating dyes. However, it was not until the 1980s that the development of the cytometer technology in general, and as a side-effect flow sorter development, made a huge leap forward, when the quantification of peripheral blood $CD4^+$ T cells became crucial to follow the development of infection with humane immune deficiency virus (Cossarizza et al., 2017). In modern flow cytometers, cells are focused by means of a laminar envelope stream of sheath buffer, whereby they pass the center of a laser beam individually (Figure 4 A).

By measurement of laser light that is scattered by cells at small angles (Forward scatter characteristics, FSC) and orthogonally (side scatter characteristics, SSC and fluorescence emission), conclusions can be drawn about the relative size (FSC), protein content/surface complexity (SSC) and fluorescence properties of the cell being examined. FSC are typically detected using a photodiode, while SSC and emitted fluorescence are captured with a collecting lens, redirected through an array of dichroic mirrors and bandpass filters and ultimately detected with photomultiplier tubes. Dichroic mirrors are transparent for specific wavelengths and reflect others. Bandpass filters are transparent for a defined band of wavelengths and block all other wavelengths. The combination of dichroic mirrors that reflect all light of smaller wavelength (long-pass dichroic mirrors) and bandpass filters specific for fluorescence light of fluorophores of interest enables the detection of different fluorophores after excitation with one laser (Figure 4 B).

Depending on the used nozzle size and sheath pressure, measurement frequencies of more than 85,000 cells per second (cells/s) are possible (BD Biosciences, Franklin Lakes, NJ, USA). This extraordinary throughput enables the investigation of large cell populations with minimal time expenditure. By using several excitation lasers and filters simultaneously, various fluorescence markers can be detected in parallel. In cytometers equipped accordingly (flow sorters), cells with previously defined properties can be isolated from cultures. For this, the stream is divided into droplets. The vibration of an ultrasonic transducer is transferred into the stream at the point of sample injection into the sheet fluid. The sample stream leaves the flow cell through a constriction called a nozzle. The vibration of the sample stream in combination with the exit of the nozzle leads to a controlled droplet formation. A charge is applied to the liquid stream immediately before to the formation of single droplets occurs, resulting in the formation of charged droplets containing the cells of interest. Subsequently, the charged droplets are deflected into separate vessels in an electric field. In order to minimize the probability of unintentional sorting of unwanted cells, the measuring rate is typically lower than the theoretical maximum of one cell per droplet. For example, in screening applications with the Aria II cell sorter (BD Biosciences, Franklin Lakes, NJ, USA) set up for bacterial samples, the event rate is usually kept at a maximum of 20,000 cells/s. Thus, the practical screening throughput for

the screening of bacterial libraries lies at 1.2×10^6 cells per minute, 7.2×10^7 cells per hour and 1.73×10^9 cells per day, respectively.

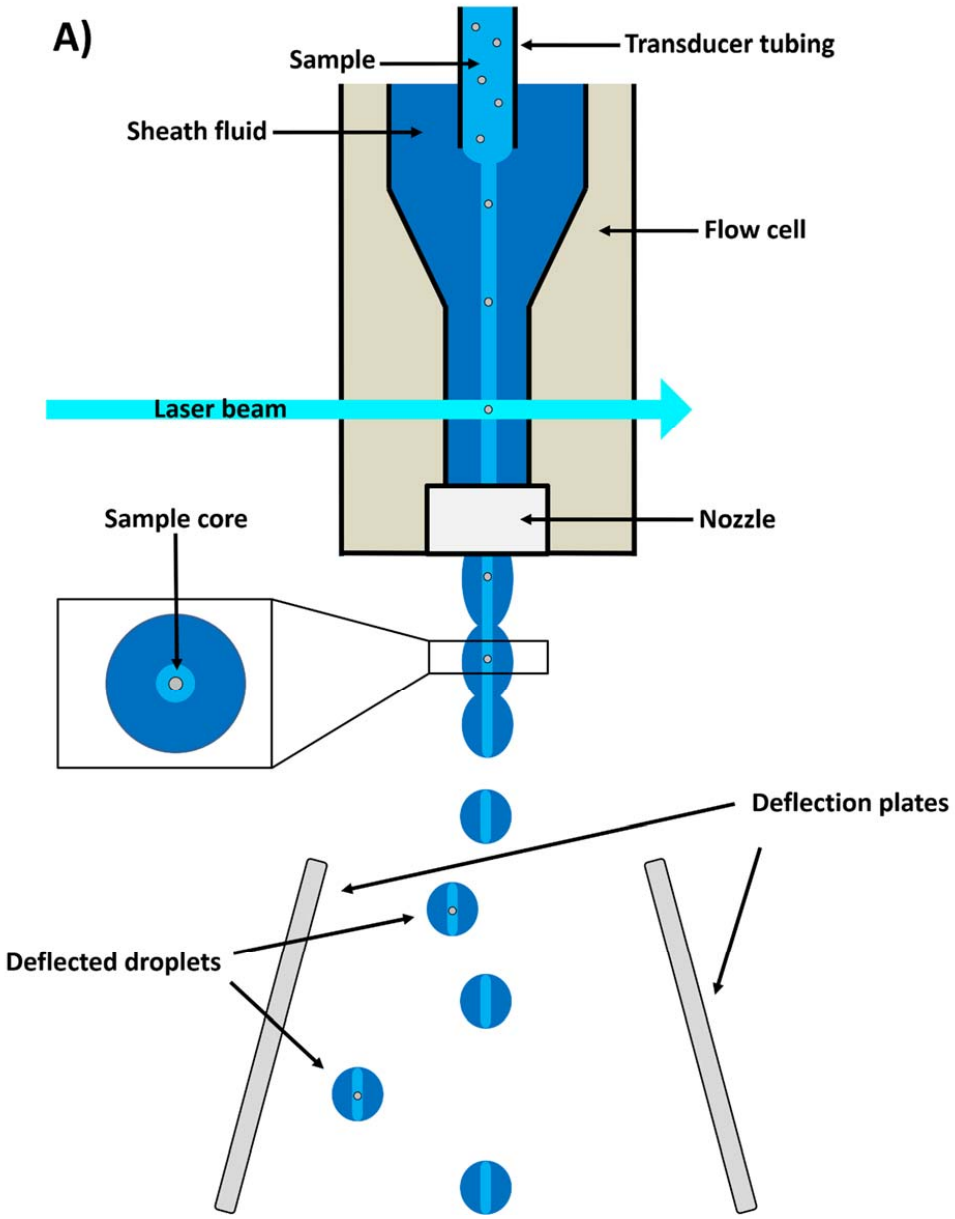

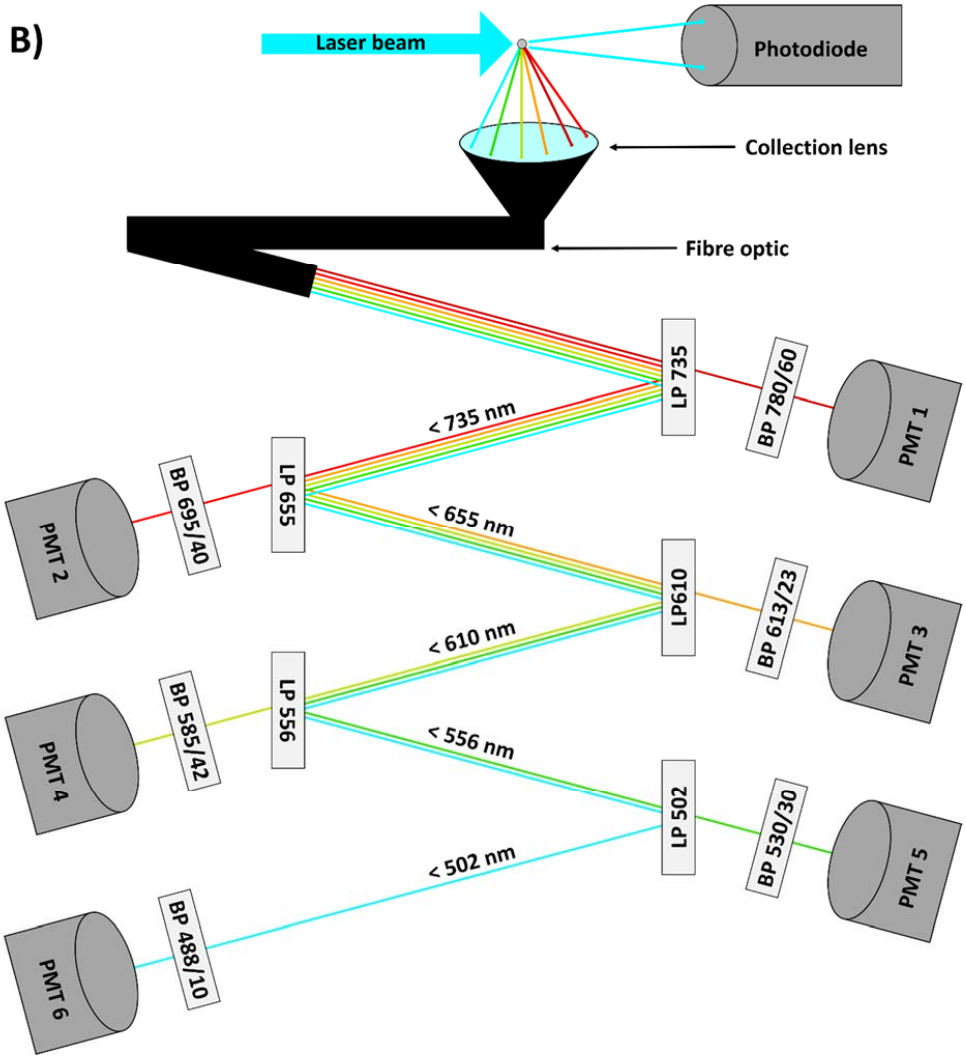

Fig. 4: (A) Overview of hydrodynamic focussing and droplet deflection in flow cell-based flow sorters. The sample is fed centrically into the sheath fluid through an ultrasonic transducer that induces a vibration of constant amplitude and frequency. The pressure of the sheath fluid is higher compared to the pressure of the sample stream, which tapers the sample fluid to a narrow column in the middle of the sheath fluid envelope stream. Thereby, cells (shown as grey circles) in the sample pass through the center of the laser separately. The nozzle narrows the flow to a smaller diameter, together with the applied pressure it determines the later drop diameter. The vibration of the fluid results in the formation of droplets with constant size, shortly after passing the nozzle. An electric field is present between the deflection plates. Target droplets are charged and deflected into a separate target vessel or onto an agar plate. **(B) Overview of laser scatter detection in Arial/II/III flow sorters.** A cell (grey circle) contains fluorophores that emit fluorescence of different wavelengths

(depicted as coloured lines). When the cell passes the laser, small angle scatter is detected as Forward scatter characteristics (FSC) in a photodiode, side scatter characteristic (SSC) and fluorescence emission are captured by a collection lens and redirected using fibre optics into an array of long-pass dichroic mirrors (LP) and band-pass filters (BP). LPs are only transparent for photons with a frequency above their threshold. The threshold (in nanometer) is indicated on the filters in the figure. Photons with a frequency below the LP threshold are reflected. Photons that passed the LP reach the BP. The BPs are transparent for a limited bandwidth (depicted on the BPs in nanometer), further narrowing the frequencies detected by the downstream Photomultiplier Tube (PMT).

For many years, the unparalleled throughput of FACS-based screenings was limited to the engineering of cells for the production of natural fluorophores or to applications coupling the target molecule to synthetic fluorophores. Examples are the production of carotenoids, gramicidin S, polyhydroxyalkanoates, poly(β)-hydroxybutyrate, and lipids (An et al., 1991; da Silva et al., 2009; Fouchet et al., 1995; Gouveia et al., 2009; Nonomura and Coder, 1988; Ukibe et al., 2008; Vidal-Mas et al., 2001). Additionally, changes in cellular physiology due to small molecule production were assessed using a pH-dependent dye enabling the isolation of *S. cerevisiae* with improved lactic acid tolerance and lactic acid production capabilities (Valli et al., 2006, 2005).

However, the combination of biosensors with FACS offers the opportunity to use FACS for the screening of strain and enzyme libraries by coupling MOI formation to a fluorescence output signal. Examples for riboswitch biosensor-based FACS screenings are the directed evolution of a caffeine demethylase, a glutamine-fructose-6-phosphate transaminase, and a haloacid dehalogenase-like phosphatase towards improved activity in *S. cerevisiae* (Lee and Oh, 2015; Michener and Smolke, 2012). TF-biosensor-based approaches were successfully applied to improve the production of branched-chain amino acids or L-lysine in *C. glutamicum* and L-tyrosine, free fatty acids or L-threonine in *E. coli*, respectively, and for the isolation of novel biosensor constructs from a promoter library (Binder et al., 2012; Liu et al., 2015; Mahr et al., 2016, 2015; Mustafi et al., 2012; Xiao et al., 2016). In addition, the suitability for TF biosensor-enabled enzyme engineering could be demonstrated by activity improvement of an alcohol dehydrogenase and the reduction of feedback inhibition in two amino acid kinases and a phosphoribosyl transferase (Schendzielorz et al., 2014; Siedler et al., 2014).

Noteworthy, publications covering the successful application of TF-based biosensors in FACS screening applications other than proof-of-principle applications are largely limited to the abovementioned examples. Nevertheless, an ever-increasing number of biosensors, mostly based on natural TFs, has been developed. The application of these TF-based biosensors in screening campaigns is mostly limited to the use of medium throughput screenings with agar plates or microtiter plate formats. This

discrepancy is probably due in part to the fact that unexpected difficulties in the transition of a constructed and characterized TF biosensor to an application in a FACS-based screening experiment can occur. Furthermore, many molecules of biotechnological interest cannot be detected with currently available regulatory elements. In these cases, a robust approach for the construction of custom-made TF-based biosensors could prove beneficial.

1.5. Microbial production of plant polyphenols

Today, there is a shortage of available TF-based biosensors for FACS-based high-throughput screening. For example, for pharmaceutically interesting compounds produced e.g. by plants. Plants produce a wide array of secondary metabolites that function as pathogen or herbivore repellents, attractants for pollinators and seed-dispersers, signalling molecules for plant-plant and plant-symbiont communication or protectants against ultraviolet radiation or oxidative stress, respectively (Wink, 2018). Terpenoids, alkaloids and polyphenols are the three major classes of secondary metabolites, delimited by their underlying synthesis route. Literature describes more than 200,000 different substances (Yonekura-Sakakibara and Saito, 2009). Three groups of plant polyphenols, namely stilbenes, flavonoids and lignanes, gained great interest due to their strong antioxidant effects, possible health-promoting effects including anti-mutagenic, anti-oxidant, anti-proliferative, anti-atherogenic effects or the reduction of the risk of cardiovascular diseases (Figure 5) (Kallscheuer et al., 2019; Korkina et al., 2011). The isolation of plant natural products from their natural source is often costly as these compounds only accumulate to low concentrations and the extraction of pure substances is difficult due to the presence of many structurally similar molecules. Furthermore, the growth of plant producers is strongly dependent on environmental and regional factors and long growth periods further reduce efficiency. The partial or total chemical synthesis avoids some of the negative aspects of plant extraction, but is usually accompanied by the accumulation of toxic byproducts and solvents and becomes increasingly inefficient with increasing complexity of the synthesized substances (Milke et al., 2018).

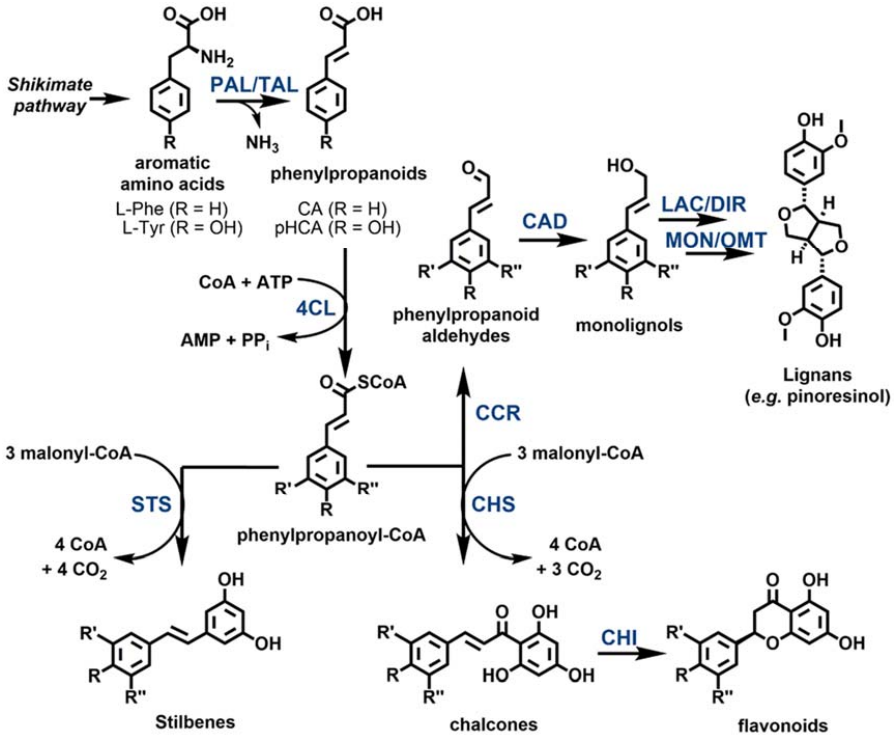

Fig. 5: Biosynthesis of lignans, stilbenes and flavonoids. Initially, nonoxidative deamination of L-Phe and L-Tyr derived from the Shikimate pathway by PAL and TAL yields the corresponding phenylpropanoids CA or pHCA, respectively. The *meta*- and *para*-positions of the benzene ring in phenylpropanoids can be further modified by hydroxylases and OMTs. CoA ligation of phenylpropanoids is performed by 4-coumaryl-CoA ligase (4CL). Phenylpropanoyl-CoA thioesters are converted to stilbenes and chalcones by stilbene synthase (STS) and chalcone synthase (CHS), respectively, via chain elongation of the phenylpropanoyl-CoA starter unit with three malonyl-CoA moieties, followed by circularization. Further isomerization, performed by chalcone isomerase (CHI), transforms chalcones into the corresponding flavonoids. Reduction of phenylpropanoyl-CoAs to the corresponding aldehyde and subsequently to the corresponding alcohol is performed by cinnamoyl-CoA reductase (CCR) and cinnamoyl alcohol dehydrogenase (CAD), respectively. Dirigent proteins (DIRs) arrange monolignols for defined radical dimerization by laccase (LAC), forming a lignan that is further modified by P450 monooxygenases (MONs) and O-methyltransferases (OMTs). **Abbreviations:** CA, *trans*-cinnamic acid; L-Phe, L-phenylalanine; L-Tyr, L-tyrosine; pHCA, *p*-coumaric acid; R, substituent in *para*-position of the benzene ring; R'/R'', substituents in *meta*-positions of the benzene ring.

The microbial production of polyphenols can be achieved by heterologous expression of the respective pathway genes (Figure 5) (Koopman et al., 2012; Santos et al., 2011). Two precursors are essential for the production of stilbenes and flavonoids. The phenylpropanoids *trans*-cinnamic acid (CA) and *p*-coumaric acid (pHCA) formed by the nonoxidative deamination of the aromatic amino acids L-phenylalanine (PHE) and L-tyrosine (TYR), respectively and the availability of the fatty acid synthesis intermediate malonyl-CoA, while the production of lignans only requires phenylpropanoids as precursor molecules (Figure 5). In several studies, malonyl-CoA availability could be increased by supplementation of the antibiotic cerulenin, which inhibits fatty acid synthase (Kallscheuer et al., 2016; Leonard et al., 2008; Milke et al., 2019b). Due to the high price of cerulenin (170 €/5 mg as of May 2019) these approaches lack practicability. Recently, metabolic engineering enabled the repeal of cerulenin dependency by reduction of the carbon flux into the tricarboxylic acid (TCA) cycle, thereby effectively reducing the drain of the malonyl-CoA precursor acetyl-CoA (Milke et al., 2019a). However, the insufficient activity of the aromatic amino acid ammonia lyases (AL) remains a major bottleneck (Eudes et al., 2013; Kallscheuer et al., 2016; Lin and Yan, 2012; Zhou et al., 2016).

1.6. Aims of this thesis

1.6.1. Application of transcription factor-based biosensors for directed enzyme evolution

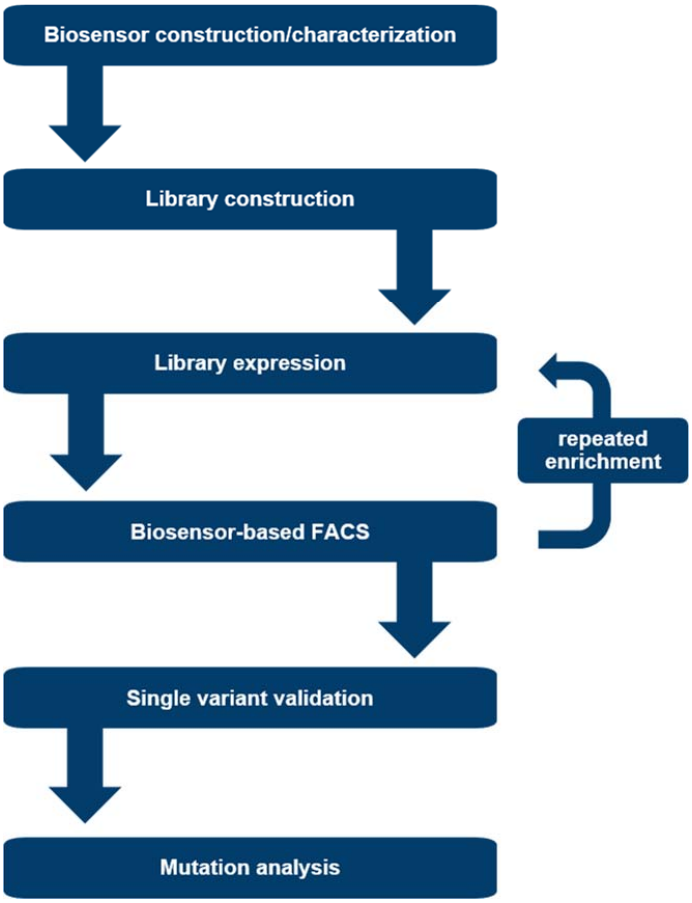

Fig. 6: Application of biosensors in directed enzyme evolutions using repeated enrichment.

The first goal of this thesis is the directed evolution of an aromatic amino acid ammonia lyase originating from the yeast *Trichosporon cutaneum* towards increased activity for future applications in microbial plant polyphenol production. The enzyme was chosen as a starting point due to its high activity in *E. coli* in comparison to aromatic amino acid ammonia lyases from different sources (Jendresen et al., 2015). This includes the construction of a transcription factor-based biosensor for the detection of *trans*-cinnamic acid to enable FACS-based screening. Suitable regulatory elements for the construction of the biosensor must be identified and the biosensor should be characterized regarding its aptitude as a transducer for intracellular CA accumulation into a detectable fluorescent output. The knowledge gained from the characterisation should then be used to develop a FACS-based screening method. The established method should allow for enrichment of improved CA producers with minimal carryover of false-positive variants. A gene library of the target gene constructed by

epPCR was to be screened using the established methodology in order to isolate variants that allow increased CA production. Isolated ammonia lyase variants were intended to be characterized *in vivo* and *in vitro*.

1.6.2. Development of transcription-factor-based biosensors

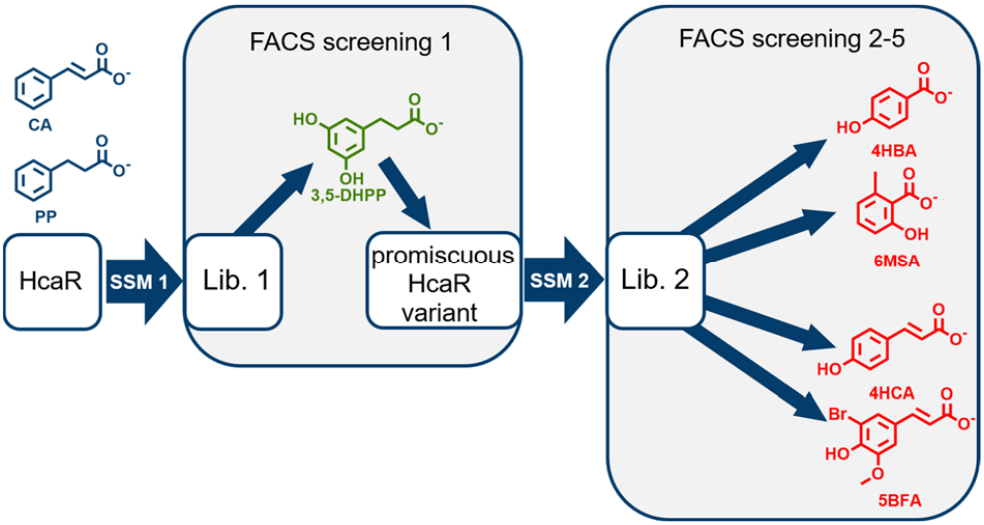

Fig. 7: Schematic representation of the stepwise specificity alteration of the HcaR regulator from *E. coli*. An initial screening campaign (Left grey box) towards a promiscuous variant of the HcaR regulator from *E. coli*, using a transition ligand shown in green. Native ligands of HcaR shown in blue. Additional screening campaigns (Right grey box, partially using the promiscuous HcaR variant as starting point) towards the isolation of regulator variants with increased specificity for one of the four target ligands shown in red. Short, thick blue arrows depict library construction, thinner blue arrows depict screening campaigns. Lib., library; SSM, site-saturation mutagenesis; CA, *trans*-cinnamic acid; PP, phenylpropionic acid; 3,5-DHPP, 3,5-dihydroxyphenylpropionic acid; 4HBA, 4 hydroxybenzoic acid; 6MSA, 6-methylsalicylic acid; 5BFA, 5-bromoferulic acid.

The aim of the second project was the development of a methodology for the rapid construction of transcriptional biosensors for small aromatic compounds of biotechnological interest. The transcriptional biosensor constructed in the first project, pSenCA, should be used as starting point for the construction of an extensive library that enables the direct isolation of specific sensors. To this end, analysis of the 3D structure of the transcriptional regulator HcaR, that is employed in the biosensor, should enable the identification of target residues for a semi-rational mutagenesis approach. Site-saturation mutagenesis (SSM) should be used to construct sensor libraries. Initially, the use of a transition ligand (3,5-dihydroxyphenylpropionic acid), which differs from the native HcaR ligands by hydroxy substitutions of the benzene ring, could enable the identification of key positions for broader ligand acceptance of the pSenCA biosensor. Based on mutations at these key positions, a library could be constructed that contains sensors for various small aromatic compounds. FACS-based screening should be used to screen these libraries for biosensors that are highly specific towards 4-hydroxybenzoic acid (4HBA), 6-methylsalicylic acid (6MSA), pHCA, and 5-bromoferrulic acid (5BFA).

1.7. Key results

Results presented in the chapters 1.7.1 to 1.7.4 are described in more detail in chapter 2.1, while results presented in the chapters 1.7.5 and 1.7.6 are described in more detail in chapter 2.2.

1.7.1. A *trans*-cinnamic acid biosensor

E. coli can catabolize the aromatic compounds phenylpropionic acid (PP) and CA via a dioxygenolytic pathway, which is partly encoded by the *hca* gene cluster. The expression of the *hca* operon, consisting of the genes *hcaEFCD*, coding for a phenylpropionate dioxygenase and *hcaB*, coding for a phenylpropionate dihydrodiol dehydrogenase, is activated by the transcriptional regulator HcaR (Díaz et al., 2001). After binding PP or CA, HcaR undergoes a structural reorganization and as a result HcaR initiates the transcription of the genes of the *hca* operon. The TF gene *hcaR*, controlled by P_{hcaR} and its target promoter, P_{hcaE}, were selected for the construction of the plasmid-based CA biosensor pSenCA. In the presence of intracellular PP or CA, HcaR induces transcription from the P_{hcaE} promoter, resulting in EYFP formation. The biosensors's origin of replication, originating from the broad host range plasmid pBBR1, results in low plasmid copy numbers of five to eight plasmids per cell in *E. coli* (Antoine and Locht, 1992; Jahn et al., 2016). A previous study described a glucose-dependent repression of P_{hcaR} in the exponential phase in both complex and minimal medium. Consequently, glycerol was used in a final concentration of 0.5 % (w/v) in all cultivations (Turlin et al., 2001). To circumvent CA degradation, *E. coli* DH10B Δ*hcaREFCBD* was constructed and used as host strain. In this strain, the biosensor pSenCA exhibits an operational range spanning from 3 µM CA to 300 µM CA. The fold induction in specific EYFP fluorescence is 120-fold. Contrasting, pHCA, supplemented in a concentration of 1 mM to the cultivation medium, triggered only a very low (2-fold) fluorescence response.

1.7.2. Optimization of heterologous gene expression enables CA production and biosensor-mediated product detection in *E. coli*

In a previous study, comparing ALs from diverse origins regarding PAL and TAL activity, the AL originating from *Trichosporon cutaneum* (Xal_{Tc}) had the highest activity with both L-Phe and L-Tyr when expressed heterologously in *E. coli* (Jendresen et al., 2015). Consequently, a synthetic gene coding for Xal_{Tc}, codon optimized for *E. coli* (xal_{Tc}), was used as starting point for the establishment of the *in vivo* evolution methodology. Initially, the widely used T7 expression system was chosen for the heterologous expression of xal_{Tc}. For this, *E. coli* BL21(DE3) was used as host strain carrying both the pSenCA biosensor plasmid and a pETDuet-1 variant with a single multiple cloning site (MCS) containing xal_{Tc}. Here, inducer concentrations widely used for GOI expression with the T7 system (10 µM, 100 µM and 1000 µM IPTG) resulted in an inverse correlation of MOI formation and fluorescence response.

Without inducer addition, the observed fluorescence was maximal, while micromolar quantities (130 µM) of CA were formed from the supplemented phenylalanine. Moreover, screening of an epPCR library of xal_{Tc} without induction of GOI expression resulted in the isolation of 300 cells of which 94 % harboured an expression plasmid without xal_{Tc} gene. Despite the occurrence of these cells already in the original library (~20 %) it was of question how they were enriched to this fraction throughout the FACS-based screening. All isolated cells harbouring an expression plasmid with the xal_{Tc} gene contained mutant XalT variants, but only one variant produced 20 % more CA than cells expressing the original xal_{Tc} gene. As this initial campaign was flawed by the presence of an excess of cells harbouring an empty expression plasmid after FACS sorting, the inferior CA production of 17 of the 18 isolated clones, and the inability to induce the system without losing sensor response, a new approach was initiated.

For this purpose, the L-arabinose (L-Ara)-inducible P_{BAD} system was chosen because of its sensitively titratable expression in combination with minimal basal expression. As host strain, *E. coli* DH10B Δ*hcaREFCBD* pSenCA was used, resulting in the strains *E. coli* DH10B Δ*hcaREFCBD* pSenCA pBAD-xal_{Tc} (CA^+) and *E. coli* DH10B Δ*hcaREFCBD* pSenCA pBAD (CA^-). In contast to other *E. coli* strains, DH10B is not capable of L-Ara metabolization. Characterization of the interplay between the expression level of xal_{Tc} and the resulting pSenCA response revealed that two L-Ara concentrations are suitable for xal_{Tc} expression in combination with a graded fluorescence output, 13 µM and 130 µM. The micromolar operating range bears the risk of saturating the pSenCA biosensor early in the cultivation. For this reason, the selection of a suitable screening time point is essential.

Within seven hours of cultivation, induction of gene expression with 130 µM L-Ara resulted in a sensor response comparable with the maximal possible response of a control strain supplemented with 3 mM CA. This strong fluorescence signal is perfectly suited to enrich CA^+ cells from CA^- cells, since it allows a large signal to noise ratio. Nonetheless, in a screening scenario, it is not possible to distinguish between cells expressing wild-type xal_{Tc} and cells expressing improved xal_{Tc} variants, as the WT allele already results in a saturation of the sensor. On the contrary, the low induction of gene expression using 13 µM L-Ara resulted in a decreased sensor response and thus a lower signal to noise ratio, hindering the distinction of CA^+ cells from CA^- cells at this time. However, it enables a more efficient distinction between cells expressing xal_{Tc} and cells expressing improved variants. Collectively, consecutive rounds of FACS screening, initially with strong *xal* gene expression (130 µM L-Ara) to reliably enrich CA^+ cells from CA^- cells, and then under weak *xal* gene expression conditions (13 µM L-Ara) to enable selection of the best variants within the pool of CA-producing cells was identified as feasible FACS screening strategy.

1.7.3. Prevention of biosensor cross-talk is a prerequisite for any FACS applications using pSenCA

Depending on their chemical structure and charge, small molecules can diffuse across biological membranes. Alternatively, they are taken up by carrier-mediated transport (facilitated diffusion or active transport) (Crane, 1977). In the context of a biosensor-based FACS screening, biosensor cross-talk between producing and non-producing variants would lead to a high number of isolated false-positive variants.

The presence of cross-talk between CA^+ cells and CA^- cells was assayed by cultivating defined mixtures of such cells for 8 h (three hours of xal_{Tc} expression and five hours of cultivation after L-Phe addition) prior to isolation of the top 5 % fluorescent cells by FACS. Of the sorted cells, 30 % were CA^- cells. A possible, but unlikely reason for this finding could be spontaneous mutations in the sensors of the CA^- strains, resulting in constitutive *eyfp* expression in the CA^- cells. A more likely scenario is CA uptake from the supernatant, which in the following activated the biosensors in the CA^- cells. Nevertheless, since none of the isolated CA^- cells showed fluorescence in the absence of CA, it was concluded that the uptake of CA produced by CA^+ cells from the supernatant was the reason for the isolation of false positive CA^- cells.

Co-cultivation of different ratios of CA^+ cells and CA^- cells (20% CA^+/80% CA^-; 50% CA^+/50% CA^-; 80% CA^+/20% CA^-; 100% CA^+/0% CA^-), starting from four different optical densities of the inoculum at 600 nm (iOD_{600}) (0.5; 0.1; 0.02 and 0.004) were performed with induction of xal_{Tc} expression by 13 µM L-Ara. The FACS analysis showed a clear reduction of the fluorescence median with reduction of the iOD_{600}, regardless of the proportion of CA^- cells in the mixture (Figure 8). This observation suggests an expression heterogeneity of the xal_{Tc} gene. At low iOD_{600}, the proportion of CA-producing CA^+ cells do not produce enough CA to induce a fluorescent response of the remaining (non-producing) CA^+ cells. If the iOD_{600} is increased, the quantity of CA-producing cells increases and thus the CA concentration in the supernatant, whereby the non-producing CA^+ cells take up CA from the supernatant and show a fluorescence response. Thereby, absence of xal_{Tc} expression in a portion of CA^+ cells is masked by cross-talk between CA^+ producing cells and non-producing cells at the higher iOD_{600} of 0.1 and 0.02. Accordingly, the number of CA-producing cells in cultivations with a lower proportion of CA^+ cells and with reduced iOD_{600} further decreases, reducing the fluorescence median of the culture even more. This significant reduction in culture fluorescence with reduced iOD_{600} (0.004 and 0.02) results in exposure of a small population with stronger fluorescence. Using FACS, the upper 5 % of the cultures

with 20% CA^+/80% CA^- and 50% CA^+/50% CA^-, cultivated from an iOD_{600} of 0.004 and 0.02, were isolated. The analysis of these cells showed that they were exclusively CA^+ cells. This dilution experiment confirmed the assumption that cross-talk can have a significant influence on the fluorescence distribution. Furthermore, with the help of this experiment, conditions could be identified under which contamination-free isolation of CA^+ cells is possible. In the following, the iOD of 0.004 was used for all FACS experiments in this project. Furthermore, the experiment showed a distinct expression heterogeneity of the P_{araB} promoter used in the *E. coli* strain, which should be further investigated in future projects.

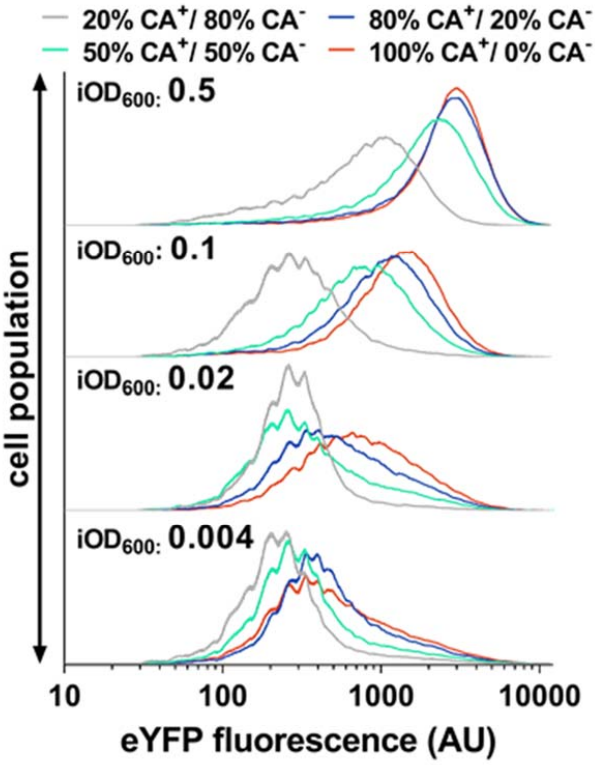

Fig. 8: EYFP fluorescence of various mixed cultures of *trans*-cinnamic acid producing and non-producing *E. coli* strains measured by flow cytometry. Cultivations were performed in yeast nitrogen base medium with 0.5 % glycerol, 25 µg/ml kanamycin and 50 µg/ml carbenicillin. All cultures were started using different inoculums (iOD_{600}) as indicated. All cultivations were performed in the in presence of 13 µM L-arabinose for induction of heterologous xal_{Tc} expression and 3 mM L-Phe as XAL-substrate, which was always added three hours after starting each cultivation. FACS measurements were performed five hours after substrate addition. Strains: CA^+, *E. coli* pSenCA pBAD-xal_{Tc}; CA^-, *E. coli* pSenCA pBAD.

1.7.4. Directed evolution of an ammonia lyase by multistep FACS screening

After appropriate expression and cultivation conditions were identified, the next step was to apply these conditions in a directed enzyme evolution experiment with the aim of isolating Xal_{Tc} variants that show increased activity in *E. coli*. At first, the xal_{Tc} epPCR product was subcloned into the pBAD expression plasmid and transferred into *E. coli* DH10B Δ*hcaREFCBD* pSenCA, yielding *E. coli* DH10B Δ*hcaREFCBD* pSenCA pBAD-xal_{Tc}LIB (CA_LIB). The total library size exceeded 2.3×10^6 variants.

In order to enrich CA-producing variants, the first three FACS enrichment steps (FES) were performed under strong xal_{Tc} induction conditions via supplementation of 130 µM L-Ara. Additionally, during each round of enrichment, the respective *E. coli* cultures were also analyzed by FACS under weak xal_{Tc}-induction conditions (13 µM L-Ara) for comparison and also without any induction of xal_{Tc} expression (no L-Ara) or addition of the Xal_{Tc} substrate L-Phe for identifying false positive variants (bearing spontaneous sensor mutations leading to constitutive *eyfp* expression). In parallel, the average CA titer of the recovered cells was also determined using HPLC. This enabled an additional confirmation of the performed enrichments and prevented use of incorrectly enriched cells for subsequent sorting, which cannot be ruled out if only the fluorescence signal is considered.

In the cause of five FES, the average CA titer increased from 232 µM in the unsorted library to 651 µM (1st FES), 706 µM (2nd FES), 734 µM (3rd FES), 780 µM (4th FES), and 850 µM (5th FES), respectively. Throughout the enrichments under strong xal_{Tc}-induction conditions (1st – 3rd FES), the fluorescence in the false positive controls did not increase notably (Figure 9). As the increase in CA titer was minimal from the 2nd FES to the 3rd FES, the 4th FES was performed with reduced induction of heterologous gene expression (13 µM L-Ara) in order to isolate predominantly variants with increased CA production. In the 3rd FES, most of the cells were presumably already CA producers which promoted a high fluorescence as a reaction to the strong induction with 130 µM L-Ara. Notably, the 4th FES in the presence of 13 µM L-Ara, after recultivation, resulted in the occurrence of a pronounced fluorescent population as shoulder in the histogram of the control FACS experiment without L-Ara or L-Phe supplementation, indicating that false positive variants were enriched under these conditions.

As a control experiment, a second FES of the library in the presence of 13 µM L-Ara (positive sort under weak induction conditions) was conducted (Figure 9, dotted line). As anticipated, the enriched cells exhibited a decreased average CA-titer of 688 µM CA as the false positive variants were further

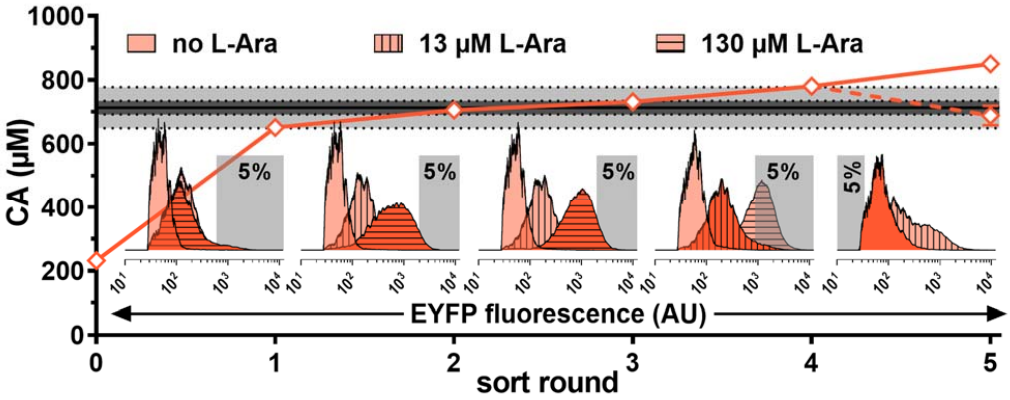

Fig. 9 Stepwise enrichment of improved CA producers from a *xal*$_{Tc}$ library using biosensor-based FACS-screening. The graph illustrates the development of the CA titer of the *xal*$_{Tc}$ library at the culture level relative to the starting variant *E. coli* DH10B Δ*hcaREFCBD* pSenCA pBAD-*xal*$_{Tc}$ (black line). The dark grey shading depicts the CA-titer range of one standard deviation from the starting variant, whereas light grey shading depicts the CA-titer range of three standard deviations. Histograms show the fluorescence distribution of the cultures of each cultivation step without induction of heterologous gene expression (no L-Ara) or substrate addition (no L-Phe) (histogram without pattern), with supplementation of 13 µM L-Ara and 3 mM L-Phe (vertical lines) and 130 µM L-Ara and 3 mM L-Phe added (horizontal lines). Conditions of each step leading to the eventually isolated *xal*$_{Tc}$ variants are highlighted in bright orange. Grey boxes visualize the respective sorting gate set in each enrichment step: steps 1-4, positive sorts (isolation of the top 5 % fluorescent cells); step 5, negative sort (isolation of the lower 5 % fluoresent cells). Cultivations for CA titer determination were always performed in triplicates, error bars depict the respective standard deviations. The dotted orange line demonstrates the development of CA production for an additional round of positive sorting in step five (supplementation of 13 µM L-Ara), which was performed in parallel for comparison. Abbreviations: CA, *trans*-cinnamic acid; L-Ara, L-arabinose; L-Phe, L-phenylalanine.

enriched. Ultimately, a final negative FES was performed without L-Ara and L-Phe supplementation, sorting of the 5 % least fluorescing cells to exclude false positive variants. This increased the average CA titer of the remaining variants to 850 µM upon recultivation.

The average CA titer of the enriched cells after the 5th FES was 20 % increased in comparison to the parent CA^{+} cells. After isolation, 182 variants were individually cultured and characterized with respect to their CA production. Of the 182 variants assayed, 8 % accumulated less CA compared to the starting strain, 16 % had a CA titer equivalent to this control. At the same time, 76 % of the isolated strains exhibited significantly (>10 %) increased titers and the upper 20 % accumulated 30 % to 50 % more CA compared to the starting variant. In order to rule out secondary undesired random mutations as cause for the increased titers, 20 selected (15 variants with highest CA titer in initial single variant screening and 5 randomly chosen clones with at least 10 % higher CA titer than starting variant) expression

plasmids were isolated and retransferred into *E. coli* DH10B Δ*hcaREFCBD.* Comparative cultivation revealed a 10 % - 60 % increased CA and pHCA accumulation from supplemented L-Phe and L-Tyr, respectively. Enzyme assays with seven purified $XalI_{Tc}$ muteins revealed an up to 12 % increased V_{max} and an increased affinity (K_m reduction of up to 20 %) to the substrates L-Phe and L-Tyr, explaining the observed increased CA and pHCA titers in the cultivations.

1.7.5. Identifying a promiscuity hotspot in the transcriptional regulator HcaR

The aim of this project was the expansion of the detection repertoire of the transcriptional biosensor pSenCA towards small aromatic substances of biotechnological interest. The three target ligands *p*-coumaric acid (4HCA), 4-hydroxybenzoic acid (4HBA), and 6-methylsalicylic acid (6MSA) were chosen due to interest in optimizing enzymes of their respective synthesis route in microbial production strains. Due to its extraordinary substitution pattern and the possibility to carry out palladium-catalyzed cross-coupling of its bromine group, the non-natural phenylpropanoid 5-bromoferulic acid (5BFA) was chosen as fourth target ligand (Aschenbrenner et al., 2018). In order to characterize the specificity of pSenCA, *E. coli* DH10B Δ*hcaREFCBD* was transformed with pSenCA and cultivated in presence of 13 different aromatic substances (Figure 10). While the native ligands of HcaR, PP and CA, triggered a 120-fold induction and a 60-fold induction of specific EYFP fluorescence, respectively, of the remaining compounds only 6MSA could induce a weak response (11-fold) (Figure 10).

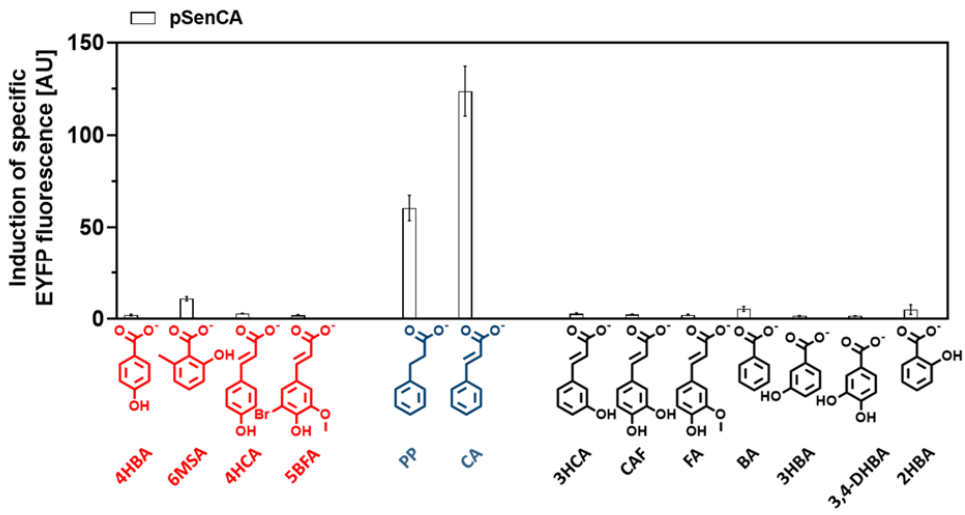

Fig. 10: Response profile of pSenCA to 13 aromatic compounds. The specificity profile of pSenCA is shown for 13 different aromatic compounds. Bars represent the mean fold induction in specific EYFP fluorescence of three biological replicates, error bars depict standard deviation. Structures of the native HcaR ligands PP and CA (shown in blue) all target ligands used for the second FACS screening (shown in red) and structures of ligands used for the characterization of biosensor constructs (black). **Abbreviations:** PP, phenylpropionic acid; CA, *trans*-cinnamic

acid; 3,5DHPP, 3,5-dihydroxyphenylpropionic acid; 4HCA, *p*-coumaric acid; CAF, caffeic acid; FA, ferulic acid; 5BFA, 5-bromoferulic acid; BA, benzoic acid; SA, salicylic acid; 6MSA, 6-methylsalicylic acid; 3HBA, 3-hydroxybenzoic acid; 4HBA, 4-hydroxybenzoic acid; 3,4DHBA, 3,4 dihydroxybenzoic acid.

To extend the ligand acceptance of HcaR, site-saturation mutagenesis (SSM) libraries were subsequently created and screened for variants with altered specificity. As no structural information regarding the ligand binding site or the ligand binding mode of HcaR was available, a homology model of HcaR was constructed using the I-Tasser suite (Roy et al., 2010; Yang et al., 2015; Zhang, 2008). Alignment and structural comparison of HcaR with CatM from *Acinetobacter baylyi* complexed with the ligand muconic acid (PDB code: 3GLB) identified 11 positions in HcaR that are in close proximity of muconic acid. SSM of the identified positions was performed. In a first step towards pSenCA variants with altered specificity, we planned to conduct a screening for HcaR variants that exhibit a less stringent ligand acceptance profile than pSenCA, which would be then engineered towards different aromatic ligands of interest. For this purpose, 3,5-dihydroxyphenylpropionic acid (3,5DHPP) was selected as “transition ligand” that shares structural similarity with the native ligands of HcaR as well as with the target ligands, to isolate such variants with a generally broadened ligand profile (Figure 11). After three consecutive rounds of FES after cultivation of the mixed SSM library in the presence of 3,5DHPP, pSenGeneral, carrying the mutations E101H and V102Y was isolated. pSenGeneral has a broadened ligand acceptance profile in comparison to pSenCA (Figure 11). pSenGeneral was used as template for additional library constructions, targeting a total of 21 positions in the binding domain of HcaR. In addition to the SSM libraries on the basis of pSenCA and pSenGeneral, epPCR libraries were constructed. To enable parallel FACS screening, all libraries were pooled.

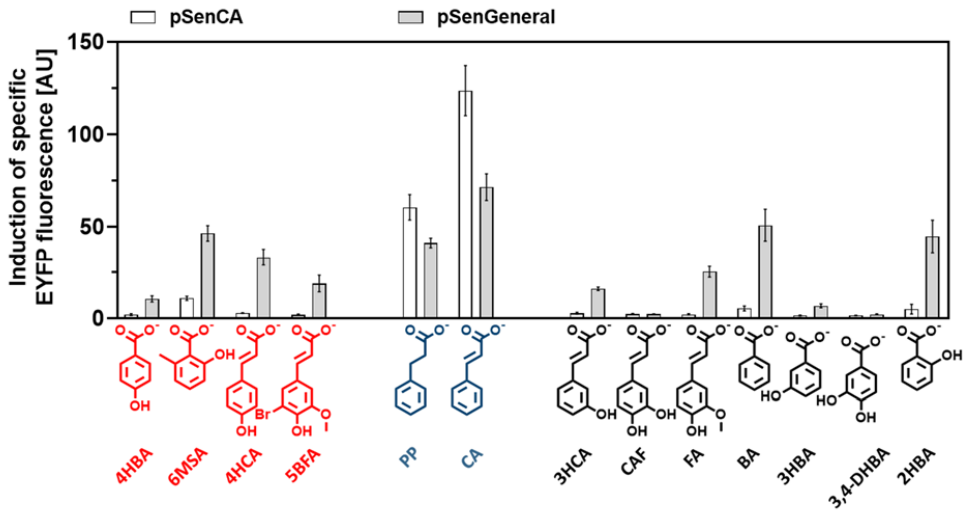

Fig. 11: Response profile of pSenGeneral to 13 aromatic compounds. The specificity profile of pSenCA (white bars) and pSenGeneral (grey bars) is shown for 13 different aromatic compounds. Bars represent the mean fold induction in specific EYFP fluorescence of three biological replicates, error bars depict standard deviation. Structures of the native HcaR ligands PP and CA (shown in blue) and all target ligands used for the second FACS screening (shown in red) and structures of ligands used for the characterization of biosensor constructs (black). **Abbreviations:** PP, phenylpropionic acid; CA, *trans*-cinnamic acid; 3,5DHPP, 3,5-dihydroxyphenylpropionic acid; 4HCA, *p*-coumaric acid; CAF, caffeic acid; FA, ferulic acid; 5BFA, 5-bromoferulic acid; BA, benzoic acid; SA, salicylic acid; 6MSA, 6-methylsalicylic acid; 3HBA, 3-hydroxybenzoic acid; 4HBA, 4-hydroxybenzoic acid; 3,4DHBA, 3,4 dihydroxybenzoic acid; SSM, site-saturation mutagenesis.

1.7.6. Multistep FACS-campaign enables the isolation of biosensors with novel specificities

The combined libraries were screened for biosensor responses to each of the individual target ligands (Figure 10) in a five-step FACS campaign. For this, positive FESs in presence of the respective target ligand were performed to enrich sensor variants with strong fluorescence response, as well as negative FESs without addition of any ligand to remove constitutively fluorescent sensor variants. After five FESs (positive, positive, negative, positive and negative), 184 single clones from each FACS campaign (736 clones) were cultivated in parallel and 24 sensors with the strongest fluorescence induction after target ligand addition were sequenced (96 in total), retransferred and characterized in detail using the set of thirteen different aromatic substances (Figure 10).

The 96 sequenced sensor variants consisted of 31 distinct mutants and exhibited diverse response profiles. Four variants, denoted pSen4HBA, pSen6MSA, pSen4HCA and pSen5BFA showed a strong fluorescence signal in the presence of the respective target ligand, whereas the inducibility of these four sensor variants by other ligands was very limited (Figure 12).

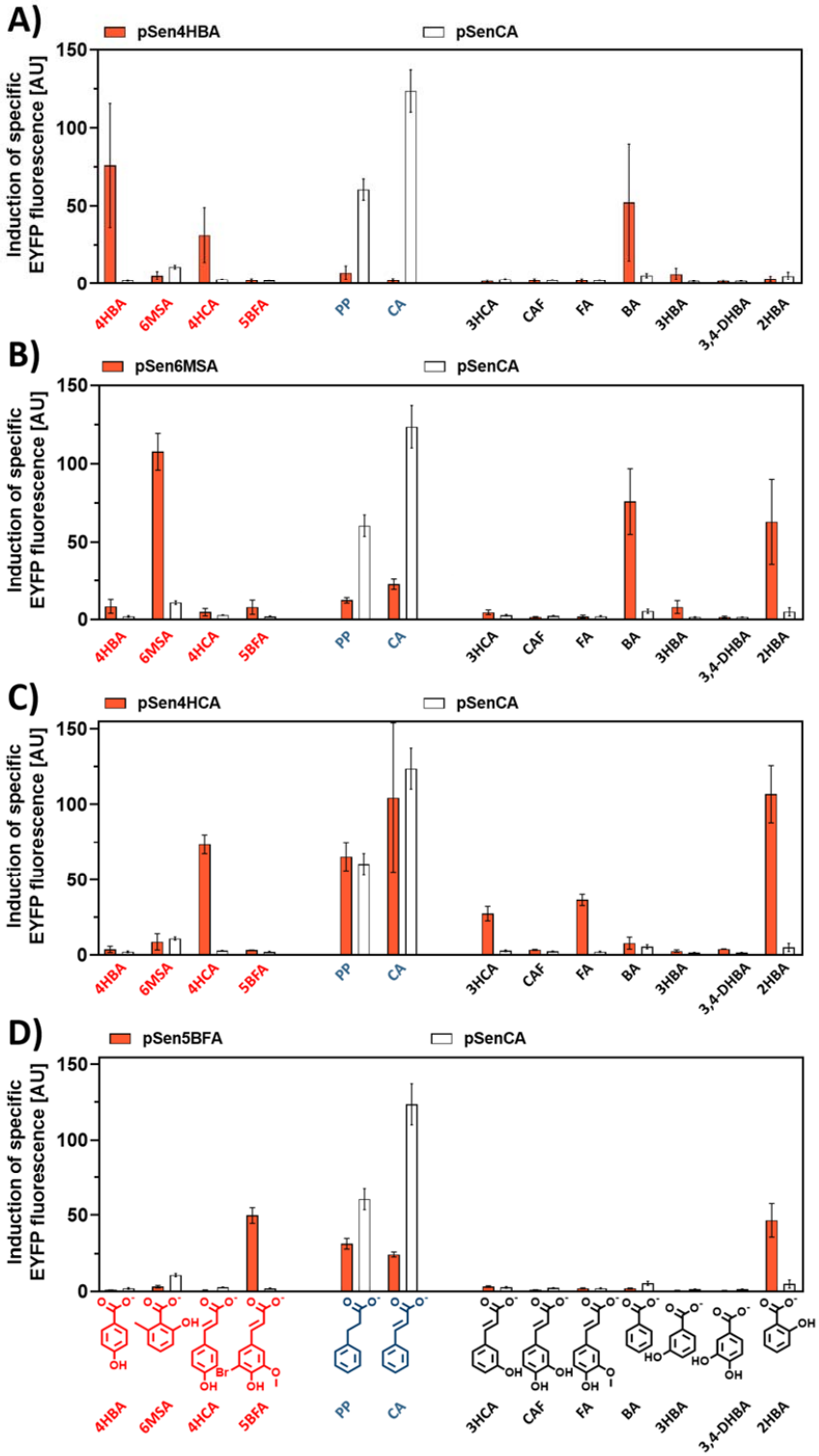
A)
pSen4HBA
pSenCA
Induction of specific EYFP fluorescence [AU]
150
100
50
0
4HBA
6MSA
4HCA
5BFA
PP
CA
3HCA
CAF
FA
BA
3HBA
3,4-DHBA
2HBA
B)
pSen6MSA
pSenCA
C)
pSen4HCA
pSenCA
D)
pSen5BFA
pSenCA

Fig. 12: Specificity profile of sensor variants isolated in the FACS screening campaigns. The specificity profile of pSenCA (white bars) and isolated sensor variants (orange bars) is shown for 13 different aromatic compounds. The sensor variants are pSen4HBA **(A)**, pSen6MSA **(B)**, pSen4HCA **(C)** and pSen5BFA **(D)**, respectively. Bars represent the mean fold induction in specific EYFP fluorescence of three biological replicates, error bars depict standard deviation. Structures of the native HcaR ligands PP and CA (shown in blue) and all target ligands used for the second FACS screening (shown in red) and structures of ligands used for the characterization of biosensor constructs (black) are shown below the diagrams. **Abbreviations:** PP, phenylpropionic acid; CA, *trans*-cinnamic acid; 3,5DHPP, 3,5-dihydroxyphenylpropionic acid; 4HCA, *p*-coumaric acid; CAF, caffeic acid; FA, ferulic acid; 5BFA, 5-bromoferulic acid; BA, benzoic acid; SA, salicylic acid; 6MSA, 6-methylsalicylic acid; 3HBA, 3-hydroxybenzoic acid; 4HBA, 4-hydroxybenzoic acid; 3,4DHBA, 3,4 dihydroxybenzoic acid; SSM, site-saturation mutagenesis.

1.8. Conclusions and Outlook

In the course of the application of the CA biosensor pSenCA in combination with FACS for the directed evolution of an AL from *T. cutaneum*, several technical obstacles were identified and solutions were worked out, which should be considered in future screening campaigns employing TF-based biosensors and FACS.

More precisely, a tightly regulated, titratable expression system (*e.g.* the L-arabinose-inducible P_{araBAD} system) should be used for expression of the target gene to enable the lowest possible basal fluorescence, thereby increasing the signal to noise ratio. Furthermore, if the MOI readily diffuses over the membrane/cell wall or is transported into the culture medium, prevention of cross-talk is crucial, whereby a low initial OD_{600} of the culture and the earliest possible screening time points are imperative. In order to investigate the presence of cross-talk, co-cultivation of producers and non-producers should be carried out. The examination of the mixed culture by means of FACS provides a precise result. In between FESs, control experiments for successful enrichment, using chromatographic or spectroscopic methods, should always be performed. In order to maximize comparability, all FES steps (and control cultures) should be stored in the form of an aliquot (*e.g.* 200 µl in PCR tubes) glycerol cultures. This prevents unwanted thawing and freezing effects as every aliquot is only used once.

More specific, the established methodology could also be applied to further optimize Xal_{Tc}. For this purpose, the identified mutational hot spots contributing to activity of the yeast enzyme in the microbial host, could be saturated in parallel. This can be achieved by using a combination of SSM and overlap extension PCR or by using a novel site-directed mutagenesis/SSM approach facilitating the parallel SSM of three codons at spatially separated positions in the target genes (Site-Directed Mutagenesis PLUS System, supplied by Geneart). The resulting library would contain variants that cannot be generated in an epPCR library-based approach due to the inherent codon bias of epPCR (Neylon, 2004). Furthermore, possible synergistic effects of the mutations could be identified following this approach without the need to construct all possible variants manually.

For future AL screening campaigns, the host strain could be optimized for very low L-arabinose induction by chromosomal integration of *araE,* coding for a high affinity L-arabinose transporter protein, under control of a constitutive promoter. By doing this, the observed population heterogeneity with regard to target gene expression in the presence of low L-arabinose concentrations could be overcome (Khlebnikov et al., 2001, 2000).

Despite the increased activity of the Xal_{Tc} mutants, the K_m of all generated variants for L-Phe is in the low mM range, which might limit the overall plant pathway performance *in vivo*. In order to reduce the K_m of Xal_{Tc}, reduced L-Phe concentrations could be used in future screenings.

Similar to the first project, the second project also opened up interesting perspectives for future biosensor applications. First, the constructed biosensors for 4HBA, 6MSA and 4HCA offer the possibility to instantly develop FACS-based screens without further modification of the biosensor variants. This concerns both the provision of precursor molecules as well as the formation of the final product. For example, pSen6MSA can be used to screen 6-methylsalicylic acid polyketide synthase libraries for variants with improved activity in *E. coli.* Since a higher substrate availability will most likely also result in an increased product formation, it should also be possible to screen strain libraries created by genome mutagenesis for increased malonyl-CoA availability. The same principle is applicable for pSen4HBA that could be used to screen chorismate pyruvate lyase (4-hydroxybenzoate synthase) libraries as well as strain libraries for increased shikimate pathway activity or pyruvate availability. The third new biosensor, pSen4HCA, detects both Xal_{Tc} products, CA and 4HCA, in contrast to the original pSenCA sensor, that only accepts CA. This enables new possibilities for the selective directed AL evolution towards PAL or TAL activity. By supplementation of the educt for the unwanted activity (*e.g.* L-Tyr for unwanted TAL activity) and sorting of cells with low fluorescence, ALs with TAL activity can be excluded. In the following FES, L-Phe could be supplemented while performing a positive sort. Toggling between these two modes should result in the enrichment of PALs with high activity and low residual TAL activity. The fourth biosensor, pSenBFA represents a starting point for the construction of future biosensors for non-natural monolignols.

In addition to the isolated biosensors, the sensor libraries created in the course of this work most likely also contain various other sensors for further aromatics, which can be isolated in additional future screenings by following the established method. The construction of combinatorial libraries of the identified positions V97, P98, S99, A100, V227, T228, M245 and N246 could further increase the versatility of this sensor library for the isolation of custom-made biosensors. Besides that, the use of transition ligands for the construction of sensor libraries could be extended to develop transcriptional biosensors for other substance classes of biotechnological interest.

2. Publications

2.1. Displaced by deceivers - Prevention of biosensor cross-talk is pivotal for successful biosensor-based high-throughput screening campaigns

2.1.1. Displaced by deceivers - Manuscript

ACS Synthetic Biology
Cite This: ACS Synth. Biol. 2019, 8, 1847−1857
Research Article
pubs.acs.org/synthbio

Displaced by Deceivers: Prevention of Biosensor Cross-Talk Is Pivotal for Successful Biosensor-Based High-Throughput Screening Campaigns

Lion Konstantin Flachbart,[†] Sascha Sokolowsky,[†] and Jan Marienhagen*[,†,‡]

[†]Institute of Bio- and Geosciences, IBG-1: Biotechnology, Forschungszentrum Jülich, D-52425 Jülich, Germany
[‡]Institute of Biotechnology, RWTH Aachen University, Worringer Weg 3, D-52074 Aachen, Germany

Supporting Information

ABSTRACT: Transcriptional biosensors emerged as powerful tools for protein and strain engineering as they link inconspicuous production phenotypes to easily measurable output signals such as fluorescence. When combined with fluorescence-activated cell sorting, transcriptional biosensors enable high throughput screening of vast mutant libraries. Interestingly, even though many published manuscripts describe the construction and characterization of transcriptional biosensors, only very few studies report the successful application of transcriptional biosensors in such high-throughput screening campaigns. Here, we describe construction and characterization of the *trans*-cinnamic acid responsive transcriptional biosensor pSenCA for *Escherichia coli* and its application in a FACS based screen. In this context, we focus on essential methodological challenges during the development of such biosensor-guided high-throughput screens such as biosensor cross-talk between producing and nonproducing cells, which could be minimized by optimization of expression and cultivation conditions. The optimized conditions were applied in a five-step FACS campaign and proved suitable to isolate phenylalanine ammonia lyase variants with improved activity in *E. coli* and *in vitro*. Findings from this study will help researchers who want to profit from the unmatched throughput of fluorescence-activated cell sorting by using transcriptional biosensors for their enzyme and strain engineering campaigns.

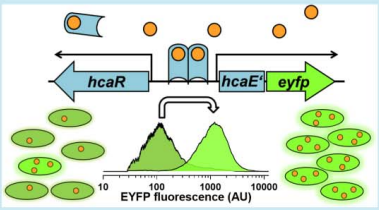

KEYWORDS: *transcriptional biosensor, library screening, product sensing, fluorescence-activated cell sorting, protein engineering, directed evolution*

Genetically encoded biosensors represent powerful tools in strain and protein engineering as they enable the high-throughput screening of large variant libraries by linking an often inconspicuous production phenotype to a readily detectable output signal.[1] In the past years, different biosensor concepts were introduced, namely, transcription factor (TF)-based biosensors, Förster resonance energy transfer (FRET) biosensors, as well as RNA-based biosensors.[2] Especially TF-based biosensors received a lot of attention as they are easy to construct and result in a relatively strong fluorescence signal.[3] Biosensors of this type take advantage of transcriptional regulator proteins, which specifically bind the molecule of interest and drive or repress expression of a reporter gene (usually encoding for a fluorescent protein or a selection marker). Examples for the application of these TF-based sensor-selector systems include screening campaigns for identifying improved producers from mutant libraries and selecting for suitable synthetic pathway variants.[4,5] Additionally, biosensors find application in synthetic sensor-actuator systems to enable the dynamic feedback regulation of heterologous pathways.[6−8] In combination with fluorescence activated cell sorting (FACS), such transcriptional biosensors unleash their true potential as they allow for ultrahigh throughput screening on single cell level and isolation of producing single cells from very large libraries.[9−13]

However, when considering the larger number of biosensors constructed over the past couple of years, studies combining transcriptional biosensors with FACS are rather scarce. For the most part, published biosensor screening applications are limited to agar plate or microtiter plate screenings, or the constructed and characterized biosensors are not put to any use at all. The transition from biosensor construction/characterization to meaningful applications involving FACS could be hampered by several factors. For instance, the engineered organism carrying the biosensor might provide a good fluorescence response in cultures, but give only a heterogeneous fluorescence response at the single cell level

Received: April 3, 2019
Published: July 3, 2019

DOI: 10.1021/acssynbio.9b00149
ACS Synth. Biol. 2019, 8, 1847−1857

prohibiting any FACS-based screening.[14] In addition, diffusion of the target metabolite from strong producing cells to weak or nonproducing strain variants could result in the isolation of mainly false-positive clones, demanding an individual and thus laborious and expensive characterization of many individual clones.

In this manuscript, we present suitable strategies by which these causes of failure can be efficiently tackled to yield robust and reliable biosensor-based FACS-ultrahigh-throughput screenings for protein and metabolic engineering campaigns. In this context, we describe construction and application of a transcriptional phenylpropanoid biosensor, which was used to engineer an ammonia lyase in *E. coli*.

MATERIALS AND METHODS

Bacterial Strains, Plasmids, Media, and Growth Conditions. All bacterial strains and plasmids used in this study and their relevant characteristics are listed in Supplementary Table S1. For recombinant DNA work and library construction, *E. coli* DH5α and *E. coli* TOP10 (Thermo Fisher Scientific, Waltham, MA, USA) were used, respectively. For recovery after electroporation, SOC-medium (super optimal broth with catabolite repression) was used (20 g/L tryptone, 5 g/L yeast extract, 0.6 g/L NaCl, 0.2 g/L KCl, 10 mM $MgCl/MgSO_4$, and 20 mM glucose, pH 7). All strains were routinely cultivated at 37 °C on plates or in liquid culture in either Lysogeny broth (LB) medium (10 g/L tryptone, 10 g/L NaCl, and 5 g/L yeast extract) or Yeast nitrogen base (YNB) medium containing carbenicillin (50 μg/mL) or kanamycin (25 μg/mL), where appropriate.[15] For the preparation of 1 l of YNB medium, 100 mL of ten-times-concentrated YNB, containing 5.1% (cultivations 48 well and 96 well microtiter plates) or 12.6% (protein expressions) glycerol was added to 900 mL YNB base medium. YNB base medium contained 6 g/L K_2HPO_4, 3 g/L KH_2PO_4, and 10 g/L 3-(*N*-morpholino)propanesulfonic acid (MOPS), pH 7. As *E. coli* DH10B is leucine auxotroph, L-leucine was supplemented to a final concentration of 2 mM for all cultivations using YNB-medium.[16]

Online monitoring of growth and formation of fluorescence was performed in 48 well microtiter FlowerPlates (FPs) using the BioLector cultivation system (m2p-laboratories GmbH, Baesweiler, Germany).[17,18] Formation of biomass was recorded as the backscatter light intensity (wavelength 620 nm; signal gain factor 25). The enhanced yellow fluorescence protein (EYFP) fluorescence was measured as fluorescence emission at 532 nm (signal gain factor of 30) after excitation at a wavelength of 510 nm. Specific fluorescence was calculated as 532 nm fluorescence per 620 nm backscatter using Biolection software version 2.2.0.6 (m2p-laboratories GmbH, Baesweiler, Germany).

The *trans*-cinnamic acid (CA) and *p*-coumaric acid (pHCA) production assays were performed using single colonies from fresh plates or 10 μL from a fresh glycerol culture to inoculate LB medium in 96 well V-bottom plates (BRAND GMBH + CO KG, Wertheim, Germany) with a total volume of 200 μL per well. Precultures were cultivated for 18 h (single colonies) or 8 h (inoculation from glycerol culture) in a Multitron Pro HT Incubator (Infors AG, Bottmingen, Suisse, 37 °C, 900 rpm, 75% humidity, 3 mm throw). Of this preculture, 100 μL were used to inoculate 900 μL YNB medium followed by 20 h incubation in the same Incubator. Subsequently, YNB precultures were cooled to 25 °C and 100 μL preculture were used to inoculate 900 μL YNB medium containing 130 μM L-arabinose and either 3 mM L-phenylalanine or 3 mM L-tyrosine, respectively. After 16 h of cultivation (25 °C, 900 rpm, 75% humidity, 3 mm throw), product titers were determined.

Molecular Biology. *Standard Techniques for Molecular Cloning.* Polymerase chain reactions, DNA restrictions and ligations were performed according to standard protocols.[19] Enzymes were obtained from Thermo Fisher Scientific (Waltham, MA, USA) and used following the manufacturer's recommendations. Genes were amplified by PCR using Pfu UltraII polymerase (Agilent, Santa Clara, CA, USA). Cloning of the amplified PCR products was performed using restriction enzyme digestion and subsequent ligation or Gibson assembly.[20] Synthesis of oligonucleotides and sequencing of DNA using Sanger sequencing were performed by Eurofins MWG Operon (Ebersberg, Germany). All oligonucleotides used in this study are listed in Supplementary Table S2.

Error-Prone PCR and Ammonia Lyase Library Construction. The xal_{Tc} gene was amplified from plasmid pCBJ296 using the Clontech Diversify kit (Takara Bio Europe, Saint-Germain-en-Laye, France) incorporating 2.3 or 4.6 mutations/kb and assembled with pBAD plasmid, previously amplified using PCR, using Gibson assembly. The resulting plasmid library was purified and transformed into One Shot TOP10 electrocompetent *E. coli* cells according to the manufacturer's recommendations. Plasmid preparations were performed using Midi kits according to the manufacturer's recommendation (Qiagen, Hilden, Germany). The plasmid library was retransformed into *E. coli DH10B* Δ*hcaREFCBD* pSenCA. Preparation of electrocompetent cells and electroporation of the plasmid library was performed as described elsewhere.[21]

Chromosomal Deletions. Deletion of chromosomal genes was performed using Lambda (λ)-Red recombineering.[22,23] Here, the recently published plasmid pSIJ8 was used according to the published protocol instead of the original two plasmid approach described by Datsenko and Wanner.[24,25]

Fluorescence Activated Cell Sorting (FACS). Single-cell fluorescence was determined and cell sortings were performed using a BD FACSAria II cell sorter (BD Biosciences, Franklin Lakes, NJ, USA) equipped with a 70 μm nozzle and run with a sheath pressure of 70 psi. A 488 nm blue solid laser was used for excitation. Forward-scatter characteristics (FSC) were recorded as small-angle scatter and side-scatter characteristics (SSC) were recorded as orthogonal scatter of the 488 nm laser. A 502 nm long-pass and 530/30 nm band-pass filter combination enabled EYFP fluorescence detection. Prior to data acquisition, debris and electronic noise were excluded from the analysis by electronic gating in the FSC-H against SSC-H plot. Another gating step was performed on the resulting population in the FSC-H against FSC-W plot to exclude doublets. Fluorescence acquisition was always performed with the population resulting from this two-step gating. For sorting applications, cells were diluted to an OD_{600} below 0.1 where necessary using YNB base buffer, and 200 000 cells were sorted into 5 mL reaction tubes (Eppendorf AG, Hamburg, Germany), prefilled with 3 mL LB medium using an in-house built adapter for 5 mL reaction tubes that was described earlier.[26] To minimize residual sheath fluid in the recovery tube, sorted cells were centrifuged (10 min, 3000*g*, 4 °C), after removal of 3 mL supernatant and addition of 4.5 mL fresh LB medium, regeneration was performed (16 h, 37 °C, 170 rpm.) Sort precision was always set to purity setting and

DOI: 10.1021/acssynbio.9b00149
ACS Synth. Biol. 2019, 8, 1847−1857

the total event rate while sorting never exceeded 16 000 events per second. FACSDiva 7.0.1 (BD Biosciences, San Jose, USA) was used for FACS control and data analysis. FlowJo for Windows 10.4.2 (FlowJo, LLC, Ashland, OR, USA) and Prism 7.04 (GraphPad Software, San Diego, CA, USA) were used to produce high-resolution graphics of FACS data.

Protein Purification and Enzyme Assays. Selected Xal_{Tc} encoding genes (xal_{Tc}) were recloned to enable their expression as fusion proteins with an N-terminal hexa histidine (His6)-tag in *E. coli* DH10B Δ*hcaREFCBD*. Single colonies were used to inoculate 5 mL LB and grown at 37 °C for 4 h. Afterward, 500 μL culture was used to inoculate 15 mL YNB (0.51% glycerol as carbon source) precultures. After 16 h of cultivation at 37 °C, these precultures were used to inoculate 100 mL YNB (1.2% glycerol as carbon source) cultures to an OD_{600} of 0.2, which were cultivated (2 h, 37 °C, and 130 rpm) prior to the addition of L-arabinose to a final concentration of 1.3 mM. Gene expression was performed (20 h, 25 °C, and 130 rpm) and cells were harvested (15 min, 4000*g*, 4 °C). After resuspension in 15 mL sonication buffer (50 mM Tris-HCl, 500 mM NaCl, 10% glycerol, pH 7.5) cells were disrupted using an ultrasonic cell disruptor (Branson Ultrasonics Corporation, Danbury, CT, USA, eight sonication cycles of 30 s, 4 °C, duty cycle 34 and output control 8). From this, crude extracts were prepared by centrifugation in an Avanti J25 centrifuge (Beckmann Coulter Life Sciences, Indianapolis, IN, USA. 19 000 rcf, 45 min, 4 °C using a JA25.5 rotor). The supernatant was applied to a gravity flow column filled with Nickel-nitrilotriacetic acid (Ni-NTA) affinity agarose (Qiagen, Hilden, Germany, 1 mL bed volume). Protein loaded onto the column was washed subsequently with 10 mL sonication buffer and 10 mL wash buffer (sonication buffer with 30 mM imidazole) prior to elution with 3 mL elution buffer (sonication buffer with 300 mM imidazole) in 500 μL fractions. Protein containing fractions were pooled and the protein solution was transferred to a hydrated Slide-A-Lyzer dialysis cassette (Thermo Fisher Scientific, Schwerte, Germany, molecular cutoff of 10 kDa) and placed in 1 L dialysis buffer/assay buffer (50 mM Tris-HCl, pH 7.5 at 30 °C, with 150 mM NaCl and 10% glycerol). Dialysis was performed (20 h, 4 °C, 30 rpm) and enzyme assays were always performed directly after protein purification.

Enzyme assays were performed in 96 well plates with UV-transparent, flat bottom (Corning, New York, USA) in a Tecan M1000 plate reader (Tecan Group, Maennedorf, Switzerland), by following the increase in absorbance at 276 nm (CA) or 310 nm (pHCA). Twenty μg purified enzyme was transferred to each well and warmed to 30 °C for 60 s. Directly afterward, the substrate was added to a final volume of 200 μL using an E4XLS 100−1200 μL multichannel pipet (Rainin Mettler-Toledo, Giessen, Germany, three mixing steps, 100 μL mixing volume). Product formation was linear in the 80 s used to determine the initial product formation rate and proportional to the protein concentration used. No product formation was detected in absence of substrate or purified enzyme.

Chemical Analyses. All standards were purchased from Sigma-Aldrich (St. Louis, MO, USA). CA and pHCA concentrations in cell-free cultures were determined using high performance liquid chromatography (HPLC) 1260 Infinity system equipped with an Infinity Diode Array Detector module (Agilent, Santa Clara, CA, USA). For this, 250 μL culture broth were centrifuged in 96 well V-bottom plates (BRAND GMBH + CO KG, Wertheim, Germany) in a Heraeus Multifuge X3 centrifuge (Heraeus, Hanau, Germany, 30 min, 6000*g* and 8 °C) and 200 μL supernatant was transferred to a new 96 well V-bottom plate and directly applied to the HPLC (8 °C sample chamber temperature). LC separation of 2 μL samples was carried out with a Kinetex 1.7u C18 100-Å-pore-size column (Phenomenex, Torrance, CA, USA, 50 mm by 2.1 mm [internal diameter], 40 °C). For elution, 2% acetic acid (solvent A) and acetonitrile supplemented with 2% acetic acid (solvent B) were used as the mobile phases at a flow rate of 1 mL/min. A gradient was used, where the amount of solvent B was changed over the course of analysis (min 0 to 5, 15% to 90%; minute 5 to 5.5, 90% to 15%). CA and pHCA were detected by determining the absorbance at 295 and 310 nm, respectively, and concentrations were calculated using an appropriate standard curve.

Bioinformatic Methods. Dose−response data of the pSenCA biosensor construct was fit using the [Agonist] *vs* response function (variable slope) of Prism 7.04 (GraphPad Software, San Diego, CA, USA) with a constraint of the minimal fold induction (μ_{min}) to 1.

$$\mu(I) = \mu_{min} + \frac{I^h \times (\mu_{max} - \mu_{min})}{(I^h + EC50^h)}$$

μ, fold induction (also referred to as induction factor); I, inducer concentration; h, Hill coefficient/Hill slope; EC50, inducer concentration resulting in an induction of 50% μ_{max}.

For the DNA sequence analysis of isolated xal_{Tc} variants, all DNA sequences obtained from Eurofins MWG Operon were aligned with the original xal_{Tc} sequence for identifying single nucleotide polymorphisms using the Clonemanager Professional software, version 9.51 (Scientific & Educational Software, Denver, CO, USA).

RESULTS

Construction and Characterization of the *trans*-Cinnamic Acid Biosensor pSenCA. In bacteria, plants and fungi, ammonia lyases catalyze the nonoxidative deamination of the aromatic amino acids L-Phe (then best referred to as phenylalanine ammonia lyases, PALs; EC 4.3.1.24) and L-Tyr (then best referred to as tyrosine ammonia lyases, TALs; EC 4.3.1.23) yielding the phenylpropanoids *trans*-cinnamic acid (CA) or *p*-coumaric acid (pHCA), respectively.[27] This reaction represents the committed step in the biosynthesis of biotechnologically and pharmaceutically interesting polyphenols such as flavonoids, stilbenes, and lignans.[28,29] The biotechnological production of plant polyphenols using microorganisms requires the functional implementation of whole plant pathways into the producing cells.[30,31] In the context of engineering microorganisms for this purpose, generally low PAL- and TAL-activities were identified to be limiting the overall performance of the heterologous pathway in the respective microbial hosts.[32−35]

Driven by the motivation to engineer a PAL/TAL-enzyme toward increased activity for future applications in microbial plant polyphenol production, a biosensor for *trans*-cinnamic acid (CA) was designed and constructed. *E. coli* can catabolize a broad range of aromatic compounds including phenylpropionic acid (PP) and phenylpropanoids such as CA, *via* a dioxygenolytic pathway, which is partly encoded by the *hca* gene cluster.[36] Transcription of the *hca* cluster is induced by HcaR, which is a LysR type transcriptional regulator (LTTR),

DOI: 10.1021/acssynbio.9b00149
ACS Synth. Biol. 2019, 8, 1847−1857

in the presence of PP or CA.[37] Therefore, HcaR and its target promoter, P_{hcaE} were selected for the construction of the plasmid-based CA biosensor pSenCA. The biosensor pSenCA harbors the regulator gene *hcaR*, under control of its native promoter, P_{hcaR}, the target promoter of HcaR, P_{hcaE}, and the first 45 bp of *hcaE* (*hcaE'*) transcriptionally fused to the *eyfp*-gene encoding for the enhanced yellow fluorescent protein (EYFP) (Figure 1A). This translational fusion was designed and constructed, because previous experiments with other regulator/promoter combinations showed that the interplay between the promoter and the 5'-end of the original open reading frame, which has been fine-tuned by evolution, enhance the overall biosensor response.[11] Earlier work on the *hca* operon showed strongly reduced expression of *hcaR* in cultivations with glucose as carbon and energy source, as the expression of *hcaR* is subject to catabolite repression.[38,39] Consequently, glycerol was used as sole carbon and energy source, resulting in a strong and homogeneous fluorescence response upon CA supplementation. To circumvent degradation of CA over the course of cultivation, the *hca* operon was subsequently deleted in *E. coli* DH10B, resulting in strain *E. coli* DH10B Δ*hcaREFCBD*. Cultures of *E. coli* DH10B Δ*hcaREFCBD* pSenCA (hereafter referred to as *E. coli* pSenCA), were supplemented with CA and also pHCA at different concentrations ranging from 1 μM to 1000 μM. The dose−response curve for CA was sigmoidal, with an operational range stretching from 3 μM CA to 300 μM CA thus spanning 2 orders of magnitude (Figure 1 B). The inducer concentrations resulting in 5% (EC5) and 95% (EC95) of the maximal fold induction are 7.5 μM CA and 126 μM CA, respectively. The maximal fold induction determined in specific EYFP fluorescence was 120-fold. In contrast, presence of pHCA in the culture medium triggered a minor fluorescence response (2-fold) of pSenCA, showing that this biosensor is indeed CA-specific.

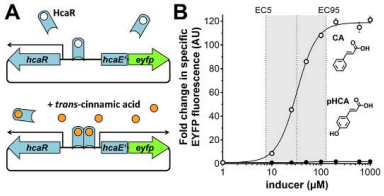

Figure 1. *trans*-Cinnamic acid biosensor pSenCA. (A) Schematic of the sensor principle. Upon binding of supplemented CA, the HcaR regulator undergoes conformational changes that enable binding to the target promoter P_{hcaE} and activation of *hcaE'* and *eyfp* expression. (B) Dose−response plot, CA (circles) or pHCA (filled circles) were supplemented extracellularly in eight different concentrations ranging from 1 to 1000 μM. The biosensor response after 24 h is shown as fold change in specific EYFP fluorescence in comparison to the background fluorescence (no inducer). Error bars represent standard deviations calculated from three biological replicates. CA, *trans*-cinnamic acid; pHCA, *p*-coumaric acid; EC5, inducer concentration that results in 5% of maximal fold induction; EC95, inducer concentration resulting in 95% of maximal fold induction.

Optimization of Heterologous Gene Expression Enables CA Production and Biosensor-Mediated Product Detection in *E. coli*. Subsequently, a codon-optimized synthetic gene for the aromatic amino acid ammonia lyase Xal_{TC} originating from *Trichosporon cutaneum*, was introduced into *E. coli* pSenCA. In a previous study, this enzyme stood out

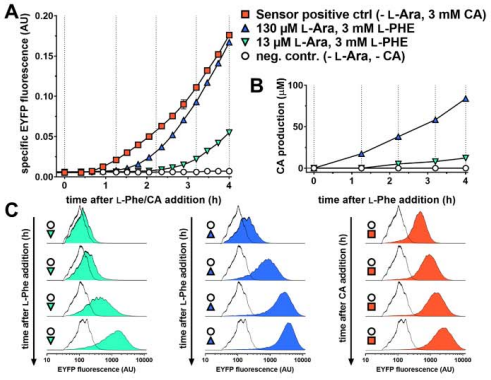

Figure 2. Influence of induction of heterologous xal_{TC} expression with 13 μM L-Ara or 130 μM L-Ara on biosensor response and CA production in *E. coli* pSenCA pBAD-xal^{1}_{TC}. After cultivation for 3 h in the presence of different L-Ara concentrations, either 3 mM L-Phe (circles and triangles) or 3 mM CA (squares) was added. Samples were taken at four time points depicted by dotted lines (A) Specific fluorescence is shown (EYFP fluorescence × biomass formation $^{-1}$, arbitrary units). (B) CA concentration in *E. coli* culture supernatants. (C) FACS measurement of EYFP fluorescence of 62 000 representative single cells in the histogram representation. Abbreviations: CA, *trans*-cinnamic acid; L-Ara, L-arabinose; and L-Phe, L-phenylalanine.

DOI: 10.1021/acssynbio.9b00149
ACS Synth. Biol. 2019, 8, 1847−1857

among 21 other ammonia lyases as highly active enzyme having both PAL- and TAL-activities.[40] Here, the L-arabinose (L-Ara) inducible pBAD expression system was used for xal_{Tc} expression in *E. coli* as it allows for tightly controlled and titratable heterologous gene expression.[41] For optimization of xal_{Tc} expression in the resulting strain *E. coli* pSenCA pBAD-xal_{Tc} at microtiter plate scale, five L-Ara concentrations (13 μM, 130 μM, 1.3 mM, 13 mM, and 130 mM) were evaluated. All cultivations were performed with supplementation of 3 mM L-Phe, which served as Xal_{Tc} substrate. The performed microtiter plate cultivations in a biolector allowed for the monitoring of EYFP fluorescence over the whole cultivation time of 48 h (Supplementary Figure S1). Interestingly, low inducer concentrations (13 μM and 130 μM) ultimately resulted in the highest specific biosensor response, whereas induction of gene expression at higher L-Ara concentrations (1.3, 13, and 130 mM) appeared to impede formation of fluorescence. In addition, with increasing L-Ara concentrations, growth rate and final biomass formation were reduced. Since different L-Ara concentrations are not known to be problematic for the cellular metabolism, it was concluded that the reduced fluorescence formation is a consequence of the metabolic burden of high level xal_{Tc} expression.[42] Therefore, cultivations with supplementation of 13 μM and 130 μM L-Ara were characterized in detail with regard to CA formation and pSenCA response to identify suitable conditions for FACS-based screenings. Noteworthy, heterologous xal_{Tc}-expression using 130 μM L-Ara yielded a fluorescence response close to the saturation of the biosensor, which was similar to the performed control experiments without xal_{Tc}-expression but supplementation of 3 mM CA (Figure 2A). Under these conditions, *E. coli* pSenCA pBAD-xal_{Tc} accumulated 84 μM CA in the supernatant within 4 h of cultivation (Figure 2B). This means that induction of gene expression with 130 μM L-Ara would be too high for distinguishing improved Xal_{Tc} variants from wild-type Xal_{Tc} during FACS-based screening campaigns using pSenCA, but allows reliable discrimination of CA-producing cells from nonproducers. In contrast, induction of gene expression with 13 μM L-Ara leads to less pronounced fluorescence response far from biosensor saturation, enabling the isolation of more active Xal_{Tc} variants from genetically diverse enzyme libraries (Figure 2A). Hence, consecutive rounds of FACS screening, first under "strong" gene expression conditions (130 μM L-Ara) to reliably enrich CA-producers, and then under "weak" gene expression conditions (13 μM L-Ara) to enable selection of the best variants within that pool of CA-producing cells could be a feasible FACS screening strategy.

Prevention of Biosensor Cross-Talk Is a Prerequisite for Any FACS Applications Using pSenCA. Many small molecules of biotechnological interest readily diffuse over biological membranes or are taken up by carrier-mediated transport (facilitated diffusion or active transport).[43] This aspect poses a major challenge during biosensor-based FACS-screenings as biosensor cross-talk between producing and nonproducing variants would lead to a high number of isolated false-positive variants. Induction of xal_{Tc}-expression in *E. coli* pSenCA pBAD-xal_{Tc} with 13 μM L-Ara allows for a product titer of 12 μM CA after 4 h of cultivation after L-Phe addition, which might already promote an undesired pSenCA cross-talk. With the aim of detecting any pSenCA cross-talk and developing a cultivation strategy for minimizing this effect prior to conducting any FACS screenings, defined mixtures of *E. coli* pSenCA pBAD-xal_{Tc} cells (CA^+) and *E. coli* pSenCA cells (CA^-) were analyzed by FACS over the course of cultivation time. In this experiment, a 50% CA^+/50% CA^- mixed culture was inoculated to a starting OD_{600} (iOD_{600}) of 0.5 and cultivated for 8 h (3 h xal_{Tc} expression and 5 h cultivation after L-Phe addition) before the top 5% fluorescing cells were isolated by FACS. Performed colony-PCRs revealed that 30% of these cells did not carry pBAD-xal_{Tc} (Supplementary Figure S2A). Reason for this could be either spontaneous mutations in pSenCA leading to constitutive *eyfp* expression in the CA^- cells, or CA uptake from the supernatant by the CA^- cells, which activated the biosensor. However, since none of the isolated CA^- cells showed fluorescence in the absence of CA, it was concluded that the uptake of CA from the supernatant was the reason for the isolation of false positive CA^- cells. These results indeed showed that pSenCA cross-talk between individual cells occurs, impeding any future FACS-screening campaigns.

Driven by the idea that reduction of the inoculum (iOD_{600}) might be useful strategy for minimizing biosensor cross-talk, four different CA^+/CA^- ratios (20% CA /80% CA^-; 50% CA^+/50% CA^-; 80% CA^+/20% CA^-; 100% CA^+/0% CA^-) at four different iOD_{600} (0.5; 0.1; 0.02; 0.004) were compared with regard to fluorescence at single cell level and FACS sorting efficiency (Figure 3). Noteworthy, the median fluorescence intensity of the culture with 100% CA^+ cells decreased with decreasing inoculum size, and a smaller population of highly fluorescing cells became apparent. This observation hints toward population heterogeneity with regard to either xal_{Tc}-expression or stochastic HcaR-binding events in the low-CA accumulation range and subsequent CA

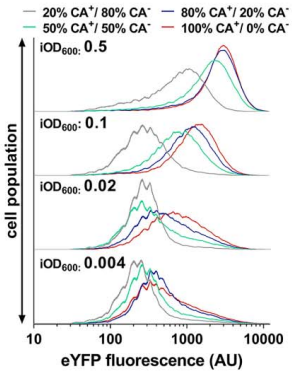

Figure 3. EYFP fluorescence of various mixed cultures of *trans*-cinnamic acid producing and nonproducing *E. coli* strains during cytometric analysis. All cultures were started using different inoculums (iOD_{600}) as indicated. All cultivations were performed in the in the presence of 13 μM L-arabinose for induction of heterologous xal_{Tc} expression and 3 mM L-Phe as XAL-substrate always added 3 h after starting each cultivation. FACS measurements were performed 5 h after substrate addition. Strains: CA^+, *E. coli* pSenCA pBAD-xal_{Tc}; CA^-, *E. coli* pSenCA pBAD.

DOI: 10.1021/acssynbio.9b00149
ACS Synth. Biol. 2019, 8, 1847−1857

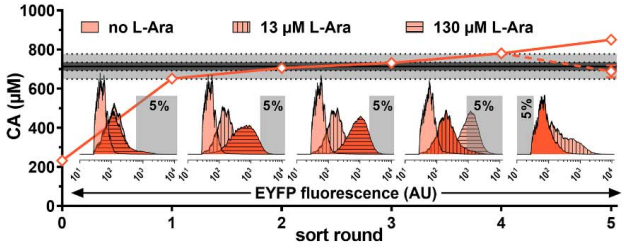

Figure 4. Stepwise enrichment of improved CA producers from a xal_{Tc} library using biosensor-based FACS-screening. The continuous orange graph depicts the development of the CA titer of the xal_{Tc} library at the culture level relative to the starting variant *E. coli* pSenCA pBAD-xal_{Tc} (black line). The dashed orange graph depicts the CA titer development in a control experiment, in which another positive sorting (fluorescence) instead of the negative sorting (no fluorescence) was performed. The dark gray shading depicts the CA-titer range of one standard deviation from the Xal_{Tc} starting variant, whereas light gray shading depicts the CA-titer range of three standard deviations. Histograms show the fluorescence distribution of the cultures of each cultivation step without induction of heterologous gene expression (no L-Ara) or substrate addition (no L-Phe) (histogram without pattern), with supplementation of 13 μM L-Ara and 3 mM L-Phe (vertical lines) and 130 μM L-Ara and 3 mM L-Phe added (horizontal lines). Conditions of each step leading to the eventually isolated xal_{Tc} variants are highlighted in bright orange relative to the conditions only used as controls that are shown in dim orange. Gray boxes visualize the respective sorting gate set in each step: Step 1−4, positive sorts (isolation of the top 5% fluorescing events); Step 5, negative sort (isolation of the lower 5% fluorescing events). Cultivations for CA titer determination were always performed in triplicates, error bars depict the respective standard deviations. The dotted line depicts development of CA production for an additional round of positive sorting in step five (Supplementation of 13 μM L-Ara), which was performed in parallel for comparison. Abbreviations: CA, *trans*-cinnamic acid; L-Ara, L-arabinose; L-Phe, L-phenylalanine.

production in these otherwise genetically homogeneous cultures. In combination with the biosensor cross-talk, the observed heterogeneity provides an explanation for the homogeneous looking population at an iOD_{600} of 0.5 as the increasing number of CA-producers among the 100% CA^- cells also produced more CA, which was then taken up by the nonproducing cells. Consequently, with a decreasing share of CA^- cells at different CA^-/CA^- ratios and decreasing iOD_{600} tested, the number of CA-producing cells was more and more reduced, resulting in a decreased median fluorescence of the respective cultures, but also a more pronounced small population of highly fluorescent CA-producing cells (Figure 3). This indicates that a reduced inoculum reduces the biosensor cross-talk between CA^+ and CA^- cells presumably enabling for the efficient biosensor-guided isolation of CA^+ cells by FACS. Subsequently performed FACS experiments in which only the top 5% fluorescent cells of the 20% CA^+/80% CA^- and 50% CA^+/50% CA^- cultures with an iOD_{600} of 0.02 or 0.004 were isolated and characterized, confirmed this assumption as all isolated cells were CA^+ cells (Supplementary Figure S2B−E).

Directed Evolution of an Ammonia Lyase by Multistep FACS Screening. The previously established and optimized gene expression and cultivation conditions were subsequently used to screen a diverse XAL_{Tc} library for isolating enzyme variants with an improved activity in *E. coli*. For this purpose, a randomly mutated xal_{Tc} library of 2.3×10^6 variants was constructed by subcloning of xal_{Tc} error-prone PCR products into the pBAD vector, and transformation into electrocompetent *E. coli* pSenCA cells.

A multistep FACS enrichment strategy was performed in which always the top 5% fluorescent cells were collected and recultivated for the next enrichment step (Figure 4). During this campaign, the average CA production of the recovered cells in the culture was determined by HPLC after every step to judge successful enrichment of CA producing cells. The first FACS enrichment steps were performed under strong xal_{Tc}-induction conditions with supplementation of 130 μM L-Ara to reliably enrich CA producing variants. In parallel, during each round of enrichment, the respective *E. coli* cultures were also analyzed by FACS under weak xal_{Tc}-induction conditions (13 μM L-Ara) for comparison and also without any induction of xal_{Tc} expression (no L-Ara) or addition of the Xal_{Tc} substrate L-Phe for identifying false positive variants bearing spontaneous mutations leading to constitutive *eyfp* expression. In the course of the enrichments under strong xal_{Tc}-induction conditions, the CA titer increased from 232 to 651 μM (1st FACS-enrichment step), from 651 to 706 μM (2nd FACS-enrichment step), and from 706 to 734 μM (3rd FACS-enrichment step), respectively, without a detectable increase in fluorescence in the false positive controls (Figure 4). A subsequent fourth enrichment step was performed with lower induction of heterologous gene expression (13 μM L-Ara) for identifying the best CA producers in the enrichments. The strategy was changed as the third step with high induction of gene expression resulted only in a small increase of the CA titer by 28 μM. Presumably this was the case because most remaining cells in the third enrichment were already CA producers, promoting strong fluorescence under high induction of heterologous gene expression (130 μM L-Ara). Surprisingly, this fourth enrichment step in the presence of 13 μM L-Ara resulted in the occurrence of a pronounced fluorescent population as a shoulder in the histogram of the control FACS experiment without L-Ara or L-Phe, indicating that false positive variants were enriched under these conditions. Hence, an additional control experiment was performed, in which a fifth positive FACS screening of the library in the presence of 13 μM L-Ara (positive sort under weak induction conditions) was conducted (Figure 4, dotted line). As expected, a decreasing average CA-titer (688 μM CA)

DOI: 10.1021/acssynbio.9b00149
ACS Synth. Biol. 2019, 8, 1847−1857

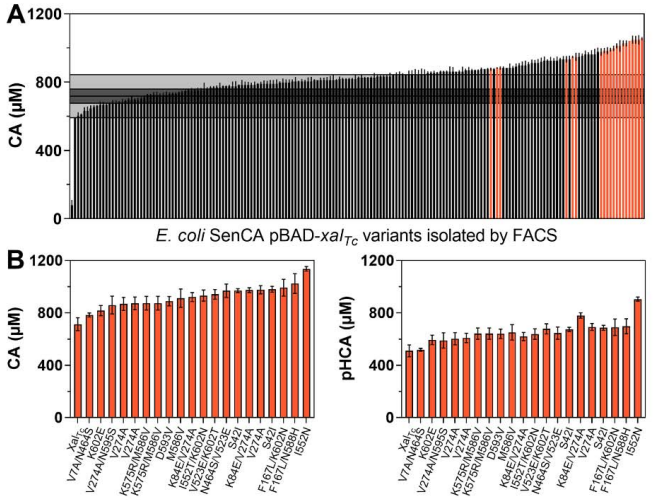

Figure 5. (A) *trans*-Cinnamic acid production of 183 FACS-isolated Xal_{Tc} variants. Presented data are means of three cultivations and error bars depict standard deviations. The dark gray shading depicts the CA-titer range of one standard deviation from the Xal_{Tc} starting variant, whereas light gray shading depicts the CA-titer range of three standard deviations. (WT cultivated as biological triplicates). Variants selected for a more detailed analysis are highlighted in orange. (B), CA (left) and pHCA (right) production of 19 strains selected during the initial characterization (Figure 5A), after retransformation of the respective pBADxal_{Tcbc} plasmid. All cultivations were performed in biological triplicates, error bars depict the standard deviation. Abbreviations: CA, *trans*-cinnamic acid; pHCA, *p*-coumaric acid.

of the enriched culture was determined as the false positives variants were further enriched. The solution was a final negative FACS-step (no L-Ara and L-Phe supplementation) and sorting of the 5% least fluorescing cells to exclude false positive variants. This increased the average CA-titer of the library to 850 μM upon recultivation.

During the FACS campaign, the stepwise enrichment resulted in a culture of *E. coli* variants, which accumulated up to 20% more CA in the supernatant in comparison to a culture of the starting variant *E. coli* pSenCA pBAD-xal_{Tc} that accumulates 713 μM CA. For comparison, prior to any FACS enrichment, the randomly mutated and unsorted Xal_{Tc}-library accumulated 232 μM CA, which is 70% less CA compared to the starting variant.

The *E. coli* cells recovered after the fifth enrichment step were spread on LB agar plates and 182 single colonies were individually cultivated and characterized with regard to their respective CA production capabilities (Figure 5A). These experiments revealed that 8% of these variants accumulated less CA compared to the starting variant, whereas 16% could not be distinguished from this control. In contrast, 76% of the strains accumulated significantly (>10%) more CA, with the upper 20% accumulating 30% to 50% more CA compared to the starting variant *E. coli* pSenCA pBAD-xal_{Tc}.

Subsequently, the pBAD-xal_{Tc} plasmids of the 15 best variants and five randomly selected variants with significantly higher CA accumulation compared to the starting variant were isolated and retransformed into *E. coli* pSenCA to exclude the potential influence of undesired random genomic mutations (Figure 5A). The resulting strains were compared to *E. coli* pSenCA pBAD-xal_{Tc} regarding their CA and pHCA accumulation from supplemented L-Phe and L-Tyr, respectively (Figure 5 B). In parallel, the DNA sequence of all 20 xal_{Tc} variants was determined. All variants accumulated 10% to 60% more CA or pHCA in the supernatant when L-Phe or L-Tyr were supplemented, respectively. Interestingly, DNA sequencing revealed that 6 strains have mutations in the P_{araB}-promoter upstream of xal_{Tc}, whereas 14 variants exclusively carry mutations in the xal_{Tc} open reading frame (Supplementary table S3).

Nonetheless, the increased CA titer of these 14 strains could be also due to improved heterologous expression of xal_{Tc} and thus higher Xal_{Tc} abundance and does not necessarily have to relate to altered enzyme kinetics of the enzyme. With the aim, to preclude any undesired expression effects, an *in vitro* characterization of seven Xal_{Tc} variants with purified proteins was performed. Seven muteins, including Xal_{Tc}-F167L-K602N, Xal_{Tc}-N464S/V523E, Xal_{Tc}-F167L/N588H, Xal_{Tc}-I552N, Xal_{Tc}-V523E/K602T, Xal_{Tc}-I552T/K602N, and Xal_{Tc}-V274A were selected to determine enzyme kinetics *in vitro*. These variants accumulated the highest CA concentrations in the *in vivo* experiments and did not carry mutations in the *araC* gene or in the P_{araBAD} promoter (except for Xal_{Tc}-I552N comprising P_{araBAD}-a10g). For the *in vitro* enzyme assays, all genes were

DOI: 10.1021/acssynbio.9b00149
ACS Synth. Biol. 2019, 8, 1847−1857

Table 1. Kinetic Characterization of Selected Xal_{Tc} Muteins Obtained during the Biosensor-Based FACS Screening Campaign

	PAL reaction		TAL reaction	
Xal_{Tc} variant	K_m (mM)	V_{max} (μmol min^{-1} mg^{-1})	K_m (mM)	V_{max} (μmol min^{-1} mg^{-1})
Xal_{Tc} "wild type"	6.1 ± 0.6	1.24 ± 0.04	0.9 ± 0.09	0.49 ± 0.02
Xal_{Tc}-V274A	6.6 ± 0.5	1.38 ± 0.04	0.7 ± 0.05	0.5 ± 0.01
Xal_{Tc}-I552N	5.3 ± 0.2	1.28 ± 0.02	0.7 ± 0.06	0.26 ± 0.01
Xal_{Tc}-I552T/K602N	5.3 ± 0.3	1.27 ± 0.03	0.9 ± 0.09	0.5 ± 0.02
Xal_{Tc}-N464S/V523E	5.1 ± 0.4	1.1 ± 0.03	0.7 ± 0.05	0.25 ± 0.01
Xal_{Tc}-V523E/K602T	5.0 ± 0.4	1.22 ± 0.03	0.6 ± 0.04	0.26 ± 0.01
Xal_{Tc}-F167L/K602N	4.9 ± 0.5	1.41 ± 0.04	0.7 ± 0.05	0.49 ± 0.01
Xal_{Tc}-F167L/N588H	4.8 ± 0.4	1.34 ± 0.04	0.6 ± 0.05	0.3 ± 0.01

individually recloned into the pBAD-N6XHIS vector allowing for the generation of N-terminally His-tagged fusions proteins and subsequent Ni-NTA affinity chromatography. Protein purification yielded 4−5 mg of pure protein as judged by SDS-PAGE analysis for enzyme assays (Supplementary Figure S3). Six of the seven muteins characterized in this detail exhibit an up to 12% increased V_{max} and an increased affinity to the substrates L-Phe and L-Tyr, respectively, which explains the observed increased CA- and pHCA-titers (Table 1). Interestingly, mutein Xal_{Tc}-V274A does have a reduced affinity toward L-Phe (6.6 mM) but exhibits one of the highest V_{max} of the mutein set (1.38 μmol min^{-1} mg^{-1}). In contrast, Xal_{Tc}-F167L/K602N and Xal_{Tc}-F167L/N588H show the lowest K_m for both L-Phe and L-Tyr (4.8 mM/4.9 mM and 0.7 mM/0.6 mM, respectively), while the V_{max} is only increased for the deamination of L-Phe in comparison to the wild-type enzyme.

■ DISCUSSION

Enzyme as well as strain engineering can be substantially accelerated when biosensor-based FACS screenings can be implemented as this technology enables screening of vast and genetically diverse libraries with a throughput that is orders of magnitude higher compared to other well-established screening strategies.[44] However, prerequisite for the application of this powerful screening technique is the availability of a suitable biosensor for the compound of interest, and detailed knowledge of the biosensor characteristics with regard to dynamic range, kinetics of the output signal, and operational range.

Characterization of the pSenCA biosensor designed and constructed in this study revealed a strong biosensor induction by CA in the micromolar range. In comparison to other TF based biosensors, the operational range of pSenCA is rather low. For example, the pJC1-lrp-brnF′-eyfp biosensor for *C. glutamicum* for L-methionine and the branched chain amino acids L-valine, L-leucine, and L-isoleucine is characterized by a maximal fold induction of 78 and an operational range from 0.2 mM to 23.5 mM (for L-methionine).[45] The lower operational range of pSenCA in comparison to pJC1-lrp-brnF′-eyfp can be explained by the role of the respective transcriptional regulators, HcaR and Lrp, in the microbial metabolism. Lrp activates the expression of the *brnFE* operon, encoding for the branched-chain amino acid exporter BrnFE, which is responsible for secretion of excess amino acids to avoid cytotoxic effects of elevated intracellular amino acid concentrations.[46] HcaR, in contrast, activates the expression of the *hca* gene cluster involved in the catabolism of aromatic acids, which can serve as valuable carbon and energy sources in absence of other more preferred substrates.[37,39] A strong expression at low inducer concentrations is therefore beneficial to compete with other microorganisms for such valuable resources.

However, despite a low operational range, a biosensor can be used in FACS screenings if screening conditions are selected, in which the expected product concentrations match with the biosensor characteristics. In the case of the directed Xal_{Tc} evolution performed in this study, only the two lowest inducer concentrations for heterologous *xalTc*-expression enabled pSenCA-guided FACS screening. As alternative for optimizing cultivation conditions, the biosensor itself can be adapted. For example, alteration of the operational range of a transcriptional biosensor can be achieved by engineering the transcriptional regulator toward reduced affinity to the ligand, thereby enabling a graded fluorescence output for higher ligand concentrations.[47] This approach was followed recently to optimize the operational range of a whole-cell biosensor for the detection and quantification of the macrodiolide antibiotic pamamycin produced by *Streptomyces alboniger*.[48] By rational engineering of the binding pocket of the PamR2 repressor, a mutein with reduced affinity for pamamycin could be constructed, extending the upper detection limit of the sensor system from 1 mg/L to more than 5 mg/L.

Additionally, given that the constructed biosensor does not provide sufficient dynamic range, often because of incompatibility between the host strain and heterologous regulatory elements, the target promoter of the regulator incorporated in the sensor or the promoter of the regulator gene can be mutated. For example, a 3,4-dihydroxy benzoate responsive biosensor based on the *pcaU* gene under control of its promoter P_{pcaU} from *Acinetobacter sp ADP1* was applied in *E. coli*.[49] By random mutagenesis, a library of 33 000 promoter mutants was constructed and subsequently screened using FACS. Applying positive and negative screening, three variants with improved dynamic range were isolated. Another example is the a biosensor comprised of PadR, a repressor specific for *p*-coumaric acid from *Bacillus subtilis*, and its cognate promoter in *E. coli*.[50] A sensor variant with improved dynamic range was constructed by screening a set of P_{padR}RBS mutants for variants with reduced expression of *padR*. In other cases where neither optimization of cultivation conditions nor adaptation of the biosensor is an option, identification of the most suitable time-point for the FACS screening during cultivation presents a possible solution to prevent saturation of the sensor system.

Cross-talk between producers and nonproducing cells as it could be observed in this study impedes any biosensor-based FACS screening if the metabolite in question can diffuse of biological membranes or is readily taken up by the microorganism. Dilution to a starting OD_{600} of 0.004 and short cultivation times (<8 h) successfully suppressed cross-talk in our case, even with an excess of producing cells in the culture.

DOI: 10.1021/acssynbio.9b00149
ACS Synth. Biol. 2019, 8, 1847−1857

A possible alternative to dilution for preventing cross-talk is compartmentalization of individual strain variants in solution, *e.g.*, by emulsion droplets, which can be sorted in microfluidic devices. By coencapsulation of an *E. coli* strain carrying a *p*-coumaric acid-responsive biosensor and *p*-coumaric acid producing *Saccharomyces cerevisiae*, yeast cells with elevated *p*-coumaric acid production capabilities could be isolated from mixtures of different producer strains.[50] However, design and construction of droplet-based screening assays is most likely more laborious, and the sorting speed in microfluidic devices is usually limited to less than 500 cells per second when reasonable sort efficiencies are desired.[50,51] Recently, successful sorting of double emulsion droplets in a FACS device could be demonstrated, increasing the throughput of droplet sorting to 1000 cells per second.[52] When performing dilution assays in this study, a pronounced heterogeneity with respect to the fluorescent response could be detected, which was presumably caused by heterogeneous expression of the xal_{Tc} gene. This heterogeneous expression in the presence of subsaturating L-Ara concentrations was described earlier and could be eliminated by expression of the L-Ara importer gene *araE* under control of either a constitutive *Lactococcus lactis* or an Isopropyl-β-D-thiogalactopyranosid-inducible *lac* promoter.[53,54]

CONCLUSIONS

In this study, a transcriptional biosensor for the phenylpropanoid *trans*-cinnamic acid could be successfully designed, constructed, and applied in a high-throughput FACS screening campaign. Key to success was a detailed characterization of the biosensor in combination with fine-tuning of cultivation and screening conditions to overcome hurdles such as biosensor cross-talk, which impede the successful application of more biosensors in the field of protein engineering or strain development. We believe that the strategies outlined in this article will help others to also develop elegant biosensor-based screening campaigns using the high-throughput capabilities of FACS.

ASSOCIATED CONTENT

Supporting Information

The Supporting Information is available free of charge on the ACS Publications website at DOI: 10.1021/acssynbio.9b00149.

Table S1: Strains and plasmids used in this study; Table S2: Oligonucleotides used in this study; Table S3: Overview of all xal_{Tc}-variants isolated in the FACS campaign, which were characterized in detail; Figure S1: Performance of the *E. coli* pSenCA pBAD-xal_{Tc} system; Figure S2: Influence of the inoculum size (iOD_{600}) on producer isolation efficiency; Figure S3: SDS-PAGE analysis of a typical Xal_{Tc} purification (PDF)

AUTHOR INFORMATION

Corresponding Author

*Tel: +49 2461 61 2843. Fax: +49 2461 61 2710. E-mail: j.marienhagen@fz-juelich.de.

ORCID

Jan Marienhagen: 0000-0001-5513-3730

Author Contributions

L.K.F. designed the experiments, L.K.F. and S.S. conducted the experiments. L.K.F. and J.M. wrote the manuscript.

Notes

The authors declare no competing financial interest.

ACKNOWLEDGMENTS

The authors thank Alex Toftgaard Nielsen and Christian Bille Jendresen for providing PCBJ296. This project has received funding from the European Research Council (ERC) under the European Union's Horizon 2020 research and innovation programme (grant agreement No 638718).

REFERENCES

(1) Daugherty, P. S., Iverson, B. L., and Georgiou, G. (2000) Flow cytometric screening of cell-based libraries. *J. Immunol. Methods 243*, 211−27.

(2) Zhang, J., Jensen, M. K., and Keasling, J. D. (2015) Development of biosensors and their application in metabolic engineering. *Curr. Opin. Chem. Biol. 28*, 1−8.

(3) Schallmey, M., Frunzke, J., Eggeling, L., and Marienhagen, J. (2014) Looking for the pick of the bunch: high-throughput screening of producing microorganisms with biosensors. *Curr. Opin. Biotechnol. 26*, 148−54.

(4) Snoek, T., Romero-Suarez, D., Zhang, J., Ambri, F., Skjoedt, M. L., Sudarsan, S., Jensen, M. K., and Keasling, J. D. (2018) An Orthogonal and pH-Tunable Sensor-Selector for Muconic Acid Biosynthesis in Yeast. *ACS Synth. Biol. 7*, 995−1003.

(5) Dietrich, J. A., Shis, D. L., Alikhani, A., and Keasling, J. D. (2013) Transcription factor-based screens and synthetic selections for microbial small-molecule biosynthesis. *ACS Synth. Biol. 2*, 47−58.

(6) Xu, P., Li, L., Zhang, F., Stephanopoulos, G., and Koffas, M. (2014) Improving fatty acids production by engineering dynamic pathway regulation and metabolic control. *Proc. Natl. Acad. Sci. U. S. A. 111*, 11299−304.

(7) Zhang, J., Sonnenschein, N., Pihl, T. P. B., Pedersen, K. R., Jensen, M. K., and Keasling, J. D. (2016) Engineering an NADPH/NADP+ Redox Biosensor in Yeast. *ACS Synth. Biol. 5*, 1546−1556.

(8) Chou, H. H., and Keasling, J. D. (2013) Programming adaptive control to evolve increased metabolite production. *Nat. Commun. 4*, 2595.

(9) Siedler, S., Schendzielorz, G., Binder, S., Eggeling, L., Bringer, S., and Bott, M. (2014) SoxR as a single-cell biosensor for NADPH-consuming enzymes in Escherichia coli. *ACS Synth. Biol. 3*, 41−7.

(10) Schendzielorz, G., Dippong, M., Grünberger, A., Kohlheyer, D., Yoshida, A., Binder, S., Nishiyama, C., Nishiyama, M., Bott, M., and Eggeling, L. (2014) Taking control over control: use of product sensing in single cells to remove flux control at key enzymes in biosynthesis pathways. *ACS Synth. Biol. 3*, 21−9.

(11) Binder, S., Schendzielorz, G., Stäbler, N., Krumbach, K., Hoffmann, K., Bott, M., and Eggeling, L. (2012) A high-throughput approach to identify genomic variants of bacterial metabolite producers at the single-cell level. *Genome Biol. 13*, R40.

(12) Mahr, R., Gätgens, C., Gätgens, J., Polen, T., Kalinowski, J., and Frunzke, J. (2015) Biosensor-driven adaptive laboratory evolution of l-valine production in Corynebacterium glutamicum. *Metab. Eng. 32*, 184−94.

(13) Xiao, Y., Bowen, C. H., Liu, D., and Zhang, F. (2016) Exploiting nongenetic cell-to-cell variation for enhanced biosynthesis. *Nat. Chem. Biol. 12*, 339−44.

(14) Dietrich, J. A., McKee, A. E., and Keasling, J. D. (2010) High-throughput metabolic engineering: advances in small-molecule screening and selection. *Annu. Rev. Biochem. 79*, 563−90.

(15) Bertani, G. (1951) Studies on lysogenesis. I. The mode of phage liberation by lysogenic Escherichia coli. *J. Bacteriol. 62*, 293−300.

DOI: 10.1021/acssynbio.9b00149
ACS Synth. Biol. 2019, 8, 1847−1857

(16) Durfee, T., Nelson, R., Baldwin, S., Plunkett, G., Burland, V., Mau, B., Petrosino, J. F., Qin, X., Muzny, D. M., Ayele, M., Gibbs, R. A., Csörgo, B., Pósfai, G., Weinstock, G. M., and Blattner, F. R. (2008) The complete genome sequence of Escherichia coli DH10B: insights into the biology of a laboratory workhorse. *J. Bacteriol. 190*, 2597−606.
(17) Kensy, F., Zang, E., Faulhammer, C., Tan, R.-K., and Büchs, J. (2009) Validation of a high-throughput fermentation system based on online monitoring of biomass and fluorescence in continuously shaken microtiter plates. *Microb. Cell Fact. 8*, 31.
(18) Funke, M., Diederichs, S., Kensy, F., Müller, C., and Büchs, J. (2009) The baffled microtiter plate: increased oxygen transfer and improved online monitoring in small scale fermentations. *Biotechnol. Bioeng. 103*, 1118−28.
(19) Sambrook, J., and Russel, D. W. (2001) *Molecular Cloning A Lab Manual* 3, Cold Spring Harbor Laboratory Press, New York.
(20) Gibson, D. G., Young, L., Chuang, R.-Y., Venter, J. C., Hutchison, C. A., and Smith, H. O. (2009) Enzymatic assembly of DNA molecules up to several hundred kilobases. *Nat. Methods 6*, 343−345.
(21) Dower, W. J., Miller, J. F., and Ragsdale, C. W. (1988) High efficiency transformation of E. coli by high voltage electroporation. *Nucleic Acids Res. 16*, 6127−45.
(22) Yu, D., Ellis, H. M., Lee, E. C., Jenkins, N. A., Copeland, N. G., and Court, D. L. (2000) An efficient recombination system for chromosome engineering in Escherichia coli. *Proc. Natl. Acad. Sci. U. S. A. 97*, 5978−83.
(23) Datsenko, K. A., and Wanner, B. L. (2000) One-step inactivation of chromosomal genes in Escherichia coli K-12 using PCR products. *Proc. Natl. Acad. Sci. U. S. A. 97*, 6640−5.
(24) Jensen, S. I., Lennen, R. M., Herrgård, M. J., and Nielsen, A. T. (2016) Seven gene deletions in seven days: Fast generation of Escherichia coli strains tolerant to acetate and osmotic stress. *Sci. Rep. 5*, 17874.
(25) Jensen, S. I., and Nielsen, A. T. (2018) Multiplex Genome Edititing in *Escherichia coli*, in *Synthetic Metabolic Pathways* (Jensen, M. K., and Keasling, J. D., Eds.), pp 119−129, Springer Science + Business Media.
(26) Freiherr von Boeselager, R., Pfeifer, E., and Frunzke, J. (2018) Cytometry meets next-generation sequencing - RNA-Seq of sorted subpopulations reveals regional replication and iron-triggered prophage induction in Corynebacterium glutamicum. *Sci. Rep. 8*, 14856.
(27) Watts, K. T., Mijts, B. N., Lee, P. C., Manning, A. J., and Schmidt-Dannert, C. (2006) Discovery of a substrate selectivity switch in tyrosine ammonia-lyase, a member of the aromatic amino acid lyase family. *Chem. Biol. 13*, 1317−26.
(28) Milke, L., Aschenbrenner, J., Marienhagen, J., and Kallscheuer, N. (2018) Production of plant-derived polyphenols in microorganisms: current state and perspectives. *Appl. Microbiol. Biotechnol. 102*, 1575−1585.
(29) Kallscheuer, N., Menezes, R., Foito, A., da Silva, M. H., Braga, A., Dekker, W., Sevillano, D. M., Rosado-Ramos, R., Jardim, C., Oliveira, J., Ferreira, P., Rocha, I., Silva, A. R., Sousa, M., Allwood, J. W., Bott, M., Faria, N., Stewart, D., Ottens, M., Naesby, M., Nunes Dos Santos, C., and Marienhagen, J. (2019) Identification and Microbial Production of the Raspberry Phenol Salidroside that Is Active against Huntington's Disease. *Plant Physiol. 179*, 969−985.
(30) Koopman, F., Beekwilder, J., Crimi, B., van Houwelingen, A., Hall, R. D., Bosch, D., van Maris, A. J., Pronk, J. T., and Daran, J.-M. (2012) De novo production of the flavonoid naringenin in engineered Saccharomyces cerevisiae. *Microb. Cell Fact. 11*, 155.
(31) Santos, C. N. S., Koffas, M., and Stephanopoulos, G. (2011) Optimization of a heterologous pathway for the production of flavonoids from glucose. *Metab. Eng. 13*, 392−400.
(32) Zhou, S., Liu, P., Chen, J., Du, G., Li, H., and Zhou, J. (2016) Characterization of mutants of a tyrosine ammonia-lyase from Rhodotorula glutinis. *Appl. Microbiol. Biotechnol. 100*, 10443−10452.
(33) Eudes, A., Juminaga, D., Baidoo, E. E. K., Collins, F., Keasling, J. D., and Loqué, D. (2013) Production of hydroxycinnamoyl anthranilates from glucose in Escherichia coli. *Microb. Cell Fact. 12*, 62.
(34) Lin, Y., and Yan, Y. (2012) Biosynthesis of caffeic acid in Escherichia coli using its endogenous hydroxylase complex. *Microb. Cell Fact. 11*, 42.
(35) Kallscheuer, N., Vogt, M., Stenzel, A., Gätgens, J., Bott, M., and Marienhagen, J. (2016) Construction of a Corynebacterium glutamicum platform strain for the production of stilbenes and (2*S*)-flavanones. *Metab. Eng. 38*, 47−55.
(36) Díaz, E., Ferrández, A., Prieto, M. A., and García, J. L. (2001) Biodegradation of aromatic compounds by Escherichia coli. *Microbiol. Mol. Biol. Rev. 65*, 523−69.
(37) Díaz, E., Ferrández, A., and García, J. L. (1998) Characterization of the hca cluster encoding the dioxygenolytic pathway for initial catabolism of 3-phenylpropionic acid in Escherichia coli K-12. *J. Bacteriol. 180*, 2915−2923.
(38) Kovářová, K., Käch, A., Chaloupka, V., and Egli, T. (1996) Cultivation of Escherichia coli with mixtures of 3-phenylpropionic acid and glucose: Dynamics of growth and substrate consumption. *Biodegradation 7*, 445−453.
(39) Turlin, E., Perrotte-Piquemal, M., Danchin, A., and Biville, F. (2001) Regulation of the early steps of 3-phenylpropionate catabolism in Escherichia coli. *J. Mol. Microbiol. Biotechnol. 3*, 127−133.
(40) Jendresen, C. B., Stahlhut, S. G., Li, M., Gaspar, P., Siedler, S., Förster, J., Maury, J., Borodina, I., and Nielsen, A. T. (2015) Novel highly active and specific tyrosine ammonia-lyases from diverse origins enable enhanced production of aromatic compounds in bacteria and yeast. *Appl. Environ. Microbiol. 81*, 4458.
(41) Guzman, L. M., Belin, D., Carson, M. J., and Beckwith, J. (1995) Tight regulation, modulation, and high-level expression by vectors containing the arabinose PBAD promoter. *J. Bacteriol. 177*, 4121−30.
(42) Desai, T. A., and Rao, C. V. (2010) Regulation of arabinose and xylose metabolism in Escherichia coli. *Appl. Environ. Microbiol. 76*, 1524−32.
(43) Crane, R. K. (1977) The gradient hypothesis and other models of carrier-mediated active transport, in *Reviews of Physiology, Biochemistry and Pharmacology*, Vol. 78, pp 99−159, Springer-Verlag, Berlin/Heidelberg.
(44) Eggeling, L., Bott, M., and Marienhagen, J. (2015) Novel screening methods—biosensors. *Curr. Opin. Biotechnol. 35*, 30−36.
(45) Mustafi, N., Grünberger, A., Kohlheyer, D., Bott, M., and Frunzke, J. (2012) The development and application of a single-cell biosensor for the detection of l-methionine and branched-chain amino acids. *Metab. Eng. 14*, 449−57.
(46) Lange, C., Mustafi, N., Frunzke, J., Kennerknecht, N., Wessel, M., Bott, M., and Wendisch, V. F. (2012) Lrp of Corynebacterium glutamicum controls expression of the brnFE operon encoding the export system for L-methionine and branched-chain amino acids. *J. Biotechnol. 158*, 231−41.
(47) Mannan, A. A., Liu, D., Zhang, F., and Oyarzún, D. A. (2017) Fundamental Design Principles for Transcription-Factor-Based Metabolite Biosensors. *ACS Synth. Biol. 6*, 1851−1859.
(48) Rebets, Y., Schmelz, S., Gromyko, O., Tistechok, S., Petzke, L., Scrima, A., and Luzhetskyy, A. (2018) Design, development and application of whole-cell based antibiotic-specific biosensor. *Metab. Eng. 47*, 263−270.
(49) Jha, R. K., Kern, T. L., Fox, D. T., and Strauss, C. E. M. (2014) Engineering an Acinetobacter regulon for biosensing and high-throughput enzyme screening in E. coli via flow cytometry. *Nucleic Acids Res. 42*, 8150−8160.
(50) Siedler, S., Khatri, N. K., Zsohár, A., Kjærbølling, I., Vogt, M., Hammar, P., Nielsen, C. F., Marienhagen, J., Sommer, M. O. A., and Joensson, H. N. (2017) Development of a Bacterial Biosensor for Rapid Screening of Yeast p-Coumaric Acid Production. *ACS Synth. Biol. 6*, 1860−1869.

DOI: 10.1021/acssynbio.9b00149
ACS Synth. Biol. 2019, 8, 1847−1857

(16) Durfee, T., Nelson, R., Baldwin, S., Plunkett, G., Burland, V., Mau, B., Petrosino, J. F., Qin, X., Muzny, D. M., Ayele, M., Gibbs, R. A., Csörgo, B., Pósfai, G., Weinstock, G. M., and Blattner, F. R. (2008) The complete genome sequence of Escherichia coli DH10B: insights into the biology of a laboratory workhorse. *J. Bacteriol. 190*, 2597−606.
(17) Kensy, F., Zang, E., Faulhammer, C., Tan, R.-K., and Büchs, J. (2009) Validation of a high-throughput fermentation system based on online monitoring of biomass and fluorescence in continuously shaken microtiter plates. *Microb. Cell Fact. 8*, 31.
(18) Funke, M., Diederichs, S., Kensy, F., Müller, C., and Büchs, J. (2009) The baffled microtiter plate: increased oxygen transfer and improved online monitoring in small scale fermentations. *Biotechnol. Bioeng. 103*, 1118−28.
(19) Sambrook, J., and Russel, D. W. (2001) *Molecular Cloning A Lab Manual* 3, Cold Spring Harbor Laboratory Press, New York.
(20) Gibson, D. G., Young, L., Chuang, R.-Y., Venter, J. C., Hutchison, C. A., and Smith, H. O. (2009) Enzymatic assembly of DNA molecules up to several hundred kilobases. *Nat. Methods 6*, 343−345.
(21) Dower, W. J., Miller, J. F., and Ragsdale, C. W. (1988) High efficiency transformation of E. coli by high voltage electroporation. *Nucleic Acids Res. 16*, 6127−45.
(22) Yu, D., Ellis, H. M., Lee, E. C., Jenkins, N. A., Copeland, N. G., and Court, D. L. (2000) An efficient recombination system for chromosome engineering in Escherichia coli. *Proc. Natl. Acad. Sci. U. S. A. 97*, 5978−83.
(23) Datsenko, K. A., and Wanner, B. L. (2000) One-step inactivation of chromosomal genes in Escherichia coli K-12 using PCR products. *Proc. Natl. Acad. Sci. U. S. A. 97*, 6640−5.
(24) Jensen, S. I., Lennen, R. M., Herrgård, M. J., and Nielsen, A. T. (2016) Seven gene deletions in seven days: Fast generation of Escherichia coli strains tolerant to acetate and osmotic stress. *Sci. Rep. 5*, 17874.
(25) Jensen, S. I., and Nielsen, A. T. (2018) Multiplex Genome Edititing in *Escherichia coli*, in *Synthetic Metabolic Pathways* (Jensen, M. K., and Keasling, J. D., Eds.), pp 119−129, Springer Science + Business Media.
(26) Freiherr von Boeselager, R., Pfeifer, E., and Frunzke, J. (2018) Cytometry meets next-generation sequencing - RNA-Seq of sorted subpopulations reveals regional replication and iron-triggered prophage induction in Corynebacterium glutamicum. *Sci. Rep. 8*, 14856.
(27) Watts, K. T., Mijts, B. N., Lee, P. C., Manning, A. J., and Schmidt-Dannert, C. (2006) Discovery of a substrate selectivity switch in tyrosine ammonia-lyase, a member of the aromatic amino acid lyase family. *Chem. Biol. 13*, 1317−26.
(28) Milke, L., Aschenbrenner, J., Marienhagen, J., and Kallscheuer, N. (2018) Production of plant-derived polyphenols in microorganisms: current state and perspectives. *Appl. Microbiol. Biotechnol. 102*, 1575−1585.
(29) Kallscheuer, N., Menezes, R., Foito, A., da Silva, M. H., Braga, A., Dekker, W., Sevillano, D. M., Rosado-Ramos, R., Jardim, C., Oliveira, J., Ferreira, P., Rocha, I., Silva, A. R., Sousa, M., Allwood, J. W., Bott, M., Faria, N., Stewart, D., Ottens, M., Naesby, M., Nunes Dos Santos, C., and Marienhagen, J. (2019) Identification and Microbial Production of the Raspberry Phenol Salidroside that Is Active against Huntington's Disease. *Plant Physiol. 179*, 969−985.
(30) Koopman, F., Beekwilder, J., Crimi, B., van Houwelingen, A., Hall, R. D., Bosch, D., van Maris, A. J., Pronk, J. T., and Daran, J.-M. (2012) De novo production of the flavonoid naringenin in engineered Saccharomyces cerevisiae. *Microb. Cell Fact. 11*, 155.
(31) Santos, C. N. S., Koffas, M., and Stephanopoulos, G. (2011) Optimization of a heterologous pathway for the production of flavonoids from glucose. *Metab. Eng. 13*, 392−400.
(32) Zhou, S., Liu, P., Chen, J., Du, G., Li, H., and Zhou, J. (2016) Characterization of mutants of a tyrosine ammonia-lyase from Rhodotorula glutinis. *Appl. Microbiol. Biotechnol. 100*, 10443−10452.
(33) Eudes, A., Juminaga, D., Baidoo, E. E. K., Collins, F., Keasling, J. D., and Loqué, D. (2013) Production of hydroxycinnamoyl anthranilates from glucose in Escherichia coli. *Microb. Cell Fact. 12*, 62.
(34) Lin, Y., and Yan, Y. (2012) Biosynthesis of caffeic acid in Escherichia coli using its endogenous hydroxylase complex. *Microb. Cell Fact. 11*, 42.
(35) Kallscheuer, N., Vogt, M., Stenzel, A., Gätgens, J., Bott, M., and Marienhagen, J. (2016) Construction of a Corynebacterium glutamicum platform strain for the production of stilbenes and (2S)-flavanones. *Metab. Eng. 38*, 47−55.
(36) Díaz, E., Ferrández, A., Prieto, M. A., and García, J. L. (2001) Biodegradation of aromatic compounds by Escherichia coli. *Microbiol. Mol. Biol. Rev. 65*, 523−69.
(37) Díaz, E., Ferrández, A., and García, J. L. (1998) Characterization of the hca cluster encoding the dioxygenolytic pathway for initial catabolism of 3-phenylpropionic acid in Escherichia coli K-12. *J. Bacteriol. 180*, 2915−2923.
(38) Kovářová, K., Käch, A., Chaloupka, V., and Egli, T. (1996) Cultivation of Escherichia coli with mixtures of 3-phenylpropionic acid and glucose: Dynamics of growth and substrate consumption. *Biodegradation 7*, 445−453.
(39) Turlin, E., Perrotte-Piquemal, M., Danchin, A., and Biville, F. (2001) Regulation of the early steps of 3-phenylpropionate catabolism in Escherichia coli. *J. Mol. Microbiol. Biotechnol. 3*, 127−133.
(40) Jendresen, C. B., Stahlhut, S. G., Li, M., Gaspar, P., Siedler, S., Förster, J., Maury, J., Borodina, I., and Nielsen, A. T. (2015) Novel highly active and specific tyrosine ammonia-lyases from diverse origins enable enhanced production of aromatic compounds in bacteria and yeast. *Appl. Environ. Microbiol. 81*, 4458.
(41) Guzman, L. M., Belin, D., Carson, M. J., and Beckwith, J. (1995) Tight regulation, modulation, and high-level expression by vectors containing the arabinose PBAD promoter. *J. Bacteriol. 177*, 4121−30.
(42) Desai, T. A., and Rao, C. V. (2010) Regulation of arabinose and xylose metabolism in Escherichia coli. *Appl. Environ. Microbiol. 76*, 1524−32.
(43) Crane, R. K. (1977) The gradient hypothesis and other models of carrier-mediated active transport, in *Reviews of Physiology, Biochemistry and Pharmacology*, Vol. 78, pp 99−159, Springer-Verlag, Berlin/Heidelberg.
(44) Eggeling, L., Bott, M., and Marienhagen, J. (2015) Novel screening methods—biosensors. *Curr. Opin. Biotechnol. 35*, 30−36.
(45) Mustafi, N., Grünberger, A., Kohlheyer, D., Bott, M., and Frunzke, J. (2012) The development and application of a single-cell biosensor for the detection of l-methionine and branched-chain amino acids. *Metab. Eng. 14*, 449−57.
(46) Lange, C., Mustafi, N., Frunzke, J., Kennerknecht, N., Wessel, M., Bott, M., and Wendisch, V. F. (2012) Lrp of Corynebacterium glutamicum controls expression of the brnFE operon encoding the export system for L-methionine and branched-chain amino acids. *J. Biotechnol. 158*, 231−41.
(47) Mannan, A. A., Liu, D., Zhang, F., and Oyarzún, D. A. (2017) Fundamental Design Principles for Transcription-Factor-Based Metabolite Biosensors. *ACS Synth. Biol. 6*, 1851−1859.
(48) Rebets, Y., Schmelz, S., Gromyko, O., Tistechok, S., Petzke, L., Scrima, A., and Luzhetskyy, A. (2018) Design, development and application of whole-cell based antibiotic-specific biosensor. *Metab. Eng. 47*, 263−270.
(49) Jha, R. K., Kern, T. L., Fox, D. T., and Strauss, C. E. M. (2014) Engineering an Acinetobacter regulon for biosensing and high-throughput enzyme screening in E. coli via flow cytometry. *Nucleic Acids Res. 42*, 8150−8160.
(50) Siedler, S., Khatri, N. K., Zsohár, A., Kjærbølling, I., Vogt, M., Hammar, P., Nielsen, C. F., Marienhagen, J., Sommer, M. O. A., and Joensson, H. N. (2017) Development of a Bacterial Biosensor for Rapid Screening of Yeast p-Coumaric Acid Production. *ACS Synth. Biol. 6*, 1860−1869.

DOI: 10.1021/acssynbio.9b00149
ACS Synth. Biol. 2019, 8, 1847−1857

(51) Baret, J.-C., Miller, O. J., Taly, V., Ryckelynck, M., El-Harrak, A., Frenz, L., Rick, C., Samuels, M. L., Hutchison, J. B., Agresti, J. J., Link, D. R., Weitz, D. A., and Griffiths, A. D. (2009) Fluorescence-activated droplet sorting (FADS): efficient microfluidic cell sorting based on enzymatic activity. *Lab Chip 9*, 1850−8.

(52) Wagner, J. M., Liu, L., Yuan, S.-F., Venkataraman, M. V., Abate, A. R., and Alper, H. S. (2018) A comparative analysis of single cell and droplet-based FACS for improving production phenotypes: Riboflavin overproduction in Yarrowia lipolytica. *Metab. Eng. 47*, 346−356.

(53) Siegele, D. a, and Hu, J. C. (1997) Gene expression from plasmids containing the araBAD promoter at subsaturating inducer concentrations represents mixed populations. *Proc. Natl. Acad. Sci. U. S. A. 94*, 8168−72.

(54) Khlebnikov, A., Skaug, T., and Keasling, J. D. (2002) Modulation of gene expression from the arabinose-inducible araBAD promoter. *J. Ind. Microbiol. Biotechnol. 29*, 34−7.

DOI:10.1021/acssynbio.9b00149
ACS Synth. Biol. 2019, 8, 1847−1857

2.1.2. Displaced by deceivers - Supporting information

Displaced by deceivers - Prevention of biosensor cross-talk is pivotal for successful biosensor-based high-throughput screening campaigns

Lion Konstantin Flachbart[1], Sascha Sokolowsky[1] and Jan Marienhagen[1,2,*]

[1]Institute of Bio- and Geosciences, IBG-1: Biotechnology, Forschungszentrum Jülich, D-52425 Jülich, Germany

[2]Institute of Biotechnology, RWTH Aachen University, Worringer Weg 3, D-52074 Aachen, Germany

* To whom correspondence should be addressed.
Tel: +49 2461 61 2843; Fax: +49 2461 61 2710; Email: j.marienhagen@fz-juelich.de

Supplementary Table S1. Strains and plasmids used in this study.

Strain or plasmid	Relevant characteristics	Reference or source
E. coli DH5α	F⁻ φ80d*lacZ*ΔM15 Δ(*lacZYA-argF*)U169 *rec* A1 *end* A1 *hsd*R17 ($r_K^-m_K^+$) *pho*A *sup*E44 *thi*-1 *gyr*A96 *rel*A1 λ⁻	Invitrogen
E. coli TOP10	F⁻ *mcr*A Δ(*mrr-hsd*RMS-*mcr*BC) φ80*lac*ZΔM15 Δ*lac*X74 *rec*A1 *ara*D139 Δ(*ara-leu*) 7697 *gal*U *gal*K *rps*L (Str^R) *end*A1 *nup*G λ⁻	Invitrogen
E. coli DH10B	F⁻ *mcr*A Δ(*mrr-hsd*RMS-*mcr*BC) φ80*lac*ZΔM15 Δ*lac*X74 *rec*A1 *end*A1 *ara*D139 Δ(*ara, leu*)7697 *gal*U *gal*K λ⁻ *rps*L *nup*G	Invitrogen
E. coli BL21(DE3)	F⁻ *omp*T *hsd*SB (rB–, mB–) gal dcm rne131 (DE3)	Invitrogen
E. coli DH10B Δ*hcaREFCBD*	F⁻ *mcr*A Δ(*mrr-hsd*RMS-*mcr*BC) φ80*lac*ZΔM15 Δ*lac*X74 *rec*A1 *end*A1 *ara*D139 Δ(*ara, leu*)7697 *gal*U *gal*K λ⁻ *rps*L *nup*G Δ*hcaREFCBD*	this work
pSIJ8	Plasmid enabling L-arabinose inducible expression of λ red recombineering genes *bet*, *gam* and *exo*. L-rhamnose inducible expression of *flp* recombinase gene.	(1)
pBBR1N-reporter-EYFP	Biosensor chassis plasmid with the *eyfp* reporter gene, Kan^R	Markus Schallmey, unpublished
pSenCA	Transcriptional biosensor construct inducing *eyfp* expression in response to the presence of *trans*-cinnamic acid or phenylpropionic acid, Kan^R	This work
pBAD/myc-His A	Cloning vector for the synthesis of His_6-tagged (c-terminal) fusion protein, Amp^R	Invitrogen
pCBJ296	pCDFDuet-1 MCS2::xal_{Tc}, Sp^R	(2)
pBAD-xal_{Tc}	Cloning vector for Xal_{Tc} protein synthesis, Amp^R	This work
pBAD-N6XHIS	Cloning vector for the synthesis of His6-tagged (n-terminal) protein, Amp^R	This work
pBAD-N6XHIS-xal_{Tc}	Cloning vector for the synthesis of His6-tagged (n-terminal) Xal_{Tc} fusion protein, Amp^R	This work

Supplementary Table S2. Oligonucleotides used in this study. Relevant restriction sites are underlined.

Primer name	Sequence	Resulting plasmid
fw_amp_hcaRE'	AATAATGAGCTCTTATGCCGTTACGCTTGCCA	pSenCA
rv_amp_hcaRE'	GAGTGAAAGCTTGGCATGCGGTGTCAATCAGTTGGTAAATGTTC	
fw_amp_xalTc	TTCATCGAAACCAATGTTGCAAAACC	pBAD-*xal*$_{Tc}$/ pBAD-*xal*$_{Tc}$ epPCR library
rv_amp_xalTc	TTAAAACATTTTACCAACTGCACCCATC	
fw_amp_pBAD	CAGTTGGTAAAATGTTTTAAAGAAGATTTTCAGCCTGATACAGATTAAATCAG	
rv_amp_pBAD	GCAACATTGGTTTCGATGAACATGGTTAATTCCTCCTGTTAGCC	
fw_amp_pBAD_N-6×HIS	CGCAGTCCATGGCGCAGTCTCGAGCTTGGCTGTTTTGGCGGATG	pBAD-N6XHIS
rv_amp_pBAD_N-6×HIS	ACTGCGCCATGGAGTGATGATGATGATGATGGCTGCCGCTCATGGTTAATTCCTCCTGTTAG	
fw_amp_6xH_xalTc	ATCATCATCATCATCACTCCATGTTCATCGAAACCAATGTTGC	pBAD-N6XHIS--*xal*$_{Tc}$
rv_amp_6xH_xalTc	ATCCGCCAAAACAGCCAAGCTTAAAACATTTTACCAACTGCACCC	

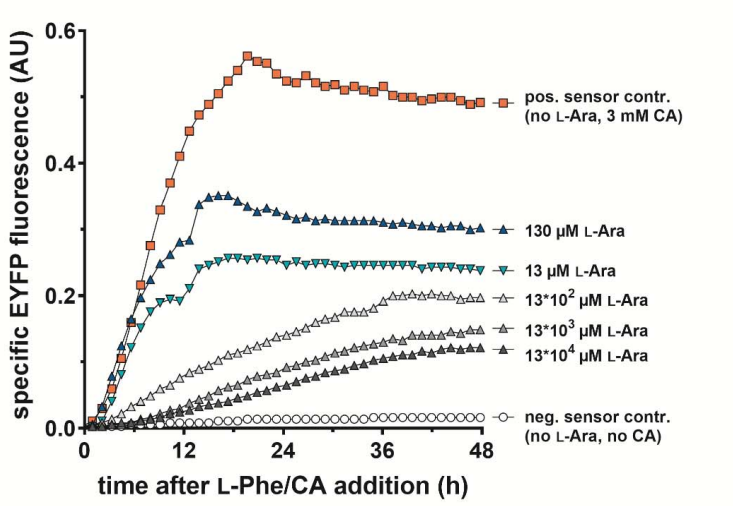

Supplementary Figure S1. Performance of the *E. coli* pSenCA pBAD-*xal*$_{Tc}$ system. After cultivation for 3 h in presence of the L-arabinose concentrations depicted in the legend, either 3 mM L-phenylalanine (circles and triangles) or 3 mM CA (squares) were added. Specific fluorescence response is shown (EYFP fluorescence×biomass formation^{-1}, arbitrary units). Abbreviations: CA, *trans*-cinnamic acid; L-Ara, L-arabinose; L-Phe, L-phenylalanine.

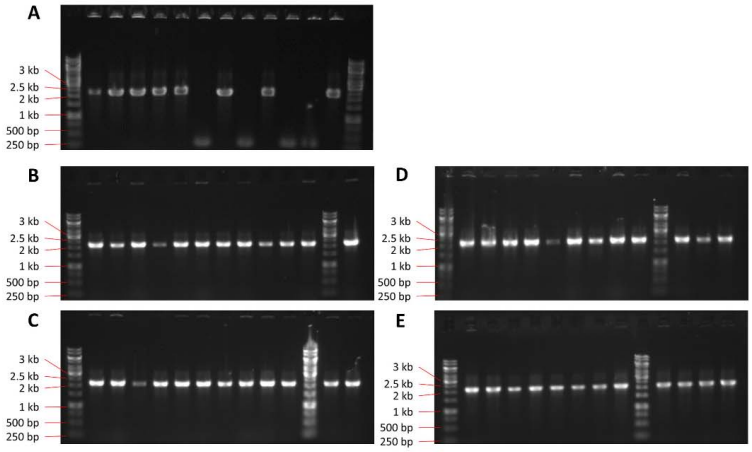

Supplementary Figure S2. Influence of the inoculum size (iOD_{600}) on producer isolation efficiency. Overall aim was the identification of suitable assay conditions for the exclusive isolation of *E. coli* pSenCA pBAD-*xal*$_{Tc}$ (CA^+-cells) from mixtures with *E. coli* pSenCA pBAD (CA^--cells). All cultivations were performed in the in presence of 13 µM L-arabinose for induction of heterologous *xal*$_{Tc}$ expression and 3 mM L-Phe as XAL-substrate was always added three hours after starting each cultivation. Fluorescence-activated cell sorting of the upper 5 % of fluorescent cells was performed five hours after substrate addition. DNA fragments amplified via PCR from isolated cells indicate pBAD (295 bp) or pBAD*xal*$_{Tc}$ (2,203 bp) presence, respectively. **(A)** Preliminary experiment with an iOD_{600} of 0.5 and 50%/50% ratio of CA^+/CA^--cells; **(B)** iOD_{600} of 0.02 and 50%/50% ratio of CA^+/CA^--cells; **(C)** iOD_{600} of 0.004 and 50%/50% ratio of CA^+/CA^--cells; **(D)** iOD_{600} of 0.02 and 20%/80% ratio of CA^+/CA^--cells; **(E)** iOD_{600} of 0.004 and 20%/80% ratio of CA^+/CA^--cells.

Supplementary Table S3. Overview of all *xalTc*-variants isolated in the FACS campaign, which were subsequently characterized in detail. Identified mutations are in the open reading frame of *xalTc*, the *xalTc*-promoter, P_{araBAD} and P_{araC}, the promoter of the *araC* gene (encoding the AraC regulator, controlling expression from the P_{araBAD} promoter), respectively. The *araC* gene did not carry mutations in any isolated plasmid. Mutations leading to AAS are highlighted in bold. Additionally, the relative CA accumulation of the mutants after isolation and after retransformation into *E. coli* DH10B Δ*hcaREFCBD* is given. Relative CA production after FACS isolation of the respective variants is given as mean of three cultivations and relative CA production after retransformation is given as mean of three biological replicates, the error is depicted as standard deviation. Abbreviations: AAS, Amino acid substitution(s); CA, *trans*-cinnamic acid.

mutations in *xalTc*	AAS in XalTc	Mutations in P_{araC} & P_{araBAD}	Relative CA production after isolation (% XalTc)	Relative CA production after retransformation (% XalTc)
t363c, **t821c**	V274A		122 ± 0.8	122 ± 6
t570c, **a1804g**	K602E		123 ± 0.9	115 ± 5
t20c, t1161c, **a1391g**, t1812c	V7A, N464S	g95a	123 ± 0.1	110 ± 2
c594t, **t821c**, **a1783t**	V274A, N595S		123 ± 0.7	120 ± 8
a1725g, **a1756g**, a1821g	M586V		132 ± 0.5	128 ± 8
t821c	V274A		134 ± 1.1	122 ± 5
g1731a, **a1778t**, t1839a	D593V		135 ± 1.3	125 ± 4
T499c, t567a, **a1806t**	F167L, K602N		136 ± 0.8	139 ± 6
a250g, **t821c**, t918c	K84E, V274A		137 ± 1.8	137 ± 2
a45g, a324g, g1365a, **a1391g**, **t1568a**, t1839g	N464S, V523E		138 ± 1.1	136 ± 5
t306c, **a1724g**, **a1756g**, t1839c, t1875c	K575R, M586V		138 ± 1.1	123 ± 6
g125t, a1185g, t1839c	S42I	t175a	139 ± 0.6	136 ± 1
g125t, a1185g, t1839c	S42I	t175a	141 ± 1.6	137 ± 2
t987c, **t1568a**, **a1805c**	V523E, K602T		141 ± 1.7	132 ± 4
t1655c, **a1806c**	I552T, K602N		141 ± 1.6	131 ± 5
t821c, t1836c	V274A		143 ± 0.9	137 ± 3
a250g, **t821c**, t918c	K84E, V274A		143 ± 0.9	129 ± 4
t306c, **a1724g**, **a1756g**, t1839c, t1875c	K575R, M586V		144 ± 0.3	113 ± 4
t1655a	I552N	a34g	146 ± <0.1	159 ± 2
t499c, t1299c, **a1762c**, t1839a	F167L, N588H		148 ± 0.7	144 ± 7

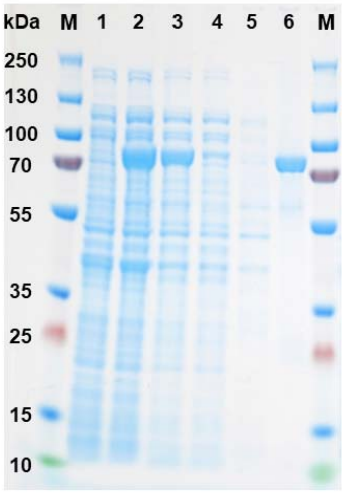

Supplementary Figure S3. SDS-PAGE analysis of a typical Xal_{Tc} purification conducted for all variants, which were characterized in more detail. Molecular weight of N-terminally His-tagged Xal_{Tc} is 74.8 kDa. Abbreviations: M, PAGE Ruler Plus Prestained protein ladder; 1, Whole cells, uninduced heterologous gene expression; 2, Whole cells, induced heterologous gene expression; 3, Crude cell extract, induced heterologous gene expression; 4, Flow through affinity chromatography; 5, Wash fraction; 6, Elution fraction.

References:

1. Jensen,S.I., Lennen,R.M., Herrgård,M.J. and Nielsen,A.T. (2015) Seven gene deletions in seven days: Fast generation of Escherichia coli strains tolerant to acetate and osmotic stress. *Sci. Rep.*, **5**, 17874.

2. Jendresen,C.B., Stahlhut,S.G., Li,M., Gaspar,P., Siedler,S., Förster,J., Maury,J., Borodina,I. and Nielsen,A.T. (2015) Novel highly active and specific tyrosine ammonia-lyases from diverse origins enable enhanced production of aromatic compounds in bacteria and yeast. *Appl. Environ. Microbiol.*, 10.1128/AEM.00405-15.

2.2. Development of a biosensor platform for phenolic compounds using a transition ligand strategy

2.2.1. Biosensor platform development - Manuscript

Development of a biosensor platform for phenolic compounds using a transition ligand strategy

Lion Konstantin Flachbart[1], Christoph Gertzen[2,3], Holger Gohlke[2,3] and Jan Marienhagen[1,4,*]

[1]Institute of Bio- and Geosciences, IBG-1: Biotechnology, Forschungszentrum Jülich, D-52425 Jülich, Germany

[2]Institute for Pharmaceutical and Medicinal Chemistry, Heinrich Heine University Düsseldorf, Universitätsstr. 1, 40225 Düsseldorf, Germany

[3]John von Neumann Institute for Computing (NIC), Jülich Supercomputing Centre (JSC) and Institute for Complex Systems – Structural Biochemistry (ICS-6), Forschungszentrum Jülich GmbH, 52425 Jülich, Germany

[4]Institute of Biotechnology, RWTH Aachen University, Worringer Weg 3, D-52074 Aachen, Germany

* To whom correspondence should be addressed.

Tel: +49 2461 61 2843; Fax: +49 2461 61 2710; Email: j.marienhagen@fz-juelich.de

Abstract

A major drawback in metabolic engineering is the often time consuming and laborious characterization of individual strain designs with regard to production performance. In recent years, the introduction of biosensors enables the conversion of an otherwise inconspicuous production phenotype into a readily detectable, semi-quantitative output signal, which allows for a rapid characterization of many strains within a short time frame. Nature's repertoire of transcription regulators is extensive; nevertheless, for many molecules of interest, no specific transcriptional regulator is available. In this study, the ligand specificity of the transcriptional biosensor pSenCA, originally developed for the detection of the biotechnologically interesting phenylpropanoid *trans*-cinnamic acid, was initially engineered towards sensing a broad range of different high-value aromatic compounds following a semi-rational transition ligand approach. The ligand binding domain of the transcriptional regulator HcaR of the resulting biosensor variant pSenGen was randomly and semi-rationally mutated and screened for a biosensor response in the presence of four different small aromatic compounds using fluorescence-activated cell sorting. A set of different biosensor variants was isolated, comprising variants with altered specificity toward 4-hydroxybenzoic acid, 6-methyl salicylic acid, *p*-coumaric acid 5-bromoferulic acid The engineered biosensors can be readily applied in metabolic engineering and protein engineering campaigns.

KEYWORDS: transcriptional biosensor, library screening, specificity alteration, fluorescence-activated cell sorting, protein engineering, directed evolution

Introduction

Directed evolution of enzymes and mutagenesis of microbial production strains are widely used approaches to improve enzyme activity, specificity, stability or strain productivity. The introduction of mutations constitutes an option to improve the desired trait when rational methods are not applicable (*e.g.* structural information is not available) or do not allow further increase in product formation. Certainly, only a miniscule fraction of mutagenesis libraries harbors advantageous mutations. Hence, the isolation of the desired mutants is either very costly when massive multiplexing approaches are used, or the screened variants represent only a spare fraction of the variant space present in the library. (Arnold, 2018; Zeymer and Hilvert, 2018) Increasingly, transcriptional biosensors are applied to screen mutant libraries. (Schallmey et al., 2014) Here, a regulator specifically binds the product of interest or an intermediate of the pathway towards the product, enabling the expression of a reporter or resistance gene, ideally in a dose-responsive manner, facilitating the isolation of cells carrying desired traits. In combination with fluorescence-activated cell sorting (FACS), this enables throughputs orders of magnitude higher than other screening methods.

If no biosensor for the molecule of interest is available, transcriptome analysis can identify suitable promoter regions to construct biosensors. (Shi et al., 2017) Furthermore, global and species-specific databases allow for excessive data mining for identifying suitable TF/promoter pairs. (Abreu et al., 2015; Keseler et al., 2013; Munch et al., 2003; Novichkov et al., 2013; Salgado et al., 2006; Wilson et al., 2008) Another strategy is the alteration of TF specificity towards the compound of interest. Successful examples for this approach are campaigns to alter the ligand specificity of AraC and LacI from *Escherichia coli* (*E. coli*). AraC, naturally accepting L-arabinose, was engineered to accept D-arabinose, mevalonate, ectoine, triacetic acid lactone, vanillin or salicylic acid, respectively. (Chen et al., 2015; Frei et al., 2018; Tang et al., 2013, 2008; Tang and Cirino, 2011) LacI, known to repress the *lac* operon in absence of allolactose or Isopropyl-β-D-thiogalactopyranoside (IPTG) was engineered to accept D-fucose, lactitol, sucralose or gentiobiose. (Taylor et al., 2015) In these examples, the crystal structure of the target protein in complex with its native inducer molecule were available, enabling the rational mutagenesis of the target regulator. In another example, the TF PobR from *Acinetobacter* sp. ADP1 was engineered towards acceptance of 3,4-hydroxybenzoate. (Jha et al., 2015) As no crystal structure was available for this study, residues for targeted mutagenesis were identified using a homology model that was constructed *ab initio* using Rosetta computational modelling.

Previously, we constructed the transcriptional biosensor pSenCA for the transduction of intracellular accumulation of *trans*-cinnamic acid (CA) into *eyfp* expression and applied it for the directed evolution of an aromatic amino acid ammonia lyase towards increased CA

production in *E. coli*. In this study, we seized to establish biosensors with altered specificity profiles relative to the pSenCA biosensor by engineering the TF HcaR in two rounds of directed evolution employing FACS. As biotechnologically interesting novel ligands 4-hydroxy benzoic acid (4HBA), *p*-coumaric acid (4HCA), 5-bromoferulic acid (5BFA) and 6-methylsalicilic acid (6MSA) were selected. Isolated biosensor variants for this ligands were characterized in detail.

Material and Methods

Bacterial strains, plasmids, media and growth conditions

All bacterial strains and plasmids used in this study and their relevant characteristics are listed in supplementary table S1. For recombinant DNA work and library construction, *E. coli* TOP10 (Thermo Fisher Scientific, Waltham, MA, USA) was used. All chemicals were purchased from Sigma Aldrich (St. Louis, MO, USA) or abcr GmbH (Karlsruhe, Germany). For recovery after electroporation, super optimal broth with catabolite repression (SOC) was used (20 g/l tryptone, 5 g/l yeast extract, 0.6 g/l NaCl, 0.2 g/l KCl, 10 mM $MgCl/MgSO_4$ and 20 mM glucose, pH 7). All strains were routinely cultivated at 37 °C in Lysogeny broth (LB) medium (10 g/l tryptone, 10 g/l NaCl and 5 g/l yeast extract). (BERTANI, 1951) Kanamycin (25 µg/ml) was used for selective propagation of pSenCA. Kanamycin stocks were prepared as 1000 × stocks in purified water and sterile filtered using a 200 nm filter. Target ligands were always prepared fresh as 100 × stocks in DMSO.

Online monitoring of growth and formation of fluorescence was performed in 48 well microtiter FlowerPlates (MFPs) using the BioLector cultivation system (m2p-labs GmbH, Baesweiler, Germany) (Funke et al., 2009; Kensy et al., 2009). Formation of biomass was recorded as the backscatter light intensity (wavelength 620 nm; signal gain factor 25). The enhanced yellow fluorescence protein (EYFP) fluorescence was measured as fluorescence emission at 532 nm (signal gain factor of 30) after excitation at a wavelength of 510 nm. Specific fluorescence was calculated as 532 nm fluorescence per 620 nm backscatter using Biolection software version 2.2.0.6 (m2p-labs GmbH, Baesweiler, Germany).

Molecular biology

Techniques for DNA manipulation were performed according to standard protocols.(Sambrook and Russel, 2001) Enzymes were used following the manufacturer's recommendations and obtained from Thermo Fisher Scientific (Waltham, MA, USA), except for Phusion High-Fidelity DNA polymerase, taq DNA ligase and T4 exonuclease, which were purchased from New England Biolabs (Ipswich, MA, USA). Genes were amplified by PCR using Pfu UltraII polymerase (Agilent, Santa Clara, CA, USA) following the manufacturer's recommendation if not stated otherwise. Cloning of amplified PCR products was performed using Gibson assembly (Gibson et al., 2009). Synthesis of oligonucleotides and sequencing of

DNA using Sanger sequencing were performed by Eurofins MWG Operon (Ebersberg, Germany). All oligonucleotides used in this study are listed in supplementary table S2.

Library construction

For error-prone libraries, the *hcaR* gene was amplified from plasmid pSenCA using the Clontech Diversify kit (Takara Bio Europe, Saint-Germain-en-Laye, France) incorporating 2.3 mutations/kb and assembled with *hcaR*-deficient pSenCA plasmid by performing Gibson assembly. For site-saturation mutagenesis (SSM), the pSenCA plasmid (6076 bp) was amplified using primers carrying degenerate codons in a PCR reaction using PfuUltra II polymerase (75 ng template DNA, 50 µl total volume, 10 pmol of each primer, 20 cycles, 300 s initial denaturation, 20 s denaturation, 20 s annealing, 372 s elongation, 420 s final elongation). Following all PCR amplifications, template plasmid removal was performed using 1 µl of Anza 10 *Dpn*I for overnight digestion at 37 °C. Plasmid libraries were purified using Nucleospin Gel and PCR Clean-up (Macherey-Nagel, Düren, Germany) and transformed into One Shot TOP10 electrocompetent *E. coli* cells following the manufacturer's recommendations (Thermo Fisher Scientific, Waltham, MA, USA). After one hour of regeneration, the cell suspensions were transferred into 50 ml LB medium and incubated for 20 h (37 °C, 120 rpm). The culture broths were used to prepare concentrated (5-fold) glycerol stocks that were snap frozen in 100 µl aliquots for single use. Appropriate library sizes for at least 3-fold coverage were confirmed by streaking serial dilutions of the regeneration cultivation on selective agar. Using the GLUE-IT algorithm, library completeness ranging from 95 % to 100 % was confirmed. (Firth and Patrick, 2008, 2005; Patrick et al., 2003)

Cytometry and Fluorescence activated cell sorting (FACS)

Fifteen (15) ml LB medium was inoculated with 100 µl glycerol stock and cultivated (16 h, 37 °C, 120 rpm). The preculture was diluted 1/100 in 15 ml LB medium and incubated (1 h, 37 °C, 120 rpm) to induce exponential growth. Afterwards, 891 µl portions of the culture were transferred into 48 well flower plate (m2p-labs GmbH, Baesweiler, Germany) wells containing 9 µL 100× stock of the target ligand of choice. The plates were sealed and incubated for 20 h in a Multitron Pro HT Incubator (Infors AG, Bottmingen, Suisse, 37 °C, 900 rpm, 75 % humidity, 3 mm throw). (Funke et al., 2009; Kensy et al., 2009) Single-cell size- and fluorescence characteristics were determined and cell sorting was performed utilizing a BD FACSAria II cell sorter (BD Biosciences, Franklin Lakes, NJ, USA) equipped with a 70 µm nozzle and using a sheath pressure of 70 psi. Excitation was performed using a 488 nm blue solid laser. Forward-scatter characteristics (FSC) were recorded as small-angle scatter and side-scatter characteristics (SSC) were recorded as orthogonal scatter of the 488-nm laser. A 502 nm long-pass, 530/30 nm band-pass filter combination enabled EYFP fluorescence detection. Prior to data acquisition, debris and electronic noise were excluded from the analysis by electronic gating in the FSC-H against SSC-H plot. Additional gating was performed on the resulting population in the FSC-H against FSC-W plot to exclude doublets. Fluorescence

acquisition was always performed with the population resulting from this two-step gating. Prior to measuring/sorting, cells were diluted to an OD_{600} below 0.1 where necessary using YNB base buffer (6 g/l K_2HPO_4, 3 g/l KH_2PO_4 and 10 g/l 3-(N-morpholino)propanesulfonic acid (MOPS), pH 7), filtered using 50 µm Cup-type filters (BD Biosciences, Franklin Lakes, NJ, USA) and analyzed. For positive sorts, the upper 5 % of most fluorescent cells were sorted, while negative sorting was performed by isolation of cells with fluorescence equivalent to the bottom 96 % of an *E. coli* TOP10 pSenCA culture without ligand supplementation. Routinely, 200,000 cells were sorted into 5 ml reaction tubes (Eppendorf AG, Hamburg, Germany), prefilled with 3 ml SOC medium using an in-house built adapter for 5 ml reaction tubes described previously. (Freiherr von Boeselager et al., 2018) To minimize residual sheath fluid in the recovery tube, sorted cells were centrifuged (10 min, 3,000 × g, 4 °C), after removal of 3 ml supernatant, 4.5 ml fresh SOC medium was added. To reduce post sorting stress for the isolated variants, cells were regenerated for 30 min (37 °C, 170 rpm) without antibiotics. Afterwards, the cells were transferred into 10 ml LB medium containing appropriate antibiotic and the cell suspension was cultivated (20 h, 37 °C, 170 rpm). The next day, the cells were used to prepare glycerol stocks and to inoculate precultures for subsequent FACS steps. Sort precision was always set to purity setting and the total event rate while sorting never exceeded 16,000 events per second. FACSDiva 7.0.1 (BD Biosciences, San Jose, USA) was used for FACS control and data analysis. FlowJo for Windows 10.4.2 (FlowJo, LLC, Ashland, OR, USA) was used to generate high-resolution graphics of the obtained FACS data for visualization.

Rescreening and characterization of isolated biosensor variants

Following FACS screening, the regeneration cultures were spread on selective agar plates. Single colonies were picked to inoculate 200 µl LB medium in 96 well V-bottom plates (BRAND GMBH + CO KG, Wertheim, Germany). Precultures were cultivated for 18 h in a Multitron Pro HT Incubator (Infors AG, Bottmingen, Suisse, 37 °C, 900 rpm, 75 % humidity, 3 mm throw). Of these precultures, 10 µl were used to inoculate 990 µl LB medium followed by 20 h of cultivation with parameters as above. Subsequently, 11 µl preculture were used to inoculate 1089 µl LB medium in a Deepwell plate (96/2000 µL, PCR clean, Eppendorf AG, Hamburg, Germany). After 2 h of cultivation using the same parameters as described above, 495 µl were transferred to two fresh deepwell plates containing 5 µl of a 100× stock solution of the respective target ligand. After 20 h of cultivation (same parameters as above), 100 µl of the culture broth was transferred to a 96 well Flat-bottom plates (BRAND GMBH + CO KG, Wertheim, Germany) and the absorbance and fluorescence were determined using a M100 plate reader (Tecan Group, Maennedorf, Switzerland; $absorbance_{600\ nm}$; $fluorescence_{530nm}$ after excitation at 500 nm, gain 65). Absorbance as well as fluorescence of cell free medium was used for background subtraction of all samples.

Bioinformatic methods

For the DNA sequence analysis of isolated *hcaR* variants, all DNA sequences obtained from Eurofins MWG Operon were aligned with the original sequence for identifying single nucleotide polymorphisms using the Clonemanager Professional software, version 9.51 (Scientific & Educational Software, Denver, CO, USA). Identification of mutagenesis targets and preparation of protein structures was performed using PyMOL Molecular Graphics System 0.99 (DeLano Scientific LLC, South San Francisco, CA, USA). (DeLano, 2005, 2002) Prism 8.02 (GraphPad Software, San Diego, CA, USA) was used for diagram preparation.

Results and Discussion

The transcriptional biosensor pSenCA for *E. coli* comprises the regulatory elements of the *hca* cluster from *E. coli*, which involved in the catabolization of phenylpropionic acid (PP) and *trans*-cinnamic acid (CA). (Díaz et al., 2001) In presence of intracellular PP or CA, HcaR induces transcription from the P_{hcaE} promoter, resulting in EYFP formation. The phenylpropanoid *p*-coumaric acid (4HCA) acid does not induce the sensor response albeit it's structural similarity to CA, a native inducer of HcaR (Figure 1 B). For this work, the expansion of the detection repertoire of pSenCA, harboring the wild type HcaR regulator ($HcaR^{WT}$) gene, was of interest. The interest in optimizing enzymes of their respective synthesis route in microbial production strains was the basis for the selection of three target ligands, namely 4HCA, 4-hydroxybenzoic acid (4HBA) and 6-methylsalicylic acid (6MSA). Additionally, a ferulic acid derivative carrying a bromine substitution in *ortho* position (5BFA) was chosen with regard to its extraordinary substitution pattern and the possibility to carry out palladium-catalyzed cross-coupling of the bromine group. (Aschenbrenner et al., 2018) The structures of all ligands used in this project are depicted in Figure 1 B.

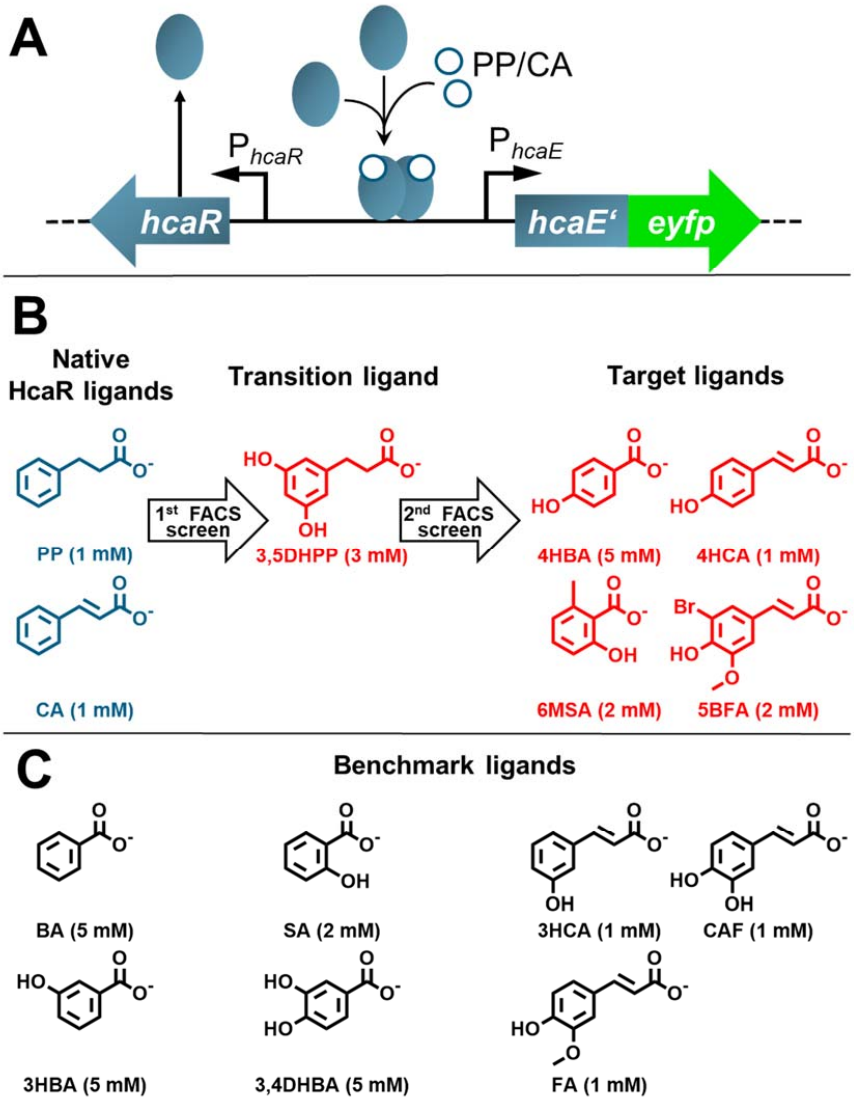

Figure 1: (A) The pSenCA biosensor. The regulator gene *hcaR* is constitutively expressed, upon binding of PP or CA, HcaR activates transcription of *hcaE'* and *eyfp*. **(B)** Structures of the native HcaR ligands PP and CA (shown in blue) and all ligands used for FACS screening (shown in red). **(C)** Structures of ligands used for the characterization of biosensor constructs. Representation in B and C) is based on structures at physiological pH. Concentrations used in all assays is listed in brackets. **Abbreviations:** PP, phenylpropionic acid; CA, *trans*-cinnamic acid; 3,5DHPP, 3,5-dihydroxyphenylpropionic acid; 4HCA, *p*-coumaric acid; CAF, caffeic acid; FA, ferulic acid; 5BFA, 5-bromoferulic acid; BA, benzoic acid; SA, salicylic acid; 6MSA, 6-methylsalicylic acid; 3HBA, 3-hydroxybenzoic acid; 4HBA, 4-hydroxybenzoic acid; 3,4DHBA, 3,4-dihydroxybenzoic acid.

Therefore, the specificity of $HcaR^{WT}$ was assayed using the four target ligands and a set of seven benchmark ligands in addition to the two native ligands PP and CA (Figure 1 B and C). As host strain, the previously constructed *E. coli* DH10BΔ*hcaREFCBD* strain (*E. coli* Δ*hca)* was used as it does not carry the *hca* operon responsible for the first steps of PP and CA degradation. (Díaz et al., 1998; Flachbart et al., 2019; Turlin et al., 2001) Interestingly, $HcaR^{WT}$ exhibits a clear preference for PP and CA, exhibiting 120-fold induction and 60-fold induction of specific EYFP fluorescence, respectively (Figure 2 A). Remarkably, the only other ligand triggering a response >10 was 6-methylsalicylic acid (6MSA), resulting in an 11-fold induction of the fluorescence signal underlining the high specificity of HcaR.

Regulation and function of the *hca* operon in *E. coli* has been studied in detail, but to the best of our knowledge, no structural information regarding the ligand binding site or the ligand binding mode of HcaR is available. (Díaz et al., 1998; Turlin et al., 2005, 2001) In order to identify the ligand binding site, an *ab initio* homology model of HcaR was constructed using the I-Tasser suite. (Roy et al., 2010; Yang et al., 2015; Zhang, 2008) Judged by a secondary structure analysis using the blastp suite (https://blast.ncbi.nlm.nih.gov/Blast.cgi) and the PROSITE database (https://prosite.expasy.org/prosite.html), HcaR, with a length of 296 amino acid, belongs to the LysR type transcriptional regulator (LTTR) family. (Marchler-Bauer et al., 2017, 2015, 2011; Marchler-Bauer and Bryant, 2004; Sigrist et al., 2013, 2005, 2002) The N-terminal DNA-binding domain (residues 1-58) of HcaR is characterized by a typical N-terminal helix-turn-helix (HTH) motif and the large ligand-binding domain is spanning from residue 90 to 292. One of the top 10 threading templates for the HcaR homology model construction, a mutant (R156H) of the ligand binding domain of the regulator CatM (PDB code: 3GLB) from *Acinetobacter baylyi* ADP1, was resolved as a homotetramer, each of the monomers binding one muconic acid molecule. (Craven et al., 2009) The structure of a CatM monomer with muconic acid, which is located in a cavity close to the protein surface was extracted from the 3GLB file and aligned with the HcaR homology model. Following the assumption that the ligand binding site for CA of HcaR is in the same location as the muconic acid binding site in CatM, we identified all residues that protrude in direction of the presumed ligand binding site, namely T128, P195, V196, Y197, S198, G199, S200, L201, V97, P98 (Figure 2 B). Additionally, the residues E101, V102, N224, I225 and L226 were selected as they form the bottom of the surmised binding cleft. In total, seven libraries were constructed, and up to three neighboring residues were saturated in parallel using site-saturation mutagenesis (Figure 2 B).

Screening of saturation libraries in presence of 3,5DHPP identified a promiscuity hotspot in the HcaR ligand binding domain.

In a first step towards HcaR variants with altered specificity, we planned to conduct a screening for HcaR variants that exhibit a less stringent ligand profile than HcaR, which would be then engineered towards different aromatic ligands of interest. For this, 3,5-dihydroxyphenylpropionic acid (3,5DHPP) was selected as “transition ligand” to isolate such variants with a generally broadened ligand profile. The propane tail of 3,5DHPP allows for the rotation of the molecule between alpha and beta carbon and presence of the two hydroxy groups of the aromatic ring in meta-position demand a larger binding pocket in comparison to the natural ligands PP and CA (Figure 1 B).

The seven biosensor libraries were pooled and three successive rounds of FACS were conducted. In each round, 3,5DHPP was supplemented and 200,000 cells were sorted using a gate that corresponds to the upper 5 % of all fluorescent cells in each round. Following this FACS enrichment, 96 single variants were cultivated without 3,5DHPP addition to keep track on the possible occurrence of biosensor variants giving a fluorescence response in absence of any ligand. The 22 strains carrying biosensors with the lowest basal response were assayed regarding fluorescence response to 3,5DHPP in microtiter plates. Sequencing of the *hcaR* gene of these 22 variants revealed six different groups of mutants in the set, all carrying mutations in the codons E101 and V102 of the ligand binding domain (supplementary table S2). As consequence of these mutations E101 was exchanged to relatively small, either neutral or negatively charged amino acids (C, S, A or T) in five variants, whereas V102 was substituted by L-phenylalanine in all cases. The sixth mutant group was the most frequent, carrying E101H and V102Y. As these mutants showed the highest fold induction in presence of 3 mM 3,5DHPP, *hcaR*_E101H,V102Y was subcloned into a new pSenCA plasmid (Using *Sac*I and *Hind*III) to exclude any possible mutations in the vector backbone, retransformed into *E. coli* Δ*hca* and characterized with regard to the response to different ligands (PP, CA, 3HCA, 4HCA, CAF, FA, 5BFA, BA, 3HBA, 4HBA, 3,4DHBA, SA and 6MSA) (Figure 1 B). The biosensor carrying the regulator variant HcaR_E101H,V102Y exhibited a reduced fold induction in presence of PP and CA while the response to 4HCA, FA, BA, 3HBA, SA and 6MSA was significantly increased (Figure 2 C). Due to its wider acceptance profile in comparison to pSenCA, it was named pSenGeneral and used as starting biosensor for further work. The mutations E101H and V102E were integrated into the HcaR homology model and their influence on the protein structure was assessed. In HcaR, V102 and I225 constrain the binding cleft by alignment towards each other. In HcaR_E101H,V102E, this alignment is missing, as E102Y rotates towards M245. This results in a widening of the estimated binding cleft and renders M245 accessible (supplementary Figure S 1).

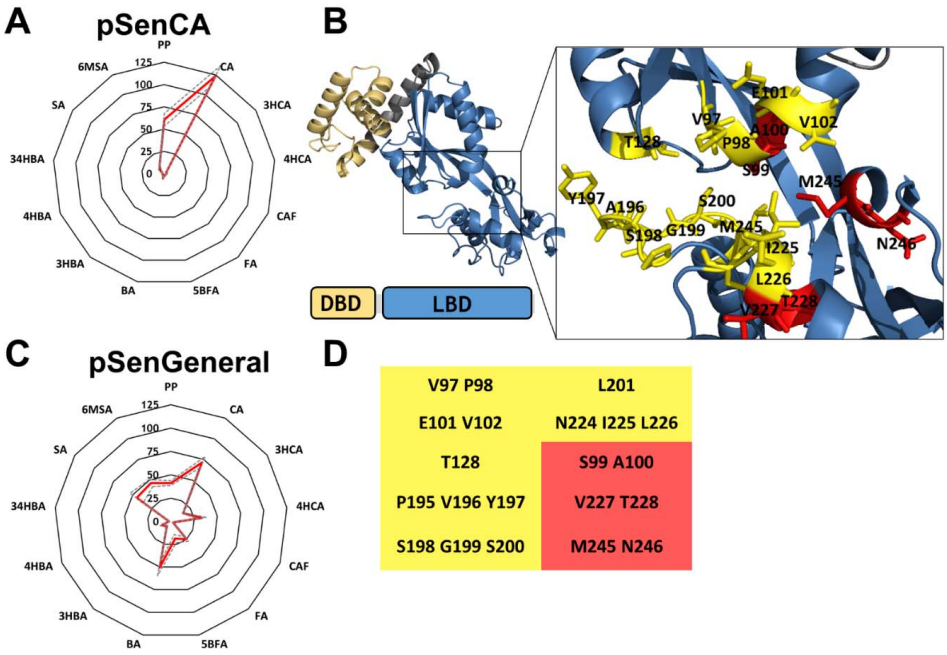

306

307 **Figure 2: Identification of a promiscuity hotspot in HcaR. (A)** Specificity profile of pSenCA is shown
308 for 13 different aromatic compounds. Red line depicts mean fold induction in specific EYFP fluorescence
309 of three biological replicates, grey dotted lines depict the respective standard deviation. **(B)** Predicted
310 structure of *E. coli* HcaR in cartoon representation. The DNA binding domain is shown in pale yellow
311 while the ligand binding domain is shown in blue. Overview of the complete structure (left) and a close
312 up of the conjectured ligand binding cleft (right). Residues targeted for SSM are highlighted and labelled.
313 Yellow colouring depicts the initial target set used to broaden the specificity profile of pSenCA, yielding
314 pSenGeneral, red depicts additional targets in the second FACS screening campaign. **(C)** Specificity
315 profile of pSenGeneral for 13 different aromatic compounds. Red line depicts mean fold induction in
316 specific EYFP fluorescence of three biological replicates, grey dotted lines depict standard deviation.
317 **(D)** All residues in the HcaR ligand binding domain targeted for SSM. Simultaneously mutagenized
318 residues are listed together. **Abbreviations:** PP, Phenylpropionic acid; CA, *trans*-cinnamic acid; 3HCA,
319 3-hydroxycinnamic acid; 4HCA, *p*-coumaric acid; CAF, caffeic acid; FA, ferulic acid; 5BFA,
320 5-bromoferulic acid; BA, benzoic acid; 3HBA, 3-hydroxybenzoic acid; 4HBA, 4-hydroxybenzoic acid;
321 3,4DHBA, 3,4-dihydroxybenzoic acid; SA, salicylic acid; 6MSA, 6-methylsalicylic acid; 3,5DHPP,
322 3,5-dihydroxyphenylpropionic acid; DBD, DNA-binding domain; LBD, Ligand binding domain; FACS,
323 Fluorescence-activated cell sorting; SSM, site-saturation mutagenesis..

324 Motivated by the identification of the mutagenic hot spots at positions G101 and V102,
325 the two neighbouring residues P98 and S99 were also targeted by SSM in the following
326 experiments. Moreover, V227 and T228 were selected for mutagenesis for investigating
327 secondary effects on HcaR ligand specificity by reorientation of the preceding residues N224,

I225 and L226 (Figure 2B). Using pSenGeneral as template, all 18 codons were saturated. Concluding that mutagenesis of pSenCA (not carrying the generalist mutations E101H and V102Y) could still yield variants with increased specificity towards the desired aromatic target ligands, the newly identified positions were also saturated in pSenCA again. In addition, considering the enormous throughput capabilities of FACS, an epPCR-based library on basis of both, pSenCA and pSenGeneral, was constructed (2×10^5 variants each) and screened, for identifying additional mutational hot spots contributing to ligand specificity outside of the ligand binding site.

Screening a diverse library for sensor variants responsive to four target ligands

In order to make the screening of all 21 libraries (21 loci in 10 libraries based on *hcaR_WT,* 19 loci in 9 libraries for *hcaR_E101H,V102Y* and two epPCR libraries, Figure 3 A) for mutants responsive to the four target ligands feasible, all libraries were pooled. The complete library, consisting of 2×10^5 variants resulting from saturation mutagenesis and 4×10^5 variants constructed using epPCR, was cultivated without target ligand addition, as a control for the presence of cells constitutively expressing *eyfp*. In addition, cultivations were started with the addition of one target ligand each. As only a few biosensor variants (< 0.1 %) with a strong fluorescence response in the absence of any ligand could be observed during FACS screening without target ligand addition, the combined library was directly used to screen for biosensor response to each of the individual target ligands (Figure 1B). For this, an initial positive sort (top 5 % fluorescent cells) was performed and 200,000 *E. coli* cells carrying a responsive biosensor variant were sorted directly into liquid medium. The sorted cells were cultivated in presence of the respective target ligand and without addition of any target ligand to quantify the proportion of constitutively fluorescent cells after the first sort (Figure 3 B). Roughly, 10 % of the variants in each library showed intermediate fluorescence in absence of any target ligand and thus possessed an undesired phenotype. However, in the cultures where the respective target ligand were added, the majority of cells exhibited strong fluorescence while a minor population (15 % - 35 %) of cells remained at lower fluorescence, which means that these cells also had undesired properties. To further enrich variants with strong fluorescence, another positive sort was performed. The sorted cells were cultivated again with and without target ligand addition. At this point, a strong fluorescence response without addition of any target ligand was detected (Figure 4 B, pseudocolor plot following after sort 2). To remove the variants constitutively expressing *eyfp*, a negative FACS was performed. To further enrich responsive variants, another round of positive- and negative FACS was performed. Upon recultivation, the majority of the remaining cells (> 80 %) in all campaigns

showed a strongly induced fluorescence response in the presence of the respective target ligand (6MSA campaign: median fluorescence 22,969), but also basal fluorescence response level without any supplementation of the aromatic target ligands (6MSA campaign: median fluorescence 227).

Figure 3. FACS-based screening of the constructed *hcaR* libraries. (A) Overview of all libraries that were pooled for the screening. Yellow and red lines depict the approximate positions of saturated amino acids in accordance to Figure 2. Orange lines depict approximate position of pSenGeneral mutations E101HV102Y and green lines depict observed random mutations originating from epPCR libraries. **(B)** Pseudocolor plots of representative data from the 6MSA screening campaign. Both plots on the far left show the pooled, unsorted libraries. Each Arrow depicts one round of FACS enrichment and recultivation. All cultivations were performed with supplementation of 2 mM 6MSA (upper diagrams) to check for population response or without ligand addition (lower diagrams) to examine the amount of false positive cells. The position and size of the green gates (positive sort) was chosen to contain the upper 5 % of all cells in the plot while position and size of the red gate (negative sort) was chosen to contain the lower 96 % of cells carrying the mutation-free sensor pSenCA, cultivated without ligand addition (in the shown example, 7 % of the cells are selected in FES 3 and 50 % of the cells are selected in FES 5 using this gate setting). **Abbreviations:** 6MSA, 6methylsalicylic acid; DBD, DNA-binding domain; FACS, Fluorescence-activated cell sorting; FES, FACS-enrichment sort; FSC-(H), Front scatter signal height; LBD, ligand binding domain; n.d., this cultivation was not performed.

Following the FACS experiments, 184 single clones from each recovery culture after the fifth FACS enrichment step were screened for response to their respective target ligand (Supplementary Figure S2). The sensor plasmid of 24 variants (96 variants in total) showing the highest response for each target ligand were sequenced, retransformed into *E. coli* Δ*hca* and characterized in detail with regard to their response to CA, PP, 4HBA, 4HCA, 5BFA, 6MSA, BA, SA, 3HBA, 3,4DHBA, 3HCA, CAF and FA (Figure 1 B). Observed amino acid substitutions in HcaR are listed in table 1.

Table 1. Amino acid substitutions in the transcriptional regulator HcaR observed in the isolated biosensor variants. The columns "Random mutations" lists due to additional amino acid substitutions found. Sensors in bold letters were subsequently characterized in more detail. **Abbreviations:** 4HCA, *p*-coumaric acid; 4HBA, 4-hydroxybenzoic acid; 5BFA, 5-bromoferulic acid; 6MSA, 6-methylsalicylic acid.

Biosensor variant	Ligand	Residues targeted by SSM										Random mutations
		97	98	99	100	101	102	227	228	245	246	
pSenCA	-	V	P	S	A	E	V	V	T	M	N	
pSenGeneral	-					H	E					
HcaR-4HCA1	4HCA	T	*			H	E					L105F
HcaR-4HCA2	4HCA	W	W			H	E					
HcaR-4HCA3	4HCA	H	W			H	E					A13T
HcaR-4HCA4	4HCA			A	*	H	E					
HcaR-4HCA5	4HCA			*	V	H	E					
HcaR-4HCA6	4HCA					H	E			I		
HcaR-4HCA7	4HCA					H	E			I	D	
HcaR-4HCA8	4HCA					H	E	*	C			
HcaR-4HCA9	4HCA							T	H			
HcaR-4HCA10	4HCA							T	H			G138D
HcaR-4HBA1	4HBA					H	E			S		A175V
HcaR-4HBA2	4HBA					H	E			S	N	
HcaR-4HBA3	4HBA					H	E			S	L	
HcaR-4HBA4	4HBA					H	E			S	L	A70V
HcaR-4HBA5	4HBA					H	E			S	H	A259V
HcaR-4HBA6	4HBA					H	E			G	F	
HcaR-4HBA7	4HBA					H	E			G	S	
HcaR-4HBA8	4HBA					H	E			G	Y	
HcaR-4HBA9	4HBA					H	E	S	E			
HcaR-5BFA1	5BFA					H	E	F	L			
HcaR-5BFA2	5BFA					H	E	M	V			
HcaR-5BFA3	5BFA					H	E	W	*			
HcaR-5BFA4	5BFA					H	E	W	C			
HcaR-5BFA5	5BFA					H	E	W	V			
HcaR-5BFA6	5BFA					H	E	W	V			A210V
HcaR-5BFA7	5BFA					H	E	Y	L			
HcaR-5BFA8	5BFA	W	W			H	E					
HcaR-6MSA1	6MSA	F	L			H	E					
HcaR-6MSA2	6MSA	H	V			H	E					
HcaR-6MSA3	6MSA	H	I			H	E					
HcaR-6MSA4	6MSA	W	L			H	E					
HcaR-6MSA5	6MSA	S	P									
HcaR-6MSA6	6MSA	S	P									T129A

*Silent mutations.

In the characterized set, a total of 32 different biosensor variants are present. All of these variants exhibit an altered ligand specificity relative to the original sensor variants pSenCA and pSenGeneral. Despite substitutions V097W and P098W that were present in two sets (HcaR-4HCA2 and HcaR-5BFA8), all other substitutions were exclusively present in the final set of one screening campaign. However, of 21 codons targeted for SSM, ten are either highly conserved or they do no contribute to ligand specificity as they were not altered in any of the isolated sensors. For each target ligand, the variant with the most specific response profile (Apart from the respective target ligand, as few ligands as possible provoke *eyfp* expression) are compared to pSenCA and pSenGeneral (Figure 4). All four sensors pSen4HBA9, pSen6MSA4, pSen4HCA10 and pSen5BFA4 exhibit the highest response for their respective target ligand in comparison to the other sensors shown. The designated 4HBA sensor, pSen4HBA9, shows nearly no residual response to CA and PP and induces a 75-fold fluorescent response to the presence of 4HBA. Other inducers are BA (50-fold) and 4HCA (27-fold). For the 6MSA sensor, pSen6MSA4, residual response to PP and CA is 10-fold and 20-fold, respectively, while 6MSA triggers a 110-fold response. Other inducers are BA (75-fold) and SA (60-fold). The 4HCA sensor, pSen4HCA10, exhibits no significant reduction of the response to PP and CA in comparison to pSenCA, but has a more than 30-fold improved response to 4HCA. Surprisingly, SA triggers a more than 100-fold response while 3HCA, closely related to the target compound 4HCA, induces a rather low response of 25-fold. The designate 5BFA sensor, pSen5BFA4 reveals a fold induction of 50 for supplementation of 5BFA, showing a comparable response only for SA. The only other inducers in the set are the native ligands PP and CA, but to a drastically lowered extent (31 and 24 fold, respectively). For comprehensibility and simplicity the four sensors compared will be called pSen4HBA, pSen6MSA, pSen4HCA and pSen5BFA in the following.

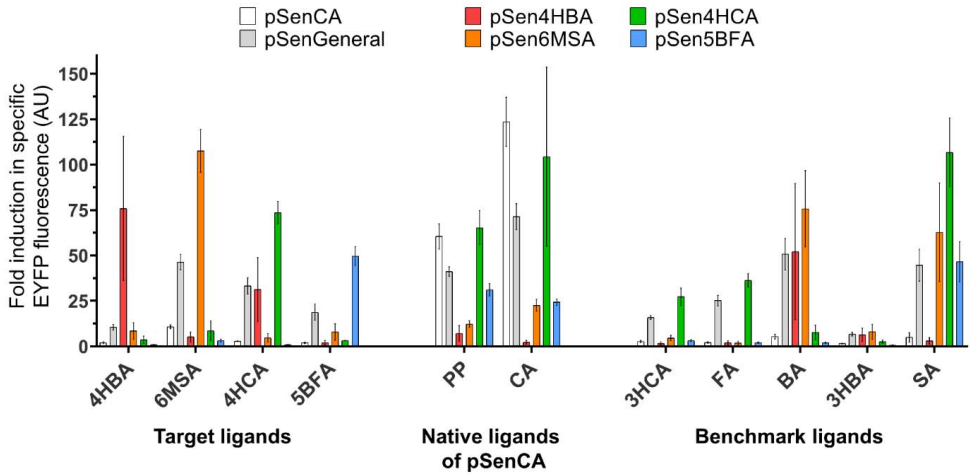

Figure 4. Specificity profiles of pSenCA, pSenGeneral, pSen4HBA, pSen6MSA, pSen4HCA and pSen5BFA, respectively. Caffeic acid and 3,4-dihydroxybenzoic acid did not induce > 3-fold induction in specific EYFP fluorescence in any of the shown variants and are therefore not shown. **Abbreviations:** PP, Phenylpropionic acid; CA, *trans*-cinnamic acid; 3HCA, 3-hydroxycinnamic acid; 4HCA, *p*-coumaric acid; FA, ferulic acid; 5BFA, 5-bromoferulic acid; BA, benzoic acid; 3HBA, 3-hydroxybenzoic acid; 4HBA, 4-hydroxybenzoic acid; SA, salicylic acid; 6MSA, 6-methylsalicylic acid.

While a small number (three and five mutants of the set of 86, respectively) of the sensors exhibit only minimal (< 10 %) residual fold induction in presence of the native ligands PP and CA, the response was only slightly reduced in most of the isolated sensors (Supplementary Figure S 3). In order to eliminate variants with WT specificity during FACS, the native ligands will be used as decoy in future projects. For this, all variants that are induced by the decoy ligand can by removed from the library by sorting all variants that do not exhibit increased fluorescence under these conditions. Unfortunately, we could not perform this approach as the *E. coli* strain used for its high transformation efficiency necessary for the construction of large libraries, carries a chromosomal copy of $hcaR^{WT}$, which results in sufficient HcaR regulator to drive *eyfp* expression from a pSenCA plasmid deficient of the *hcaR gene* (data not shown).

An unexpected observation was the occurrence of two DBD mutants carrying only the substitution R37H, in the set of mutants responsive to 6MSA. After retransformation of the respective plasmids, the mutants showed only 30 % and 10 % residual response to PP and CA (in comparison to pSenCA), respectively. Noteworthy, no other ligand induced notable biosensor response. Therefore, the mutation R37H most likely impairs DNA binding of HcaR and the initial response to 6MSA was caused by mutations in the chromosomally encoded *hcaR* gene.

No HcaR mutants constructed via epPCR was isolated during the FACS screening campaing. One explanation is the low genetic variation typically introduced by epPCR, yielding only single nucleotide polymorphisms. The set of isolated mutants contained at least two and a maximum of five mutations (Table 1). Moreover, variants resulting from epPCR could show lower induction levels than the variants resulting from site saturation mutagenesis. As the epPCR- and SSM-libraries were pooled to facilitate the parallel screening with four target ligands, these variants were possibly not sorted in the positive sorts due to their lower response. Investigation of the variants that showed low response in the parallel cultivation assay could be performed to answer this question (Supplementary Figure S 2). Similar findings were reported for the alteration of the ligand specificity of AraC, were mutants specific for D-arabinose isolated from epPCR libraries, but showed a significantly lower response than mutants isolated from saturation mutagenesis libraries. (Tang et al., 2008)

The importance of specificity for other substances depends on the desired application of the respective sensor. For example, 6MSA is formed by 6-methylsalicylic acid polyketide synthases via subsequent condensation of three malonyl-CoA moieties to an acetyl-CoA starter unit. (Cox et al., 2018; Dimroth et al., 1970; Fujii, Y. Ono, H. Tada, K. Gomi, Y. et al., 1996; Kealey et al., 1998) Throughout the condensation, no intermediate with structural similarity to 6MSA is formed, enabling the use of pSen6MSA despite its BA- and SA-sensitivity. Furthermore, if SA is the target ligand, pSen6MSA can be used for screening approaches as SA is derived from chorismate without formation of other inducers of pSen6MSA. (Kallscheuer and Marienhagen, 2018)

Henceforth, the comprehensive library established in the course of this project can be used as platform for the isolation of sensor variants with specificity towards other substances. By following the workflow used for the isolation of pSen4HCA, pSen4HBA, pSen5BFA and pSen6MSA, many other sensors could be constructed. The structural restrictions of target ligands for HcaR-derived biosensors will be investigated in future studies; it can be assumed that the ligand spectrum is limited to aromatic/ pseudoaromatic structures. Additionally, the presence of the carboxy function could prove to be imperative for ligand binding of HcaR. Certainly, further structural insights would be beneficial for future work with HcaR.

Furthermore, sensor libraries for other compound classes of biotechnological interest could be constructed following the described principle. The libraries would be based on sensors that proved suitable for the detection of a molecule from the respective compound class. The libraries ideally contain combined degeneracy for all residues of the ligand binding cleft. If a sensor for a specific substance is needed, the respective library can be screened for responsive variants.

Conclusions

In this work, we engineered the ligand specificity of the transcriptional repressor HcaR, being part of the biosensor pSenCA, towards the acceptance of the biotechnologically interesting aromatic compounds 4HCA, 4HBA, 5BFA and 6MSA. In this context, the FACS-based dual screening in the presence or absence of a ligand proved its suitability for the effective screening of large mutant libraries. Ten positions, influencing the ligand specificity of HcaR were identified in the course of the work, paving the way for future engineering of this regulator. Characterization of the specificity profile of the isolated sensors identified HcaR mutants that will act as valuable starting points for future sensor constructions. This approach can easily be translated to other transcriptional regulators, which would give rise of many new biosensors for biotechnologically interesting small molecules.

Associated content

Supporting information

The supporting information is available free of charge on the ACS Publication website:

Supplementary tables

Table S1: Strains and plasmids used in this study.

Table S2: Mutants isolated in the screening towards pSenGeneral.

Table S3: Oligonucleotides used in this study.

Supplementary figures

Figure S1: Structural consequences of amino acid substitutions E101H and V102Y in HcaR.

Figure S2: Response of 184 single variants from each endpoint population to the addition of the respective target ligand.

Figure S3: Residual response to native inducers.

Figure S4: RMSF and RMSD over time.

Figure S5: Comparison of the predicted binding modes of 4HBA and 4HCA in pSen4HBA.

Author information

Corresponding Author

*(J.M.) Tel: +49 2461 61 2843; Fax: +49 2461 61 2710. E-mail: j.marienhagen@fz-juelich.de

ORCID

Lion Konstantin Flachbart: https://orcid.org/0000-0003-0701-7019

Christoph Gerhard Wilhelm Gertzen: https://orcid.org/0000-0002-9562-7708

Holger Gohlke: https://orcid.org/0000-0001-8613-1447

Jan Marienhagen: https://orcid.org/0000-0001-5513-3730

Author Contributions

L.K.F. designed and conducted the mutagenesis, cultivations, FACS screening and plate-based screenings and characterizations. C.G.W.G. performed the homology modeling, MD simulations, and molecular docking, and C.G.W.G. and H.G. evaluated the molecular modeling and simulation work. L.K.F., C.G.W.G., H.G., and J.M. wrote the manuscript.

Notes

The author declare no competing financial interest.

Acknowledgements

This project has received funding from the European Research Council (ERC) under the European Union's Horizon 2020 research and innovation programme (grant agreement No 638718). The Center for Structural Studies is funded by the Deutsche Forschungsgemeinschaft (DFG Grant number 417919780). We are grateful for computational support by the "Zentrum für Informations und Medientechnologie" at the Heinrich-Heine-Universität Düsseldorf and the computing time provided by the John von Neumann Institute for Computing (NIC) to HG on the supercomputer JURECA at Jülich Supercomputing Centre (JSC) (user ID: HKF7). Funding by Deutsche Forschungsgemeinschaft (DFG) (INST 208/704-1 FUGG) to purchase the hybrid computer cluster used in this study is gratefully acknowledged.

References

Abreu, V.A.C., Almeida, S., Tiwari, S., Hassan, S.S., Mariano, D., Silva, A., Baumbach, J., Azevedo, V., Röttger, R., 2015. CMRegNet–An interspecies reference database for corynebacterial and mycobacterial regulatory networks. BMC Genomics 16, 452. https://doi.org/10.1186/s12864-015-1631-0

Arnold, F.H., 2018. Directed Evolution: Bringing New Chemistry to Life. Angew. Chem. Int. Ed. Engl. 57, 4143–4148. https://doi.org/10.1002/anie.201708408

Aschenbrenner, J., Marx, P., Pietruszka, J., Marienhagen, J., 2018. Microbial production of natural and non-natural monolignols with Escherichia coli. ChemBioChem cbic.201800673. https://doi.org/10.1002/cbic.201800673

BERTANI, G., 1951. Studies on lysogenesis. I. The mode of phage liberation by lysogenic Escherichia coli. J. Bacteriol. 62, 293–300. https://doi.org/citeulike-article-id:149214

Chen, W., Zhang, S., Jiang, P., Yao, J., He, Y., Chen, L., Gui, X., Dong, Z., Tang, S., 2015. Design of an ectoine-responsive AraC mutant and its application in metabolic engineering of ectoine biosynthesis. Metab. Eng. 30, 149–155. https://doi.org/10.1016/J.YMBEN.2015.05.004

Cox, R.J., Skellam, E., Williams, K., 2018. Biosynthesis of Fungal Polyketides, in: Physiology and Genetics. Springer International Publishing, Cham, pp. 385–412. https://doi.org/10.1007/978-3-319-71740-1_13

Craven, S.H., Ezezika, O.C., Haddad, S., Hall, R.A., Momany, C., Neidle, E.L., 2009. Inducer responses of BenM, a LysR-type transcriptional regulator from Acinetobacter baylyi ADP1. Mol. Microbiol. 72, 881–94. https://doi.org/10.1111/j.1365-2958.2009.06686.x

DeLano, W.L., 2005. The case for open-source software in drug discovery. Drug Discov. Today 10, 213–7. https://doi.org/10.1016/S1359-6446(04)03363-X

DeLano, W.L., 2002. Pymol: An open-source molecular graphics tool. CCP4 Newsl. Protein Crystallogr. 40, 82–92.

Díaz, E., Ferrández, A., García, J.L., 1998. Characterization of the hca cluster encoding the dioxygenolytic pathway for initial catabolism of 3-phenylpropionic acid in Escherichia coli K-12. J. Bacteriol. 180, 2915–23.

Díaz, E., Ferrández, A., Prieto, M.A., García, J.L., 2001. Biodegradation of aromatic compounds by Escherichia coli. Microbiol. Mol. Biol. Rev. 65, 523–69. https://doi.org/10.1128/MMBR.65.4.523-569.2001

580 Dimroth, P., Walter, H., Lynen, F., 1970. [Biosynthesis of 6-methylsalicylic acid]. Eur. J.
581 Biochem. 13, 98–110.

582 Firth, A.E., Patrick, W.M., 2008. GLUE-IT and PEDEL-AA: new programmes for analyzing
583 protein diversity in randomized libraries. Nucleic Acids Res. 36.
584 https://doi.org/10.1093/nar/gkn226

585 Firth, A.E., Patrick, W.M., 2005. Statistics of protein library construction. Bioinformatics 21,
586 3314–3315. https://doi.org/10.1093/bioinformatics/bti516

587 Flachbart, L.K., Sokolowsky, S., Marienhagen, J., 2019. Displaced by deceivers - Prevention
588 of biosensor cross-talk is pivotal for successful biosensor-based high-throughput
589 screening campaigns. ACS Synth. Biol. 8, acssynbio.9b00149.
590 https://doi.org/10.1021/acssynbio.9b00149

591 Frei, C.S., Qian, S., Cirino, P.C., 2018. New engineered phenolic biosensors based on the
592 AraC regulatory protein. Protein Eng. Des. Sel. 31, 213–220.
593 https://doi.org/10.1093/protein/gzy024

594 Freiherr von Boeselager, R., Pfeifer, E., Frunzke, J., 2018. Cytometry meets next-generation
595 sequencing – RNA-Seq of sorted subpopulations reveals regional replication and iron-
596 triggered prophage induction in *Corynebacterium glutamicum*. Sci. Rep. 8, 14856.
597 https://doi.org/10.1038/s41598-018-32997-9

598 Fujii, Y. Ono, H. Tada, K. Gomi, Y., I., Ono, Y., Tada, H., Gomi, K., Ebizuka, Y., Sankawa, U.,
599 1996. Cloning of the polyketide synthase gene atX from Aspergillus terreus and its
600 identification as the 6-Methylsalicylic acid synthase gene by heterologous expression.
601 Mol. Gen. Genet. MGG 253, 1–10. https://doi.org/10.1007/s004380050289

602 Funke, M., Diederichs, S., Kensy, F., Müller, C., Büchs, J., 2009. The baffled microtiter plate:
603 increased oxygen transfer and improved online monitoring in small scale fermentations.
604 Biotechnol. Bioeng. 103, 1118–28. https://doi.org/10.1002/bit.22341

605 Gibson, D.G., Young, L., Chuang, R.-Y., Venter, J.C., Hutchison, C.A., Smith, H.O., 2009.
606 Enzymatic assembly of DNA molecules up to several hundred kilobases. Nat. Methods 6,
607 343–345. https://doi.org/10.1038/nmeth.1318

608 Jha, R.K., Chakraborti, S., Kern, T.L., Fox, D.T., Strauss, C.E.M., 2015. Rosetta comparative
609 modeling for library design: Engineering alternative inducer specificity in a transcription
610 factor. Proteins 83, 1327–40. https://doi.org/10.1002/prot.24828

611 Kallscheuer, N., Marienhagen, J., 2018. *Corynebacterium glutamicum* as platform for the
612 production of hydroxybenzoic acids. Microb. Cell Fact. 17, 70.

https://doi.org/10.1186/s12934-018-0923-x

Kealey, J.T., Liu, L., Santi, D. V, Betlach, M.C., Barr, P.J., 1998. Production of a polyketide natural product in nonpolyketide-producing prokaryotic and eukaryotic hosts. Proc. Natl. Acad. Sci. U. S. A. 95, 505–9. https://doi.org/10.1073/PNAS.95.2.505

Kensy, F., Zang, E., Faulhammer, C., Tan, R.-K., Büchs, J., 2009. Validation of a high-throughput fermentation system based on online monitoring of biomass and fluorescence in continuously shaken microtiter plates. Microb. Cell Fact. 8, 31. https://doi.org/10.1186/1475-2859-8-31

Keseler, I.M., Mackie, A., Peralta-Gil, M., Santos-Zavaleta, A., Gama-Castro, S., Bonavides-Martínez, C., Fulcher, C., Huerta, A.M., Kothari, A., Krummenacker, M., Latendresse, M., Muñiz-Rascado, L., Ong, Q., Paley, S., Schröder, I., Shearer, A.G., Subhraveti, P., Travers, M., Weerasinghe, D., Weiss, V., Collado-Vides, J., Gunsalus, R.P., Paulsen, I., Karp, P.D., 2013. EcoCyc: fusing model organism databases with systems biology. Nucleic Acids Res. 41, D605–D612. https://doi.org/10.1093/nar/gks1027

Marchler-Bauer, A., Bo, Y., Han, L., He, J., Lanczycki, C.J., Lu, S., Chitsaz, F., Derbyshire, M.K., Geer, R.C., Gonzales, N.R., Gwadz, M., Hurwitz, D.I., Lu, F., Marchler, G.H., Song, J.S., Thanki, N., Wang, Z., Yamashita, R.A., Zhang, D., Zheng, C., Geer, L.Y., Bryant, S.H., 2017. CDD/SPARCLE: functional classification of proteins via subfamily domain architectures. Nucleic Acids Res. 45, D200–D203. https://doi.org/10.1093/nar/gkw1129

Marchler-Bauer, A., Bryant, S.H., 2004. CD-Search: protein domain annotations on the fly. Nucleic Acids Res. 32, W327-31. https://doi.org/10.1093/nar/gkh454

Marchler-Bauer, A., Derbyshire, M.K., Gonzales, N.R., Lu, S., Chitsaz, F., Geer, L.Y., Geer, R.C., He, J., Gwadz, M., Hurwitz, D.I., Lanczycki, C.J., Lu, F., Marchler, G.H., Song, J.S., Thanki, N., Wang, Z., Yamashita, R.A., Zhang, D., Zheng, C., Bryant, S.H., 2015. CDD: NCBI's conserved domain database. Nucleic Acids Res. 43, D222–D226. https://doi.org/10.1093/nar/gku1221

Marchler-Bauer, A., Lu, S., Anderson, J.B., Chitsaz, F., Derbyshire, M.K., DeWeese-Scott, C., Fong, J.H., Geer, L.Y., Geer, R.C., Gonzales, N.R., Gwadz, M., Hurwitz, D.I., Jackson, J.D., Ke, Z., Lanczycki, C.J., Lu, F., Marchler, G.H., Mullokandov, M., Omelchenko, M. V., Robertson, C.L., Song, J.S., Thanki, N., Yamashita, R.A., Zhang, D., Zhang, N., Zheng, C., Bryant, S.H., 2011. CDD: a Conserved Domain Database for the functional annotation of proteins. Nucleic Acids Res. 39, D225–D229. https://doi.org/10.1093/nar/gkq1189

Munch, R., Hiller, K., Barg, H., Heldt, D., Linz, S., Wingender, E., Jahn, D., 2003. PRODORIC:

prokaryotic database of gene regulation. Nucleic Acids Res. 31, 266–269. https://doi.org/10.1093/nar/gkg037

Novichkov, P.S., Kazakov, A.E., Ravcheev, D.A., Leyn, S.A., Kovaleva, G.Y., Sutormin, R.A., Kazanov, M.D., Riehl, W., Arkin, A.P., Dubchak, I., Rodionov, D.A., 2013. RegPrecise 3.0 – A resource for genome-scale exploration of transcriptional regulation in bacteria. BMC Genomics 14, 745. https://doi.org/10.1186/1471-2164-14-745

Patrick, W.M., Firth, A.E., Blackburn, J.M., 2003. User-friendly algorithms for estimating completeness and diversity in randomized protein-encoding libraries. Protein Eng. 16, 451–7.

Roy, A., Kucukural, A., Zhang, Y., 2010. I-TASSER: a unified platform for automated protein structure and function prediction. Nat. Protoc. 5, 725–38. https://doi.org/10.1038/nprot.2010.5

Salgado, H., Gama-Castro, S., Peralta-Gil, M., Díaz-Peredo, E., Sánchez-Solano, F., Santos-Zavaleta, A., Martínez-Flores, I., Jiménez-Jacinto, V., Bonavides-Martínez, C., Segura-Salazar, J., Martínez-Antonio, A., Collado-Vides, J., 2006. RegulonDB (version 5.0): *Escherichia coli* K-12 transcriptional regulatory network, operon organization, and growth conditions. Nucleic Acids Res. 34, D394–D397. https://doi.org/10.1093/nar/gkj156

Sambrook, J., Russel, D.W., 2001. Molecular Cloning A Lab Manual, 3. ed. Cold Spring Harbor Laboratory Press, New York.

Schallmey, M., Frunzke, J., Eggeling, L., Marienhagen, J., 2014. Looking for the pick of the bunch: high-throughput screening of producing microorganisms with biosensors. Curr. Opin. Biotechnol. 26, 148–54. https://doi.org/10.1016/j.copbio.2014.01.005

Shi, S., Choi, Y.W., Zhao, H., Tan, M.H., Ang, E.L., 2017. Discovery and engineering of a 1-butanol biosensor in Saccharomyces cerevisiae. Bioresour. Technol. https://doi.org/10.1016/j.biortech.2017.06.114

Sigrist, C.J.A., Cerutti, L., Hulo, N., Gattiker, A., Falquet, L., Pagni, M., Bairoch, A., Bucher, P., 2002. PROSITE: a documented database using patterns and profiles as motif descriptors. Brief. Bioinform. 3, 265–74. https://doi.org/10.1093/bib/3.3.265

Sigrist, C.J.A., De Castro, E., Cerutti, L., Cuche, B.A., Hulo, N., Bridge, A., Bougueleret, L., Xenarios, I., 2013. New and continuing developments at PROSITE. Nucleic Acids Res. 41, D344-7. https://doi.org/10.1093/nar/gks1067

Sigrist, C.J.A., De Castro, E., Langendijk-Genevaux, P.S., Le Saux, V., Bairoch, A., Hulo, N., 2005. ProRule: a new database containing functional and structural information on

PROSITE profiles. Bioinformatics 21, 4060–6. https://doi.org/10.1093/bioinformatics/bti614

Tang, S.-Y., Cirino, P.C., 2011. Design and application of a mevalonate-responsive regulatory protein. Angew. Chem. Int. Ed. Engl. 50, 1084–6. https://doi.org/10.1002/anie.201006083

Tang, S.-Y., Fazelinia, H., Cirino, P.C., 2008. AraC regulatory protein mutants with altered effector specificity. J. Am. Chem. Soc. 130, 5267–71. https://doi.org/10.1021/ja7109053

Tang, S.-Y., Qian, S., Akinterinwa, O., Frei, C.S., Gredell, J.A., Cirino, P.C., 2013. Screening for enhanced triacetic acid lactone production by recombinant *Escherichia coli* expressing a designed triacetic acid lactone reporter. J. Am. Chem. Soc. 135, 10099–103. https://doi.org/10.1021/ja402654z

Taylor, N.D., Garruss, A.S., Moretti, R., Chan, S., Arbing, M.A., Cascio, D., Rogers, J.K., Isaacs, F.J., Kosuri, S., Baker, D., Fields, S., Church, G.M., Raman, S., 2015. Engineering an allosteric transcription factor to respond to new ligands. Nat. Methods 13, 177–183. https://doi.org/10.1038/nmeth.3696

Turlin, E., Perrotte-piquemal, M., Danchin, A., Biville, F., 2001. Regulation of the early steps of 3-phenylpropionate catabolism in *Escherichia coli*. J. Mol. Microbiol. Biotechnol. 3, 127–33.

Turlin, E., Sismeiro, O., Le Caer, J.P., Labas, V., Danchin, A., Biville, F., 2005. 3-phenylpropionate catabolism and the *Escherichia coli* oxidative stress response. Res. Microbiol. 156, 312–21. https://doi.org/10.1016/j.resmic.2004.10.012

Wilson, D., Charoensawan, V., Kummerfeld, S.K., Teichmann, S.A., 2008. DBD—taxonomically broad transcription factor predictions: new content and functionality. Nucleic Acids Res. 36, D88–D92. https://doi.org/10.1093/nar/gkm964

Yang, J., Yan, R., Roy, A., Xu, D., Poisson, J., Zhang, Y., 2015. The I-TASSER Suite: protein structure and function prediction. Nat. Methods 12, 7–8. https://doi.org/10.1038/nmeth.3213

Zeymer, C., Hilvert, D., 2018. Directed Evolution of Protein Catalysts. Annu. Rev. Biochem. 87, 131–157. https://doi.org/10.1146/annurev-biochem-062917-012034

Zhang, Y., 2008. I-TASSER server for protein 3D structure prediction. BMC Bioinformatics 9, 40. https://doi.org/10.1186/1471-2105-9-40

2.2.2. Biosensor platform development - Supporting information

Supporting information

Development of a biosensor platform for phenolic compounds using a transition ligand strategy

Lion Konstantin Flachbart[1], Christoph Gertzen[2,3], Holger Gohlke[2,3] and Jan Marienhagen[1,4,*]

[1]Institute of Bio- and Geosciences, IBG-1: Biotechnology, Forschungszentrum Jülich, D-52425 Jülich, Germany

[2]Institute for Pharmaceutical and Medicinal Chemistry, Heinrich Heine University Düsseldorf, Universitätsstr. 1, 40225 Düsseldorf, Germany

[3]John von Neumann Institute for Computing (NIC), Jülich Supercomputing Centre (JSC) and Institute for Complex Systems – Structural Biochemistry (ICS-6), Forschungszentrum Jülich GmbH, 52425 Jülich, Germany

[4]Institute of Biotechnology, RWTH Aachen University, Worringer Weg 3, D-52074 Aachen, Germany

* To whom correspondence should be addressed.
Tel: +49 2461 61 2843; Fax: +49 2461 61 2710; Email: j.marienhagen@fz-juelich.de

Supplementary Table S1. Strains and plasmids used in this study.

Strain or plasmid	Relevant characteristics	Reference or source
E. coli TOP10	F⁻ *mcr*A Δ(*mrr-hsd*RMS-*mcr*BC) φ80*lac*ZΔM15 Δ*lac*X74 *rec*A1 *ara*D139 Δ(*ara-leu*) 7697 *gal*U *gal*K *rps*L (Str^R) *end*A1 *nup*G λ⁻	Invitrogen
E. coli DH10B Δ*hcaREFCBD*	F⁻ *mcr*A Δ(*mrr-hsd*RMS-*mcr*BC) φ80*lac*ZΔM15 Δ*lac*X74 *rec*A1 *end*A1 *ara*D139 Δ(*ara, leu*)7697 *gal*U *gal*K λ⁻ *rps*L *nup*G Δ*hcaREFCBD*	Chapter 2.1
pSenCA	Transcriptional biosensor construct inducing *eyfp* expression in response to the presence of *trans*-cinnamic acid or phenylpropionic acid, Kan^R	Chapter 2.1

Supplementary Table S2. Oligonucleotides used in this study. Underlined positions indicate degenerate codons.

Primer name	Sequence (5'-3')
seq_hcaR_fw	CACACGGTCACACTGCTTCC
seq_hcaR_rv	TGAACAGCTCCTCGCCCTTG
amp_hcaR_fw	TGCCGTTACGCTTGCCAAACGTTC
amp_hcaR_rv	GAACTACGGCATTTACGCTATTTCGTCGCAG
amp_pSenCA_w/o_hcaR_fw	GTAAATGCCGTAGTTCCATCACCTTCCCCTTGTTATCGAAAAAAC G
amp_pSenCA_w/o_hcaR_rv	GCAAGCGTAACGGCATAAGAGCTCCCGGGCCCG
hcaR-V97/P98-rv	GCAATAAATTCACTTCCGCCGAMNNMNNAAAGCCAATGGTTA ATTGTCTGTCTTCCTGAACAATTTTCCGC
hcaR-V97/P98-fw	GCGGAAAATTGTTCAGGAAGACAGACAATTAACCATTGGCTTTNN KNNKTCGGCGGAAGTGAATTTATTGC
hcaR-T128-rv	CGAATTTTTTCCTCCTGTTGCGTMNNGATTAAACTCACCAGCTCA ATCAAG
hcaR-T128-fw	CTTGATTGAGCTGGTGAGTTTAATCNNKACGCAACAGGAGGAAA AAATTCG
hcaR-P195/V196/Y197-fw	GGATGGCGTGAATTTCGTCAGTACCGATNNKNNKNNKTCCGGTT CGCTTGCGCCGATCGTTAA
hcaR-P195/V196/Y197-rv	TTAACGATCGGCGCAAGCGAACCGGAMNNMNNMNNATCGGTAC TGACGAAATTCACGCCATCC

hcaR-S198/G199/S200-fw	GGCGTGAATTTCGTCAGTACCGATCCGGCGTATNNKNNKNNKCTTGCGCCGATCGTTA
hcaR-S198/G199/S200-rv	TAACGATCGGCGCAAGMNNMNNMNNATACGCCGGATCGGTACTGACGAAATTCACGCC
hcaR-L201-rv	GCTTTAACGATCGGCGCMNNCGAACCGGAATACGCCG
hcaR-L201-fw	CGGCGTATTCCGGTTCGNNKGCGCCGATCGTTAAAGC
hcaR-E101/V102-rv	CGAAACATCGGTAATACTTTTGGCAATAAATTMNNMNNCGCCGATGGCACAAAGCCAATGGTTAATTGTC
hcaR-E101/V102-fw	GACAATTAACCATTGGCTTTGTGCCATCGGCGNNKNNKAATTTATTGCCAAAAGTATTACCGATGTTTCG
hcaR-N224/I225/L226-rv	CCCCATGCCCACCAGATTCATGGTCACMNNMNNMNNCGTTGCCACCTGGACGATATTTGGCTG
hcaR-N224/I225/L226-fw	CAGCCAAATATCGTCCAGGTGGCAACGNNKNNKNNKGTGACCATGAATCTGGTGGGCATGGGG
hcaR-S99/A100-rv	CATCGGTAATACTTTTGGCAATAAATTCACTTCMNNMNNTGGCACAAAGCCAATGGTTAATTGTCTGTCTTC
hcaR-S99/A100-fw	GAAGACAGACAATTAACCATTGGCTTTGTGCCANNKNNKGAAGTGAATTTATTGCCAAAAGTATTACCGATG
hcaR-V227/T228-rv	CCAGCCCCATGCCCACCAGATTCATMNNMNNCAGAATATTCGTTGCCACCTGGACG
hcaR-V227/T228-fw	CGTCCAGGTGGCAACGAATATTCTGNNKNNKATGAATCTGGTGGGCATGGGGCTGG
hcaR-M245/N246-rv	CGAAAAACAACCTGCCCGGTATTAAAATTMNNMNNATAACCGGGTATCAAAGTGACGCCCAGCC
hcaR-M245/N246-fw	GGCTGGGCGTCACTTTGATACCCGGTTATNNKNNKAATTTTAATACCGGGCAGGTTGTTTTTCG
hcaR_mutH101Y102-V97/P98-rv	GGCAATAAATTATAATGCGCCGAMNNMNNAAAGCCAATGGTTAATTGTCTGTCTTCCTGAACAATTTTCCGCGC
hcaR_mutH101Y102-V97/P98-fw	GCGCGGAAAATTGTTCAGGAAGACAGACAATTAACCATTGGCTTTNNKNNKTCGGCGCATTATAATTTATTGCC
hcaR_mutH101Y102-S99/A100-rv	AAACATCGGTAATACTTTTGGCAATAAATTATAATGMNNMNNTGGCACAAAGCCAATGGTTAATTGTCTGTCTTCCTG
hcaR_mutH101Y102-S99/A100-fw	CAGGAAGACAGACAATTAACCATTGGCTTTGTGCCANNKNNKCATTATAATTTATTGCCAAAAGTATTACCGATGTTT

35
36

Supplementary Table S2. Mutants isolated in the screening towards a generalist HcaR regulator. In contrast to other data presented in this manuscript, this cultivation was performed with an inoculum OD_{600} of 1 and fluorescence measurements were performed 4 h after cultivation (37 °C) of the respective compounds.

					Fold induction in specific EYFP fluorescence				
Variant	Codon 101	Codon 102	residue 101	residue 102	CA	PP	3HPP	3HCl	3,5DHPP
WT-HcaR	GAA	GTG	E	V	45.7	43.4	2.0	2.5	1.9
1	TGT	TTT	C	F	3.2	3.5	2.9	3.4	3.3
2	AGT	TTT	S	F	4.8	5.1	4.2	5.0	7.7
3	GCT	TTT	A	F	4.8	5.1	4.2	5.0	1.5
4	ACT	TTT	T	F	5.3	6.8	4.9	5.4	9.3
5	ACG	TTT	T	F	3.8	4.1	3.7	4.2	3.9
6	CAT	TAT	H	Y	10.9	11.8	10.4	11.5	8.4

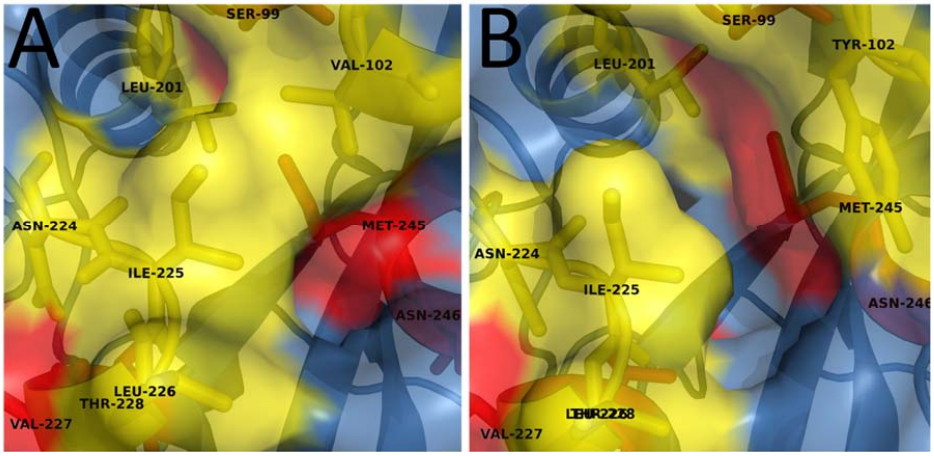

Supplementary Figure S1. Effect of mutation E101H and V102Y on HcaR structure. Figures show a close up of the Hcar binding cleft. Residues targeted in first screening campaign shown in yellow and additional targets of subsequent screenings shown in red. **(A)** Structure of Hcar. V102 and I225 align towards each other, constraining the binding cleft. **(B)** Structure of HcaR_E101H,V102Y. By rotation of Y102, the binding cleft opens and M245 is accessible.

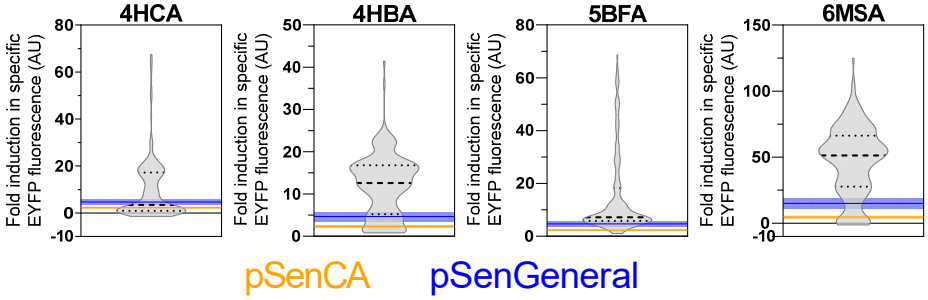

Supplementary Figure S2. Response of 184 single variants from each endpoint population to the addition of the respective target compound. Distribution shown as violin plots, dashed lines depict median, dotted lines depict quartiles of each distribution. Yellow and blue lines and shading depict mean fold induction and standard deviation of *E. coli* Top10 pSenCA and *E. coli* TOP10 pSenGeneral, respectively.

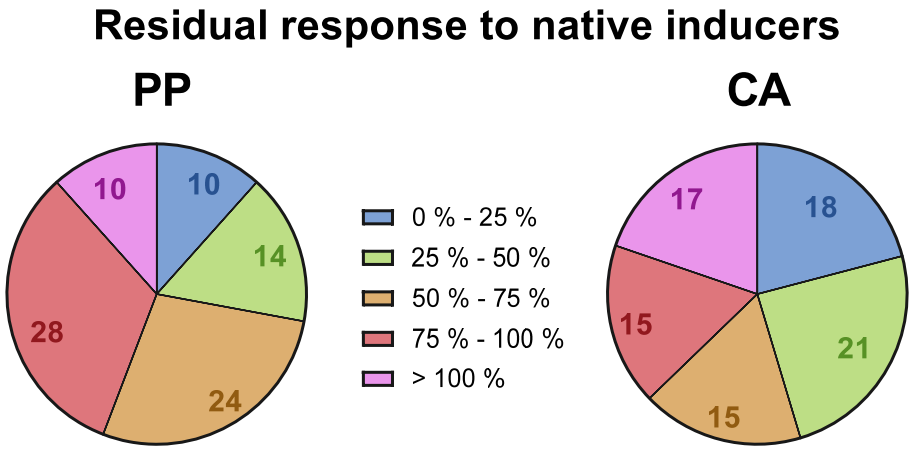

55
56

57 **Supplementary Figure S3.** Residual response to native inducers of 96 isolated variants. Distribution of
58 fold induction in specific EYFP fluorescence response is shown, relative to the response of pSenCA as
59 depicted in the legend. Total number is 86, as two R37H mutants were not considered due to insufficient
60 overall performance. **Abbreviations:** PP, phenylpropionic acid; CA, trans-cinnamic acid.

3. Bibliography

Aboul-ela, F., Huang, W., Abd Elrahman, M., Boyapati, V., Li, P., 2015. Linking aptamer-ligand binding and expression platform folding in riboswitches: prospects for mechanistic modeling and design. Wiley Interdiscip. Rev. RNA 6, 631–650. https://doi.org/10.1002/wrna.1300

Abreu-Goodger, C., Merino, E., 2005. RibEx: a web server for locating riboswitches and other conserved bacterial regulatory elements. Nucleic Acids Res. 33, W690-2. https://doi.org/10.1093/nar/gki445

Abreu, V.A.C., Almeida, S., Tiwari, S., Hassan, S.S., Mariano, D., Silva, A., Baumbach, J., Azevedo, V., Röttger, R., 2015. CMRegNet–An interspecies reference database for corynebacterial and mycobacterial regulatory networks. BMC Genomics 16, 452. https://doi.org/10.1186/s12864-015-1631-0

Ameen, S., Ahmad, M., Mohsin, M., Qureshi, M.I., Ibrahim, M.M., Abdin, M.Z., Ahmad, A., 2016. Designing, construction and characterization of genetically encoded FRET-based nanosensor for real time monitoring of lysine flux in living cells. J. Nanobiotechnology 14, 49. https://doi.org/10.1186/s12951-016-0204-y

An, G.-H., Bielich, J., Auerbach, R., Johnson, E.A., 1991. Isolation and Characterization of Carotenoid Hyperproducing Mutants of Yeast by Flow Cytometry and Cell Sorting. Nat. Biotechnol. 9, 70–73. https://doi.org/10.1038/nbt0191-70

Antoine, R., Locht, C., 1992. Isolation and molecular characterization of a novel broad-host-range plasmid from Bordetella bronchiseptica with sequence similarities to plasmids from Gram-positive organisms. Mol. Microbiol. 6, 1785–1799. https://doi.org/10.1111/j.1365-2958.1992.tb01351.x

Arnold, F.H., Georgiou, G., 2003. Directed Enzyme Evolution. Humana Press, New Jersey. https://doi.org/10.1385/1592593968

Aschenbrenner, J., Marx, P., Pietruszka, J., Marienhagen, J., 2018. Microbial production of natural and non-natural monolignols with *Escherichia coli*. ChemBioChem cbic.201800673. https://doi.org/10.1002/cbic.201800673

Bengert, P., Dandekar, T., 2004. Riboswitch finder--a tool for identification of riboswitch RNAs. Nucleic Acids Res. 32, W154-9. https://doi.org/10.1093/nar/gkh352

Bilan, D.S., Pase, L., Joosen, L., Gorokhovatsky, A.Y., Ermakova, Y.G., Gadella, T.W.J., Grabher, C., Schultz, C., Lukyanov, S., Belousov, V. V, 2013. HyPer-3: a genetically encoded H(2)O(2) probe

with improved performance for ratiometric and fluorescence lifetime imaging. ACS Chem. Biol. 8, 535–42. https://doi.org/10.1021/cb300625g

Billinton, N., Barker, M.G., Michel, C.E., Knight, A.W., Heyer, W.D., Goddard, N.J., Fielden, P.R., Walmsley, R.M., 1998. Development of a green fluorescent protein reporter for a yeast genotoxicity biosensor. Biosens. Bioelectron. 13, 831–838. https://doi.org/10.1016/S0956-5663(98)00049-9

Binder, S., Schendzielorz, G., Stäbler, N., Krumbach, K., Hoffmann, K., Bott, M., Eggeling, L., 2012. A high-throughput approach to identify genomic variants of bacterial metabolite producers at the single-cell level. Genome Biol. 13, R40. https://doi.org/10.1186/gb-2012-13-5-r40

Bornscheuer, U.T., Hauer, B., Jaeger, K.E., Schwaneberg, U., 2019. Directed Evolution Empowered Redesign of Natural Proteins for the Sustainable Production of Chemicals and Pharmaceuticals. Angew. Chemie Int. Ed. 58, 36–40. https://doi.org/10.1002/anie.201812717

Bott, M., 2015. Need for speed - finding productive mutations using transcription factor-based biosensors, fluorescence-activated cell sorting and recombineering. Microb. Biotechnol. 8, 8–10. https://doi.org/10.1111/1751-7915.12248

Bulter, T., Alcalde, M., Sieber, V., Meinhold, P., Schlachtbauer, C., Arnold, F.H., 2003. Functional Expression of a Fungal Laccase in Saccharomyces cerevisiae by Directed Evolution. Appl. Environ. Microbiol. 69, 987–995. https://doi.org/10.1128/AEM.69.2.987-995.2003

Carroll, D., 2011. Genome Engineering With Zinc-Finger Nucleases. Genetics 188, 773–782. https://doi.org/10.1534/GENETICS.111.131433

Chan, C.T.Y., Lee, J.W., Cameron, D.E., Bashor, C.J., Collins, J.J., 2016. “Deadman” and “Passcode” microbial kill switches for bacterial containment. Nat. Chem. Biol. 12, 82–86. https://doi.org/10.1038/nchembio.1979

Chou, H.H., Keasling, J.D., 2013. Programming adaptive control to evolve increased metabolite production. Nat. Commun. 4, 2595. https://doi.org/10.1038/ncomms3595

Church, G.M., Elowitz, M.B., Smolke, C.D., Voigt, C.A., Weiss, R., 2014. Realizing the potential of synthetic biology. Nat. Rev. Mol. Cell Biol. 15, 289–294. https://doi.org/10.1038/nrm3767

Cirino, P.C., Mayer, K.M., Umeno, D., 2003. Generating mutant libraries using error-prone PCR, in: Directed Evolution Library Creation. Springer, pp. 3–9.

Cossarizza, A., Chang, H.-D., Radbruch, A., Akdis, M., Andrä, I., Annunziato, F., Bacher, P., Barnaba, V., Battistini, L., Bauer, W.M., Baumgart, S., Becher, B., Beisker, W., Berek, C., Blanco, A., Borsellino,

G., Boulais, P.E., Brinkman, R.R., Büscher, M., Busch, D.H., Bushnell, T.P., Cao, X., Cavani, A., Chattopadhyay, P.K., Cheng, Q., Chow, S., Clerici, M., Cooke, A., Cosma, A., Cosmi, L., Cumano, A., Dang, V.D., Davies, D., De Biasi, S., Del Zotto, G., Della Bella, S., Dellabona, P., Deniz, G., Dessing, M., Diefenbach, A., Di Santo, J., Dieli, F., Dolf, A., Donnenberg, V.S., Dörner, T., Ehrhardt, G.R.A., Endl, E., Engel, P., Engelhardt, B., Esser, C., Everts, B., Dreher, A., Falk, C.S., Fehniger, T.A., Filby, A., Fillatreau, S., Follo, M., Förster, I., Foster, J., Foulds, G.A., Frenette, P.S., Galbraith, D., Garbi, N., García-Godoy, M.D., Geginat, J., Ghoreschi, K., Gibellini, L., Goettlinger, C., Goodyear, C.S., Gori, A., Grogan, J., Gross, M., Grützkau, A., Grummitt, D., Hahn, J., Hammer, Q., Hauser, A.E., Haviland, D.L., Hedley, D., Herrera, G., Herrmann, M., Hiepe, F., Holland, T., Hombrink, P., Houston, J.P., Hoyer, B.F., Huang, B., Hunter, C.A., Iannone, A., Jäck, H.-M., Jávega, B., Jonjic, S., Juelke, K., Jung, S., Kaiser, T., Kalina, T., Keller, B., Khan, S., Kienhöfer, D., Kroneis, T., Kunkel, D., Kurts, C., Kvistborg, P., Lannigan, J., Lantz, O., Larbi, A., LeibundGut-Landmann, S., Leipold, M.D., Levings, M.K., Litwin, V., Liu, Y., Lohoff, M., Lombardi, G., Lopez, L., Lovett-Racke, A., Lubberts, E., Ludewig, B., Lugli, E., Maecker, H.T., Martrus, G., Matarese, G., Maueröder, C., McGrath, M., McInnes, I., Mei, H.E., Melchers, F., Melzer, S., Mielenz, D., Mills, K., Mirrer, D., Mjösberg, J., Moore, J., Moran, B., Moretta, A., Moretta, L., Mosmann, T.R., Müller, S., Müller, W., Münz, C., Multhoff, G., Munoz, L.E., Murphy, K.M., Nakayama, T., Nasi, M., Neudörfl, C., Nolan, J., Nourshargh, S., O'Connor, J.-E., Ouyang, W., Oxenius, A., Palankar, R., Panse, I., Peterson, P., Peth, C., Petriz, J., Philips, D., Pickl, W., Piconese, S., Pinti, M., Pockley, A.G., Podolska, M.J., Pucillo, C., Quataert, S.A., Radstake, T.R.D.J., Rajwa, B., Rebhahn, J.A., Recktenwald, D., Remmerswaal, E.B.M., Rezvani, K., Rico, L.G., Robinson, J.P., Romagnani, C., Rubartelli, A., Ruckert, B., Ruland, J., Sakaguchi, S., Sala-de-Oyanguren, F., Samstag, Y., Sanderson, S., Sawitzki, B., Scheffold, A., Schiemann, M., Schildberg, F., Schimisky, E., Schmid, S.A., Schmitt, S., Schober, K., Schüler, T., Schulz, A.R., Schumacher, T., Scotta, C., Shankey, T.V., Shemer, A., Simon, A.-K., Spidlen, J., Stall, A.M., Stark, R., Stehle, C., Stein, M., Steinmetz, T., Stockinger, H., Takahama, Y., Tarnok, A., Tian, Z., Toldi, G., Tornack, J., Traggiai, E., Trotter, J., Ulrich, H., van der Braber, M., van Lier, R.A.W., Veldhoen, M., Vento-Asturias, S., Vieira, P., Voehringer, D., Volk, H.-D., von Volkmann, K., Waisman, A., Walker, R., Ward, M.D., Warnatz, K., Warth, S., Watson, J. V., Watzl, C., Wegener, L., Wiedemann, A., Wienands, J., Willimsky, G., Wing, J., Wurst, P., Yu, L., Yue, A., Zhang, Q., Zhao, Y., Ziegler, S., Zimmermann, J., 2017. Guidelines for the use of flow cytometry and cell sorting in immunological studies. Eur. J. Immunol. 47, 1584–1797. https://doi.org/10.1002/eji.201646632

Crane, R.K., 1977. The gradient hypothesis and other models of carrier-mediated active transport, in: Reviews of Physiology, Biochemistry and Pharmacology, Volume 78. Springer-Verlag, Berlin/Heidelberg, pp. 99–159. https://doi.org/10.1007/BFb0027722

da Silva, T.L., Reis, A., Medeiros, R., Oliveira, A.C., Gouveia, L., 2009. Oil production towards biofuel

from autotrophic microalgae semicontinuous cultivations monitorized by flow cytometry. Appl. Biochem. Biotechnol. 159, 568–78. https://doi.org/10.1007/s12010-008-8443-5

De Lorenzo, V., Fernandez, S., Herrero, M., Jakubzik, U., Timmis, K.N., 1993. Engineering of alkyl- and haloaromatic-responsive gene expression with mini-transposons containing regulated promoters of biodegradative pathways of Pseudomonas. Gene 130, 41–46. https://doi.org/10.1016/0378-1119(93)90344-3

Díaz, E., Ferrández, A., Prieto, M.A., García, J.L., 2001. Biodegradation of aromatic compounds by *Escherichia coli*. Microbiol. Mol. Biol. Rev. 65, 523–69. https://doi.org/10.1128/MMBR.65.4.523-569.2001

Dietrich, J.A., McKee, A.E., Keasling, J.D., 2010. High-throughput metabolic engineering: advances in small-molecule screening and selection. Annu. Rev. Biochem. 79, 563–90. https://doi.org/10.1146/annurev-biochem-062608-095938

Dietrich, J.A., Shis, D.L., Alikhani, A., Keasling, J.D., 2013. Transcription factor-based screens and synthetic selections for microbial small-molecule biosynthesis. ACS Synth. Biol. 2, 47–58. https://doi.org/10.1021/sb300091d

Ellington, A.D., Szostak, J.W., 1990. In vitro selection of RNA molecules that bind specific ligands. Nature 346, 818–822. https://doi.org/10.1038/346818a0

Elowitz, M.B., Leibler, S., 2000. A synthetic oscillatory network of transcriptional regulators. Nature 403, 335–8. https://doi.org/10.1038/35002125

Endy, D., 2005. Foundations for engineering biology. Nature 438, 449–453. https://doi.org/10.1038/nature04342

Eudes, A., Juminaga, D., Baidoo, E.E.K., Collins, F., Keasling, J.D., Loqué, D., 2013. Production of hydroxycinnamoyl anthranilates from glucose in *Escherichia coli*. Microb. Cell Fact. 12, 62. https://doi.org/10.1186/1475-2859-12-62

Fasan, R., Chen, M.M., Crook, N.C., Arnold, F.H., 2007. Engineered Alkane-Hydroxylating Cytochrome P450BM3 Exhibiting Nativelike Catalytic Properties. Angew. Chemie Int. Ed. 46, 8414–8418. https://doi.org/10.1002/anie.200702616

Feng, J., Jester, B.W., Tinberg, C.E., Mandell, D.J., Antunes, M.S., Chari, R., Morey, K.J., Rios, X., Medford, J.I., Church, G.M., Fields, S., Baker, D., 2015. A general strategy to construct small molecule biosensors in eukaryotes. Elife 4. https://doi.org/10.7554/eLife.10606

Fouchet, P., Jan, S., Courtois, J., Courtois, B., Frelat, G., Barbotin, J.., 1995. Quantitative single-cell

detection of poly(Î²-hydroxybutyrate) accumulation in Rhizobium meliloti by flow cytometry. FEMS Microbiol. Lett. 126, 31–35. https://doi.org/https://doi.org/10.1002/anie.200702616

Fredens, J., Wang, K., de la Torre, D., Funke, L.F.H., Robertson, W.E., Christova, Y., Chia, T., Schmied, W.H., Dunkelmann, D.L., Beránek, V., Uttamapinant, C., Llamazares, A.G., Elliott, T.S., Chin, J.W., 2019. Total synthesis of *Escherichia coli* with a recoded genome. Nature 569, 514–518. https://doi.org/10.1038/s41586-019-1192-5

Furusawa, C., Horinouchi, T., Hirasawa, T., Shimizu, H., 2013. Systems metabolic engineering: the creation of microbial cell factories by rational metabolic design and evolution. Adv. Biochem. Eng. Biotechnol. 131, 1–23. https://doi.org/10.1007/10_2012_137

Gaj, T., Gersbach, C.A., Barbas, C.F., 2013. ZFN, TALEN, and CRISPR/Cas-based methods for genome engineering. Trends Biotechnol. 31, 397–405. https://doi.org/10.1016/J.TIBTECH.2013.04.004

Gardner, T.S., Cantor, C.R., Collins, J.J., 2000. Construction of a genetic toggle switch in *Escherichia coli*. Nature 403, 339–42. https://doi.org/10.1038/35002131

Ghribi, D., Zouari, N., Jaoua, S., 2004. Improvement of bioinsecticides production through mutagenesis of Bacillus thuringiensis by u.v. and nitrous acid affecting metabolic pathways and/or delta-endotoxin synthesis. J. Appl. Microbiol. 97, 338–346. https://doi.org/10.1111/j.1365-2672.2004.02323.x

Gibson, D.G., Benders, G.A., Andrews-Pfannkoch, C., Denisova, E.A., Baden-Tillson, H., Zaveri, J., Stockwell, T.B., Brownley, A., Thomas, D.W., Algire, M.A., Merryman, C., Young, L., Noskov, V.N., Glass, J.I., Venter, J.C., Hutchison, C.A., Smith, H.O., 2008. Complete chemical synthesis, assembly, and cloning of a Mycoplasma genitalium genome. Science 319, 1215–20. https://doi.org/10.1126/science.1151721

Gouveia, L., Marques, A.E., da Silva, T.L., Reis, A., 2009. Neochloris oleabundans UTEX #1185: a suitable renewable lipid source for biofuel production. J. Ind. Microbiol. Biotechnol. 36, 821–6. https://doi.org/10.1007/s10295-009-0559-2

Gutmann, M., Hoischen, C., Krämer, R., 1992. Carrier-mediated glutamate secretion by *Corynebacterium glutamicum* under biotin limitation. Biochim. Biophys. Acta - Biomembr. 1112, 115–123. https://doi.org/10.1016/0005-2736(92)90261-J

Hall, B.G., 1981. Changes in the substrate specificities of an enzyme during directed evolution of new functions. Biochemistry 20, 4042–9. https://doi.org/10.1021/bi00517a015

Hamers, D., van Voorst Vader, L., Borst, J.W., Goedhart, J., 2014. Development of FRET biosensors for

mammalian and plant systems. Protoplasma 251, 333–47. https://doi.org/10.1007/s00709-013-0590-z

Harmsen, P.F.H., Hackmann, M.M., Bos, H.L., 2014. Green building blocks for bio-based plastics. Biofuels, Bioprod. Biorefining 8, 306–324. https://doi.org/10.1002/bbb.1468

Hessels, A.M., Merkx, M., 2015. Genetically-encoded FRET-based sensors for monitoring Zn 2+ in living cells. Metallomics 7, 258–266. https://doi.org/10.1039/C4MT00179F

Hoppe, G.K., Hansford, G.S., 1984. The effect of micro-aerobic conditions on continuous ethanol production by Saccharomyces cerevisiae. Biotechnol. Lett. 6, 681–686. https://doi.org/10.1007/BF00133837

Hughes, S.R., Gibbons, W.R., Bang, S.S., Pinkelman, R., Bischoff, K.M., Slininger, P.J., Qureshi, N., Kurtzman, C.P., Liu, S., Saha, B.C., Jackson, J.S., Cotta, M.A., Rich, J.O., Javers, J.E., 2012. Random UV-C mutagenesis of Scheffersomyces (formerly Pichia) stipitis NRRL Y-7124 to improve anaerobic growth on lignocellulosic sugars. J. Ind. Microbiol. Biotechnol. 39, 163–173. https://doi.org/10.1007/s10295-011-1012-x

Ikariyama, Y., Nishiguchi, S., Koyama, T., Kobatake, E., Aizawa, M., Tsuda, M., Nakazawa, T., 1997. Fiber-optic-based biomonitoring of benzene derivatives by recombinant E. coli bearing luciferase gene-fused TOL-plasmid immobilized on the fiber-optic end. Anal. Chem. 69, 2600–5. https://doi.org/10.1021/ac961311o

Jahn, M., Vorpahl, C., Hübschmann, T., Harms, H., Müller, S., 2016. Copy number variability of expression plasmids determined by cell sorting and Droplet Digital PCR. Microb. Cell Fact. 15, 211. https://doi.org/10.1186/s12934-016-0610-8

Jakočiūnas, T., Pedersen, L.E., Lis, A. V., Jensen, M.K., Keasling, J.D., 2018. CasPER, a method for directed evolution in genomic contexts using mutagenesis and CRISPR/Cas9. Metab. Eng. 48, 288–296. https://doi.org/10.1016/j.ymben.2018.07.001

Jang, S., Yang, J., Seo, S.W., Jung, G.Y., 2015. Riboselector: riboswitch-based synthetic selection device to expedite evolution of metabolite-producing microorganisms. Methods Enzymol. 550, 341–62. https://doi.org/10.1016/bs.mie.2014.10.039

Jendresen, C.B., Stahlhut, S.G., Li, M., Gaspar, P., Siedler, S., Förster, J., Maury, J., Borodina, I., Nielsen, A.T., 2015. Novel highly active and specific tyrosine ammonia-lyases from diverse origins enable enhanced production of aromatic compounds in bacteria and yeast. Appl. Environ. Microbiol. AEM.00405-15. https://doi.org/10.1128/AEM.00405-15

Jinek, M., Chylinski, K., Fonfara, I., Hauer, M., Doudna, J.A., Charpentier, E., 2012. A programmable dual-RNA-guided DNA endonuclease in adaptive bacterial immunity. Science 337, 816–21. https://doi.org/10.1126/science.1225829

Kallscheuer, N., Menezes, R., Foito, A., da Silva, M.H., Braga, A., Dekker, W., Sevillano, D.M., Rosado-Ramos, R., Jardim, C., Oliveira, J., Ferreira, P., Rocha, I., Silva, A.R., Sousa, M., Allwood, J.W., Bott, M., Faria, N., Stewart, D., Ottens, M., Naesby, M., Nunes Dos Santos, C., Marienhagen, J., 2019. Identification and Microbial Production of the Raspberry Phenol Salidroside that Is Active against Huntington's Disease. Plant Physiol. 179, 969–985. https://doi.org/10.1104/pp.18.01074

Kallscheuer, N., Vogt, M., Stenzel, A., Gätgens, J., Bott, M., Marienhagen, J., 2016. Construction of a *Corynebacterium glutamicum* platform strain for the production of stilbenes and (2S)-flavanones. Metab. Eng. 38, 47–55. https://doi.org/10.1016/j.ymben.2016.06.003

Kang, Z., Zhang, C., Zhang, J.J., Jin, P., Zhang, J.J., Du, G., Chen, J., 2014. Small RNA regulators in bacteria: powerful tools for metabolic engineering and synthetic biology. Appl. Microbiol. Biotechnol. 98, 3413–24. https://doi.org/10.1007/s00253-014-5569-y

Kaplan, N.L., Hudson, R.R., Langley, C.H., 1989. The "hitchhiking effect" revisited. Genetics 123, 887–99.

Kaschubowski, K.E., Kraft, A.E., Nikolaev, V.O., Haag, F., 2020. Using FRET-Based Fluorescent Sensors to Monitor Cytosolic and Membrane-Proximal Extracellular ATP Levels, in: Pelegrín, P. (Ed.), Purinergic Signaling: Methods and Protocols. Springer New York, New York, NY, pp. 223–231. https://doi.org/10.1007/978-1-4939-9717-6_16

Keseler, I.M., Mackie, A., Peralta-Gil, M., Santos-Zavaleta, A., Gama-Castro, S., Bonavides-Martínez, C., Fulcher, C., Huerta, A.M., Kothari, A., Krummenacker, M., Latendresse, M., Muñiz-Rascado, L., Ong, Q., Paley, S., Schröder, I., Shearer, A.G., Subhraveti, P., Travers, M., Weerasinghe, D., Weiss, V., Collado-Vides, J., Gunsalus, R.P., Paulsen, I., Karp, P.D., 2013. EcoCyc: fusing model organism databases with systems biology. Nucleic Acids Res. 41, D605–D612. https://doi.org/10.1093/nar/gks1027

Khlebnikov, A., Datsenko, K.A., Skaug, T., Wanner, B.L., Keasling, J.D., 2001. Homogeneous expression of the P(BAD) promoter in *Escherichia coli* by constitutive expression of the low-affinity high-capacity AraE transporter. Microbiology 147, 3241–7. https://doi.org/10.1099/00221287-147-12-3241

Khlebnikov, A., Risa, O., Skaug, T., Carrier, T.A., Keasling, J.D., 2000. Regulatable arabinose-inducible gene expression system with consistent control in all cells of a culture. J. Bacteriol. 182, 7029–34.

https://doi.org/10.1128/JB.182.24.7029-7034.2000.Updated

Kiviet, D.J., Nghe, P., Walker, N., Boulineau, S., Sunderlikova, V., Tans, S.J., 2014. Stochasticity of metabolism and growth at the single-cell level. Nature 514, 376–9. https://doi.org/10.1038/nature13582

Knight, T., 2003. Idempotent vector design for standard assembly of biobricks.

Koopman, F., Beekwilder, J., Crimi, B., van Houwelingen, A., Hall, R.D., Bosch, D., van Maris, A.J., Pronk, J.T., Daran, J.-M., 2012. De novo production of the flavonoid naringenin in engineered Saccharomyces cerevisiae. Microb. Cell Fact. 11, 155. https://doi.org/10.1186/1475-2859-11-155

Kopniczky, M.B., Moore, S.J., Freemont, P.S., 2015. Multilevel Regulation and Translational Switches in Synthetic Biology. IEEE Trans. Biomed. Circuits Syst. 9, 485–96. https://doi.org/10.1109/TBCAS.2015.2451707

Korkina, L., Kostyuk, V., De Luca, C., Pastore, S., 2011. Plant Phenylpropanoids as Emerging Anti-Inflammatory Agents. Mini-Reviews Med. Chem. 11, 823–835. https://doi.org/10.2174/138955711796575489

Kucherov, F.A., Romashov, L. V, Galkin, K.I., Ananikov, V.P., 2018. Chemical Transformations of Biomass-Derived C6-Furanic Platform Chemicals for Sustainable Energy Research, Materials Science, and Synthetic Building Blocks. ACS Sustain. Chem. Eng. 6, 8064–8092. https://doi.org/10.1021/acssuschemeng.8b00971

Lee, S.-W., Oh, M.-K., 2015. A synthetic suicide riboswitch for the high-throughput screening of metabolite production in Saccharomyces cerevisiae. Metab. Eng. 28, 143–150. https://doi.org/10.1016/j.ymben.2015.01.004

Lee, S.Y., Kim, H.U., Park, J.H., Park, J.M., Kim, T.Y., 2009. Metabolic engineering of microorganisms: general strategies and drug production. Drug Discov. Today 14, 78–88. https://doi.org/10.1016/J.DRUDIS.2008.08.004

Leonard, E., Yan, Y., Fowler, Z.L., Li, Z., Lim, C.-G., Lim, K.-H., Koffas, M.A.G., 2008. Strain Improvement of Recombinant *Escherichia coli* for Efficient Production of Plant Flavonoids. Mol. Pharm. 5, 257–265. https://doi.org/10.1021/mp7001472

Liang, J.C., Bloom, R.J., Smolke, C.D., 2011. Engineering biological systems with synthetic RNA molecules. Mol. Cell 43, 915–26. https://doi.org/10.1016/j.molcel.2011.08.023

Lin, J.-L., Wagner, J.M., Alper, H.S., 2017. Enabling tools for high-throughput detection of metabolites: Metabolic engineering and directed evolution applications. Biotechnol. Adv. 0–1.

https://doi.org/10.1016/j.biotechadv.2017.07.005

Lin, Y., Yan, Y., 2012. Biosynthesis of caffeic acid in *Escherichia coli* using its endogenous hydroxylase complex. Microb. Cell Fact. 11, 42. https://doi.org/10.1186/1475-2859-11-42

Liu, Ya'nan, Li, Q., Zheng, P., Zhang, Z., Liu, Yongfei, Sun, C., Cao, G., Zhou, W., Wang, X., Zhang, D., Zhang, T., Sun, J., Ma, Y., 2015. Developing a high-throughput screening method for threonine overproduction based on an artificial promoter. Microb. Cell Fact. 14, 121. https://doi.org/10.1186/s12934-015-0311-8

Lutz, S., Iamurri, S.M., 2018. Protein Engineering: Past, Present, and Future, in: Protein Engineering. Springer, pp. 1–12. https://doi.org/10.1007/978-1-4939-7366-8_1

Mahr, R., Frunzke, J., 2015. Transcription factor-based biosensors in biotechnology: current state and future prospects. Appl. Microbiol. Biotechnol. https://doi.org/10.1007/s00253-015-7090-3

Mahr, R., Gätgens, C., Gätgens, J., Polen, T., Kalinowski, J., Frunzke, J., 2015. Biosensor-driven adaptive laboratory evolution of l-valine production in *Corynebacterium glutamicum*. Metab. Eng. 32, 184–94. https://doi.org/10.1016/j.ymben.2015.09.017

Mahr, R., von Boeselager, R.F., Wiechert, J., Frunzke, J., 2016. Screening of an *Escherichia coli* promoter library for a phenylalanine biosensor. Appl. Microbiol. Biotechnol. https://doi.org/10.1007/s00253-016-7575-8

Martin, V.J.J., Pitera, D.J., Withers, S.T., Newman, J.D., Keasling, J.D., 2003. Engineering a mevalonate pathway in *Escherichia coli* for production of terpenoids. Nat. Biotechnol. 21, 796–802. https://doi.org/10.1038/nbt833

McVey, M., Lee, S.E., 2008. MMEJ repair of double-strand breaks (director's cut): deleted sequences and alternative endings. Trends Genet. 24, 529–38. https://doi.org/10.1016/j.tig.2008.08.007

Michener, J.K., Smolke, C.D., 2012. High-throughput enzyme evolution in Saccharomyces cerevisiae using a synthetic RNA switch. Metab. Eng. 14, 306–316. https://doi.org/10.1016/j.ymben.2012.04.004

Milke, L., Aschenbrenner, J., Marienhagen, J., Kallscheuer, N., 2018. Production of plant-derived polyphenols in microorganisms: current state and perspectives. Appl. Microbiol. Biotechnol. 102, 1575–1585. https://doi.org/10.1007/s00253-018-8747-5

Milke, L., Ferreira, P., Kallscheuer, N., Braga, A., Vogt, M., Kappelmann, J., Oliveira, J., Silva, A.R., Rocha, I., Bott, M., Noack, S., Faria, N., Marienhagen, J., 2019a. Modulation of the central carbon metabolism of *Corynebacterium glutamicum* improves malonyl-CoA availability and increases

plant polyphenol synthesis. Biotechnol. Bioeng. 116, 1380–1391. https://doi.org/10.1002/bit.26939

Milke, L., Kallscheuer, N., Kappelmann, J., Marienhagen, J., 2019b. Tailoring *Corynebacterium glutamicum* towards increased malonyl-CoA availability for efficient synthesis of the plant pentaketide noreugenin. Microb. Cell Fact. 18, 71. https://doi.org/10.1186/s12934-019-1117-x

Miller, J.C., Tan, S., Qiao, G., Barlow, K.A., Wang, J., Xia, D.F., Meng, X., Paschon, D.E., Leung, E., Hinkley, S.J., Dulay, G.P., Hua, K.L., Ankoudinova, I., Cost, G.J., Urnov, F.D., Zhang, H.S., Holmes, M.C., Zhang, L., Gregory, P.D., Rebar, E.J., 2011. A TALE nuclease architecture for efficient genome editing. Nat. Biotechnol. 29, 143–148. https://doi.org/10.1038/nbt.1755

Möglich, A., Hegemann, P., 2013. Programming genomes with light. Nature 500, 406–408. https://doi.org/10.1038/500406a

Mohsin, M., Abdin, M.Z., Nischal, L., Kardam, H., Ahmad, A., 2013. Genetically encoded FRET-based nanosensor for in vivo measurement of leucine. Biosens. Bioelectron. 50, 72–7. https://doi.org/10.1016/j.bios.2013.06.028

Mohsin, M., Ahmad, A., 2014. Genetically-encoded nanosensor for quantitative monitoring of methionine in bacterial and yeast cells. Biosens. Bioelectron. 59, 358–64. https://doi.org/10.1016/j.bios.2014.03.066

Munch, R., Hiller, K., Barg, H., Heldt, D., Linz, S., Wingender, E., Jahn, D., 2003. PRODORIC: prokaryotic database of gene regulation. Nucleic Acids Res. 31, 266–269. https://doi.org/10.1093/nar/gkg037

Mustafi, N., Grünberger, A., Kohlheyer, D., Bott, M., Frunzke, J., 2012. The development and application of a single-cell biosensor for the detection of l-methionine and branched-chain amino acids. Metab. Eng. 14, 449–57. https://doi.org/10.1016/j.ymben.2012.02.002

Mustafi, N., Grünberger, A., Mahr, R., Helfrich, S., Nöh, K., Blombach, B., Kohlheyer, D., Frunzke, J., 2014. Application of a genetically encoded biosensor for live cell imaging of L-valine production in pyruvate dehydrogenase complex-deficient *Corynebacterium glutamicum* strains. PLoS One 9, e85731. https://doi.org/10.1371/journal.pone.0085731

Nadler, D.C., Morgan, S.-A., Flamholz, A., Kortright, K.E., Savage, D.F., 2016. Rapid construction of metabolite biosensors using domain-insertion profiling. Nat. Commun. 7, 12266. https://doi.org/10.1038/ncomms12266

Nahvi, A., Sudarsan, N., Ebert, M.S., Zou, X., Brown, K.L., Breaker, R.R., 2002. Genetic Control by a

Metabolite Binding mRNA. Chem. Biol. 9, 1043–1049. https://doi.org/10.1016/S1074-5521(02)00224-7

Neylon, C., 2004. Chemical and biochemical strategies for the randomization of protein encoding DNA sequences: library construction methods for directed evolution. Nucleic Acids Res. 32, 1448–59. https://doi.org/10.1093/nar/gkh315

Niedenführ, S., Wiechert, W., Nöh, K., 2015. How to measure metabolic fluxes: a taxonomic guide for 13C fluxomics. Curr. Opin. Biotechnol. 34, 82–90. https://doi.org/10.1016/J.COPBIO.2014.12.003

Nielsen, J., 2001. Metabolic engineering. Appl. Microbiol. Biotechnol. 55, 263–283. https://doi.org/10.1007/s002530000511

Nonomura, A.M., Coder, D.M., 1988. Improved phycocatalysis of carotene production by flow cytometry and cell sorting. Biocatalysis 1, 333–338.

Novichkov, P.S., Kazakov, A.E., Ravcheev, D.A., Leyn, S.A., Kovaleva, G.Y., Sutormin, R.A., Kazanov, M.D., Riehl, W., Arkin, A.P., Dubchak, I., Rodionov, D.A., 2013. RegPrecise 3.0 – A resource for genome-scale exploration of transcriptional regulation in bacteria. BMC Genomics 14, 745. https://doi.org/10.1186/1471-2164-14-745

Pasteur, L., 1857. Mémoire sur la fermentation appelée lactique (Extrait par l'auteur). Comptes rendus des seances l'Academie des Sci. 45, 913–916.

Petzold, C.J., Chan, L.J.G., Nhan, M., Adams, P.D., 2015. Analytics for Metabolic Engineering. Front. Bioeng. Biotechnol. 3, 135. https://doi.org/10.3389/fbioe.2015.00135

Pfleger, B.F., Pitera, D.J., Newman, J.D., Martin, V.J.J., Keasling, J.D., 2007. Microbial sensors for small molecules: development of a mevalonate biosensor. Metab. Eng. 9, 30–8. https://doi.org/10.1016/j.ymben.2006.08.002

Pitera, D.J., Paddon, C.J., Newman, J.D., Keasling, J.D., 2007. Balancing a heterologous mevalonate pathway for improved isoprenoid production in *Escherichia coli*. Metab. Eng. 9, 193–207. https://doi.org/10.1016/j.ymben.2006.11.002

Potzkei, J., Kunze, M., Drepper, T., Gensch, T., Jaeger, K.-E.E., Buechs, J., Büchs, J., 2012. Real-time determination of intracellular oxygen in bacteria using a genetically encoded FRET-based biosensor. BMC Biol. 10, 28. https://doi.org/10.1186/1741-7007-10-28

Reisch, C.R., Prather, K.L.J., 2015. The no-SCAR (Scarless Cas9 Assisted Recombineering) system for genome editing in *Escherichia coli*. Sci. Rep. 5, 15096. https://doi.org/10.1038/srep15096

Rogers, J.K., Church, G.M., 2016. Genetically encoded sensors enable real-time observation of

metabolite production. Proc. Natl. Acad. Sci. U. S. A. 113, 2388–93. https://doi.org/10.1073/pnas.1600375113

Ronda, C., Pedersen, L.E., Sommer, M.O.A., Nielsen, A.T., 2016. CRMAGE: CRISPR Optimized MAGE Recombineering. Sci. Rep. 6, 19452. https://doi.org/10.1038/srep19452

Rovner, A.J., Haimovich, A.D., Katz, S.R., Li, Z., Grome, M.W., Gassaway, B.M., Amiram, M., Patel, J.R., Gallagher, R.R., Rinehart, J., Isaacs, F.J., 2015. Recoded organisms engineered to depend on synthetic amino acids. Nature 518, 89–93. https://doi.org/10.1038/nature14095

Roy, A., Kucukural, A., Zhang, Y., 2010. I-TASSER: a unified platform for automated protein structure and function prediction. Nat. Protoc. 5, 725–38. https://doi.org/10.1038/nprot.2010.5

Salgado, H., Gama-Castro, S., Peralta-Gil, M., Díaz-Peredo, E., Sánchez-Solano, F., Santos-Zavaleta, A., Martínez-Flores, I., Jiménez-Jacinto, V., Bonavides-Martínez, C., Segura-Salazar, J., Martínez-Antonio, A., Collado-Vides, J., 2006. RegulonDB (version 5.0): *Escherichia coli* K-12 transcriptional regulatory network, operon organization, and growth conditions. Nucleic Acids Res. 34, D394–D397. https://doi.org/10.1093/nar/gkj156

San Martín, A., Ceballo, S., Ruminot, I., Lerchundi, R., Frommer, W.B., Barros, L.F., 2013. A genetically encoded FRET lactate sensor and its use to detect the Warburg effect in single cancer cells. PLoS One 8, e57712. https://doi.org/10.1371/journal.pone.0057712

Santos, C.N.S., Koffas, M., Stephanopoulos, G., 2011. Optimization of a heterologous pathway for the production of flavonoids from glucose. Metab. Eng. 13, 392–400. https://doi.org/10.1016/J.YMBEN.2011.02.002

Sauer, U., 2001. Evolutionary Engineering of Industrially Important Microbial Phenotypes, in: Advances in Biochemical Engineering/Biotechnology. pp. 129–169. https://doi.org/10.1007/3-540-45300-8_7

Scarlat, N., Dallemand, J.F., Monforti-Ferrario, F., Nita, V., 2015. The role of biomass and bioenergy in a future bioeconomy: Policies and facts. Environ. Dev. 15, 3–34. https://doi.org/10.1016/j.envdev.2015.03.006

Schallmey, M., Frunzke, J., Eggeling, L., Marienhagen, J., 2014. Looking for the pick of the bunch: high-throughput screening of producing microorganisms with biosensors. Curr. Opin. Biotechnol. 26, 148–54. https://doi.org/10.1016/j.copbio.2014.01.005

Schendzielorz, G., Dippong, M., Grünberger, A., Kohlheyer, D., Yoshida, A., Binder, S., Nishiyama, C., Nishiyama, M., Bott, M., Eggeling, L., 2014. Taking control over control: use of product sensing in

single cells to remove flux control at key enzymes in biosynthesis pathways. ACS Synth. Biol. 3, 21–9. https://doi.org/10.1021/sb400059y

Schürrle, K., 2018. History, Current State, and Emerging Applications of Industrial Biotechnology. Springer Fachmedien, Wiesbaden, pp. 1–39. https://doi.org/10.1007/10_2018_81

Serganov, A., Nudler, E., 2013. A decade of riboswitches. Cell 152, 17–24. https://doi.org/10.1016/j.cell.2012.12.024

Sibbesson, E., 2019. Reclaiming the Rotten: Understanding Food Fermentation in the Neolithic and Beyond. Environ. Archaeol. 1–12. https://doi.org/10.1080/14614103.2018.1563374

Siedler, S., Schendzielorz, G., Binder, S., Eggeling, L., Bringer, S., Bott, M., 2014. SoxR as a single-cell biosensor for NADPH-consuming enzymes in *Escherichia coli*. ACS Synth. Biol. 3, 41–7. https://doi.org/10.1021/sb400110j

Snoek, T., Romero-Suarez, D., Zhang, J., Ambri, F., Skjoedt, M.L., Sudarsan, S., Jensen, M.K., Keasling, J.D., 2018. An Orthogonal and pH-Tunable Sensor-Selector for Muconic Acid Biosynthesis in Yeast. ACS Synth. Biol. 7, 995–1003. https://doi.org/10.1021/acssynbio.7b00439

Sowa, S.W., Gelderman, G., Contreras, L.M., 2015. Advances in synthetic dynamic circuits design: using novel synthetic parts to engineer new generations of gene oscillations. Curr. Opin. Biotechnol. 36, 161–167. https://doi.org/10.1016/J.COPBIO.2015.08.020

Sticher, P., Jaspers, M.C.M., Stemmler, K., Harms, H., Zehnder, A.J.B., Van Der Meer, J.R., 1997. Development and characterization of a whole-cell bioluminescent sensor for bioavailable middle-chain alkanes in contaminated groundwater samples. Appl. Environ. Microbiol. 63, 4053–4060.

Turlin, E., Perrotte-piquemal, M., Danchin, A., Biville, F., 2001. Regulation of the early steps of 3-phenylpropionate catabolism in *Escherichia coli*. J. Mol. Microbiol. Biotechnol. 3, 127–33.

Uchiyama, T., Miyazaki, K., 2010. Product-induced gene expression, a product-responsive reporter assay used to screen metagenomic libraries for enzyme-encoding genes. Appl. Environ. Microbiol. 76, 7029–35. https://doi.org/10.1128/AEM.00464-10

Ukibe, K., Katsuragi, T., Tani, Y., Takagi, H., 2008. Efficient screening for astaxanthin-overproducing mutants of the yeast Xanthophyllomyces dendrorhous by flow cytometry. FEMS Microbiol. Lett. 286, 241–248.

Valli, M., Sauer, M., Branduardi, P., Borth, N., Porro, D., Mattanovich, D., 2006. Improvement of lactic acid production in Saccharomyces cerevisiae by cell sorting for high intracellular pH. Appl. Environ. Microbiol. 72, 5492–5499.

Valli, M., Sauer, M., Branduardi, P., Borth, N., Porro, D., Mattanovich, D., 2005. Intracellular pH distribution in Saccharomyces cerevisiae cell populations, analyzed by flow cytometry. Appl. Environ. Microbiol. 71, 1515–1521.

Vidal-Mas, J., Resina-Pelfort, O., Haba, E., Comas, J., Manresa, A., Vives-Rego, J., 2001. Rapid flow cytometry--Nile red assessment of PHA cellular content and heterogeneity in cultures of Pseudomonas aeruginosa 47T2 (NCIB 40044) grown in waste frying oil. Antonie Van Leeuwenhoek 80, 57–63.

Wang, H.H., Isaacs, F.J., Carr, P.A., Sun, Z.Z., Xu, G., Forest, C.R., Church, G.M., 2009. Programming cells by multiplex genome engineering and accelerated evolution. Nature 460, 894–898. https://doi.org/10.1038/nature08187

Watts, N., Adger, W.N., Agnolucci, P., Blackstock, J., Byass, P., Cai, W., Chaytor, S., Colbourn, T., Collins, M., Cooper, A., Cox, P.M., Depledge, J., Drummond, P., Ekins, P., Galaz, V., Grace, D., Graham, H., Grubb, M., Haines, A., Hamilton, I., Hunter, A., Jiang, X., Li, M., Kelman, I., Liang, L., Lott, M., Lowe, R., Luo, Y., Mace, G., Maslin, M., Nilsson, M., Oreszczyn, T., Pye, S., Quinn, T., Svensdotter, M., Venevsky, S., Warner, K., Xu, B., Yang, J., Yin, Y., Yu, C., Zhang, Q., Gong, P., Montgomery, H., Costello, A., 2015. Health and climate change: policy responses to protect public health. Lancet 386, 1861–1914. https://doi.org/10.1016/S0140-6736(15)60854-6

Wieschalka, S., Blombach, B., Bott, M., Eikmanns, B.J., 2013. Bio-based production of organic acids with *Corynebacterium glutamicum*. Microb. Biotechnol. 6, 87–102. https://doi.org/10.1111/1751-7915.12013

Williamson, L.L., Borlee, B.R., Schloss, P.D., Guan, C., Allen, H.K., Handelsman, J., 2005. Intracellular screen to identify metagenomic clones that induce or inhibit a quorum-sensing biosensor. Appl. Environ. Microbiol. 71, 6335–44. https://doi.org/10.1128/AEM.71.10.6335-6344.2005

Wilson, D., Charoensawan, V., Kummerfeld, S.K., Teichmann, S.A., 2008. DBD—taxonomically broad transcription factor predictions: new content and functionality. Nucleic Acids Res. 36, D88–D92. https://doi.org/10.1093/nar/gkm964

Wink, M., 2018. Introduction: Biochemistry, Physiology and Ecological Functions of Secondary Metabolites, in: Annual Plant Reviews Online. John Wiley & Sons, Ltd, Chichester, UK, pp. 1–19. https://doi.org/10.1002/9781119312994.apr0423

Winkler, W.C., Cohen-Chalamish, S., Breaker, R.R., 2002a. An mRNA structure that controls gene expression by binding FMN. Proc. Natl. Acad. Sci. U. S. A. 99, 15908–13. https://doi.org/10.1073/pnas.212628899

Winkler, W.C., Nahvi, A., Breaker, R.R., 2002b. Thiamine derivatives bind messenger RNAs directly to regulate bacterial gene expression. Nature 419, 952–6. https://doi.org/10.1038/nature01145

Woolston, B.M., Edgar, S., Stephanopoulos, G., 2013. Metabolic engineering: past and future. Annu. Rev. Chem. Biomol. Eng. 4, 259–88. https://doi.org/10.1146/annurev-chembioeng-061312-103312

Xiao, Y., Bowen, C.H., Liu, D., Zhang, F., 2016. Exploiting nongenetic cell-to-cell variation for enhanced biosynthesis. Nat. Chem. Biol. 12, 339–44. https://doi.org/10.1038/nchembio.2046

Xu, P., Li, L., Zhang, F., Stephanopoulos, G., Koffas, M., 2014. Improving fatty acids production by engineering dynamic pathway regulation and metabolic control. Proc. Natl. Acad. Sci. U. S. A. 111, 11299–304. https://doi.org/10.1073/pnas.1406401111

Yang, J., Seo, S.W., Jang, S., Shin, S.-I., Lim, C.H., Roh, T.-Y., Jung, G.Y., 2013. Synthetic RNA devices to expedite the evolution of metabolite-producing microbes. Nat. Commun. 4, 1413. https://doi.org/10.1038/ncomms2404

Yang, J., Yan, R., Roy, A., Xu, D., Poisson, J., Zhang, Y., 2015. The I-TASSER Suite: protein structure and function prediction. Nat. Methods 12, 7–8. https://doi.org/10.1038/nmeth.3213

Yano, T., Oku, M., Akeyama, N., Itoyama, A., Yurimoto, H., Kuge, S., Fujiki, Y., Sakai, Y., 2010. A novel fluorescent sensor protein for visualization of redox states in the cytoplasm and in peroxisomes. Mol. Cell. Biol. 30, 3758–66. https://doi.org/10.1128/MCB.00121-10

Yeom, S.-J., Kim, M., Kwon, K.K., Fu, Y., Rha, E., Park, S.-H., Lee, H., Kim, H., Lee, D.-H., Kim, D.-M., Lee, S.-G., 2018. A synthetic microbial biosensor for high-throughput screening of lactam biocatalysts. Nat. Commun. 9, 5053. https://doi.org/10.1038/s41467-018-07488-0

Yonekura-Sakakibara, K., Saito, K., 2009. Functional genomics for plant natural product biosynthesis. Nat. Prod. Rep. 26, 1466. https://doi.org/10.1039/b817077k

Zhang, J., Sonnenschein, N., Pihl, T.P.B., Pedersen, K.R., Jensen, M.K., Keasling, J.D., 2016. Engineering an NADPH/NADP+ Redox Biosensor in Yeast. ACS Synth. Biol. 5, 1546–1556. https://doi.org/10.1021/acssynbio.6b00135

Zhang, Y., 2008. I-TASSER server for protein 3D structure prediction. BMC Bioinformatics 9, 40. https://doi.org/10.1186/1471-2105-9-40

Zhou, L.-B., Zeng, A.-P., 2015. Engineering a Lysine-ON Riboswitch for Metabolic Control of Lysine Production in *Corynebacterium glutamicum*. ACS Synth. Biol. 4, 1335–40. https://doi.org/10.1021/acssynbio.5b00075

Zhou, S., Liu, P., Chen, J., Du, G., Li, H., Zhou, J., 2016. Characterization of mutants of a tyrosine ammonia-lyase from *Rhodotorula glutinis*. Appl. Microbiol. Biotechnol. 100, 10443–10452. https://doi.org/10.1007/s00253-016-7672-8

Zhu, Q., Wang, L., Dong, Q., Chang, S., Wen, K., Jia, S., Chu, Z., Wang, H., Gao, P., Zhao, H., Han, S., Wang, Y., 2017. FRET-based glucose imaging identifies glucose signalling in response to biotic and abiotic stresses in rice roots. J. Plant Physiol. 215, 65–72. https://doi.org/10.1016/j.jplph.2017.05.007

4. Appendix

4.1. Author contributions

Flachbart, L.K., Sokolowsky, S., Marienhagen, J. (2019). **Displaced by deceivers - Prevention of biosensor cross-talk is pivotal for successful biosensor-based high-throughput screening campaigns.** ACS Synth. Biol. 8, acssynbio.9b00149. https://doi.org/10.1021/acssynbio.9b00149 Copyright 2019 American Chemical Society

LKF performed the literature and database search, constructed plasmids, strains and libraries, planned and performed all cultivations, FACS experiments and HPLC analyses, established enzyme expression, purification and enzyme assay protocols and wrote the manuscript. SS carried out the protein purification and SS and LKF performed the enzyme assays of the $XalI_{Tc}$ mutants. JM revised the manuscript.

Overall contribution LKF: 90 %

Flachbart, L. K., Gertzen, C., Gohlke, H. & Marienhagen, J. (2020). **Development of a biosensor platform for various phenolic compounds using a transition ligand strategy**. To be submitted.

LKF performed the literature and database search, identified targets, constructed plasmids, strains and libraries. and planned and performed all cultivations and FACS experiments. CG performed docking and MD experiments. CG and HG analysed docking and MD experiments. LKF and JM wrote the manuscript.

Overall contribution LKF: 75 %

Danksagung

Bei **Herrn Prof. Dr. Michael Bott** bedanke ich mich für die Möglichkeit meine Doktorarbeit am IBG-1 anzufertigen, für die Übernahme des Erstgutachtens und für das Interesse am Fortgang dieser Arbeit.

Herr Prof. Dr. Holger Gohlke danke ich für die Übernahme des Korreferats und die Bereitschaft, meine Doktorandenzeit als Mentor zu begleiten.

Bei **Herrn Prof. Dr. Jan Marienhagen** bedanke ich mich für die Überlassung des sehr interessanten Themas und die engagierte, gleichsam fördernd wie fordernde Betreuung des Projektes.

Der Arbeitsgruppe **„Synthetische Zellfabriken“** danke ich für viele anregende Diskussionen über Aspekte des Labor- und Büroalltags, die hervorragende Arbeitsatmosphäre, die immer vorhandene Hilfsbereitschaft, unterhaltsame Kaffeepausen und schöne Gruppenausflüge.

Den helfenden Händen der **Infrastruktur** danke ich für die stets schnelle und freundliche Unterstützung bei bürokratischen und organisatorischen Hürden.

Den über die Jahre wechselnden Teilnehmern der **Fahrgemeinschaften** von Düsseldorf ins FZ und zurück, allen voran Andi, Cedric, Eva, Marc und Max danke ich für die erinnerungswürdige Zeit in Auberginen, Discomäusen und anderen Gefährten.

Meiner Familie danke ich für die Unterstützung im Verlauf des gesamten Studiums, das stete Interesse an meiner Arbeit und das offene Ohr für die Nöte des Alltags.

Meiner **Ehefrau Samantha** danke ich für die tägliche Unterstützung beim Bewältigen des Doktorandenalltags, für die Geduld an den vielen Tagen die, entgegen vorheriger Planung, bis spät in die Nacht reichten, für den Halt in Zeiten großer Belastung und das schönste Geschenk, unseren Sohn Caspar. Twoje na zawsze, moje serce.

Erklärung

Ich versichere an Eides Statt, dass die Dissertation von mir selbständig und ohne unzulässige fremde Hilfe unter Beachtung der „Grundsätze zur Sicherung guter wissenschaftlicher Praxis an der Heinrich-Heine-Universität Düsseldorf“ erstellt worden ist. Die Dissertation wurde in der vorgelegten oder einer ähnlichen Form noch bei keiner anderen Institution eingereicht. Ich habe bisher keine erfolglosen Promotionsversuche unternommen.

Jülich, 07.10.2020

L. K. Flachbart

Lion Konstantin Flachbart

Band / Volume 212
First-principles study of collective spin excitations in noncollinear magnets
F.J. dos Santos (2020), 270 pp
ISBN: 978-3-95806-459-1

Band / Volume 213
Direct measurement of anisotropic resistivity in thin films using a 4-probe STM
T. Flatten (2020), viii, 129 pp
ISBN: 978-3-95806-460-7

Band / Volume 214
The guided self-assembly of magnetic nanoparticles into two- and three- dimensional nanostructures using patterned substrates
W. Ji (2020), VI, 140 pp
ISBN: 978-3-95806-462-1

Band / Volume 215
Molecular layer deposition and protein interface patterning for guided cell growth
M. Glass (2020), iv, 81 pp
ISBN: 978-3-95806-463-8

Band / Volume 216
Development of a surface acoustic wave sensor for in situ detection of molecules
D. Finck (2020), 63 pp
ISBN: 978-3-95806-464-5

Band / Volume 217
Detection and Statistical Evaluation of Spike Patterns in Parallel Electrophysiological Recordings
P. Quaglio (2020), 128 pp
ISBN: 978-3-95806-468-3

Band / Volume 218
Automatic Analysis of Cortical Areas in Whole Brain Histological Sections using Convolutional Neural Networks
H. Spitzer (2020), xii, 162 pp
ISBN: 978-3-95806-469-0

Band / Volume 219
Postnatale Ontogenesestudie (Altersstudie) hinsichtlich der Zyto- und Rezeptorarchitektonik im visuellen Kortex bei der grünen Meerkatze
D. Stibane (2020), 135 pp
ISBN: 978-3-95806-473-7

Band / Volume 220
Inspection Games over Time: Fundamental Models and Approaches
R. Avenhaus und T. Krieger (2020), VIII, 455 pp
ISBN: 978-3-95806-475-1

Band / Volume 221
High spatial resolution and three-dimensional measurement of charge density and electric field in nanoscale materials using off-axis electron holography
F. Zheng (2020), xix, 182 pp
ISBN: 978-3-95806-476-8

Band / Volume 222
Tools and Workflows for Data & Metadata Management of Complex Experiments
Building a Foundation for Reproducible & Collaborative Analysis in the Neurosciences
J. Sprenger (2020), X, 168 pp
ISBN: 978-3-95806-478-2

Band / Volume 223
Engineering of *Corynebacterium glutamicum* towards increased malonyl-CoA availability for polyketide synthesis
L. Milke (2020), IX, 117 pp
ISBN: 978-3-95806-480-5

Band / Volume 224
Morphology and electronic structure of graphene supported by metallic thin films
M. Jugovac (2020), xi, 151 pp
ISBN: 978-3-95806-498-0

Band / Volume 225
Single-Molecule Characterization of FRET-based Biosensors and Development of Two-Color Coincidence Detection
H. Höfig (2020), XVIII, 160 pp
ISBN: 978-3-95806-502-4

Band / Volume 226
Development of a transcriptional biosensor and reengineering of its ligand specificity using fluorescence-activated cell sorting
L. K. Flachbart (2020), VIII, 102 pp
ISBN: 978-3-95806-515-4

Weitere ***Schriften des Verlags im Forschungszentrum Jülich*** unter
http://wwwzb1.fz-juelich.de/verlagextern1/index.asp

Schlüsseltechnologien / Key Technologies
Band / Volume 226
ISBN 978-3-95806-515-4

Mitglied der Helmholtz-Gemeinschaft

JÜLICH
Forschungszentrum